October 2021

Amyloidogenesis of β-2-microglobulin Studied by Mass Spectrometry and Covalent Labeling

Blaise G. Arden
University of Massachusetts Amherst

AMYLOIDOGENESIS OF β-2-MICROGLOBULIN STUDIED BY MASS SPECTROMETRY AND COVALENT LABELING

A Dissertation Presented

by

BLAISE GABRIEL ARDEN

Submitted to the Graduate School of the
University of Massachusetts Amherst in partial fulfillment
of the requirements for the degree of

DOCTOR OF PHILOSOPHY

September 2021

Chemistry Department

Amyloidogenesis of β-2-microglobulin Studied by Mass Spectrometry and Covalent Labeling

A Dissertation Presented

by

BLAISE GABRIEL ARDEN

Approved as to style and content by:

_____
Richard W. Vachet, Chair

_____
Igor A. Kaltashov, Member

_____
Lynmarie K. Thompson, Member

_____
Scott C. Garman, Member

_____
Ricardo B. Metz, Head
Department of Chemistry

ACKNOWLEDGEMENTS

I would like to take the time to thank everyone who has supported, assisted, and guided me on my journey to completing this dissertation, without whom none of this would be possible.

I first and foremost would like to sincerely thank Professor Richard Vachet who advised, directed, and guided me through the work leading to this dissertation. I am immensely grateful to him for accepting me into his research group in a time of need. Richard is an incredible example of not only how to be a good scientist and analytical thinker, but also how to be a caring, compassionate human being and some of that always rubs off on those he mentors. His patience and understanding are an asset in leading such a large and spirited research group. His unwavering support during the trials and tribulations of graduate school will forever be appreciated. I feel very privileged to have been allowed this experience to learn and grow under his instruction.

I would also like to extend my gratitude to my committee members, Professors Igor Kaltashov, Lynmarie Thompson, and Scott Garman. They have been wonderfully patient in committee meetings and massively helpful in my pursuit of this degree. I have also been lucky enough to have interacted with all of them outside of their committee duties, as a teaching assistant, as a student in their classes, and through the Chemistry-Biology Interface program. They are three of the most intelligent people I know, and their advice and guidance has been invaluable.

Additional thanks are due to Dr. Matt Holden who gave me my start in his research lab at UMass. I greatly appreciate the chance he gave me at the beginning of my graduate

career. Thanks also to Steve Eyles, Lizz Bartlett, Adam Graichen, and Ruthanne Paradise for use of and help with instrumentation. They have all been a great asset to the planning and execution of many experiments. I am also grateful to them for always being up for a friendly chat, scientific or otherwise. I would like to extend my thanks to the staff of the Chemistry Department: Bob Sabola, Ryan Feyrer, Ellen Kalt, JMS, Kay Fenlason, and Rebecca David. You keep the department running smoothly and we are all eternally grateful.

Thanks to all of the Vachet Lab members, past and present, who have created a welcoming and inclusive group, not only within the lab, but at social events and conferences as well. To those who came before me: Professors Nick Borotto, Alyssa Marsico, and Sukru Gokhan Elçi and Drs. Zhe Zhang, M.A.C. Serrano, Tyler Marcinko, Meizhe Wang, Bo Zhao, and Tianying Liu, I am grateful for all the knowledge you passed down to me when I started in the group and all the continued help over the years. Special thanks to Dr. Tyler Marcinko who, in addition to being the first to teach me how to use a mass spectrometer when I started at UMass, has always been a great sounding board for my ideas (the good ones and the crazy ones) and a good friend. Thanks also to the undergraduate and post-baccalaureate students who performed valuable supporting work for this dissertation, especially Pablo Quinteros Jr. who also became a good friend. I would also like to thank Drs. Kristen Sikora and Patanachai ‘Kong’ Limpikirati. Thank you both for being wonderful cohort-mates and true friends. I am honored to have undergone this entire journey with you. Finally, thank you to all current members of the Vachet Lab: Laura Castellanos, Catherine Tremblay, Xiao Pan, Stacey Nash, Zack Kirsch, Dheeraj Agrohia,

Jack Bell, Jeerapat ‘Ping’ Doungchawee, and Akaansha Rampal. It has been a pleasure working with you all and good luck to you in the future.

Over my graduate career I have been fortunate to make many wonderful friends who have made the entire experience much richer and fuller and, though there are too many to name all individually (I hope you will forgive me), I would like to highlight a few. Firstly, the Amherst town softball team The Isotopes (TOPES!). It has been an absolute pleasure playing with you all these years and I hope the team tradition continues to live on. Massive thanks to Jillian Denhardt, Kevin Guay, Brendan Sheehan, and Keenan Bailey who got me through the extraordinary circumstances of a global pandemic during my final year of graduate school and helped keep me sane. Additional thanks to my high school and college friends who have kept in touch and supported me throughout graduate school, particularly Tyler Denning, Ari Girelli, and Josh Squire

Lastly, I’d like to extend the largest thank yous to my family, whose undying support has meant the world to me, not only in graduate school, but through my whole life. To my grandparents, Frederic and Eleanore Arden and Joseph and Mary Gavin, I have always tried to make you proud, and I am grateful for the wonderful influence you’ve had on my life. Thanks to my amazing sister Ariana, who constantly amazes and impresses me, for her love and support in all aspects of my life. I am incredibly lucky to have her as my sister. Finally, and by no means least, I need to thank my parents, Janet and Ronald Arden, for their unwavering love and support in my life, including through many years of schooling. They exposed me to a wide variety of culture, nature, and information and always fed and encouraged my natural curiosity. In more ways than one, I truly would not be the person I

am today without them. It is an honor to call them my parents and I will never be able to thank them enough.

ABSTRACT

AMYLOIDOGENESIS OF β-2-MICROGLOBULIN STUDIED BY MASS SPECTROMETRY AND COVALENT LABELING

SEPTEMBER 2021

BLAISE GABRIEL ARDEN

B.S, UNIVERSITY OF CONNECTICUT

Ph.D., UNIVERSITY OF MASSACHUSETTS AMHERST

Directed by: Professor Richard W. Vachet

Amyloid-forming proteins are implicated in a number of debilitating diseases. While many amyloid-forming proteins are well studied, the early stages of amyloidosis are still not well understood on a molecular level. Covalent labeling, combined with mass spectrometry (CL-MS), is uniquely well suited to provide molecular-level insight into the factors governing the early stages of amyloidosis. This dissertation leverages CL-MS techniques to examine the early stages of β-2-microglobulin (β2m) amyloidosis. β2m is the protein that forms amyloids in the condition known as dialysis-related amyloidosis. An automated CL-MS technique that uses dimethyl(2-hydroxy-5-nitrobenzyl) sulfonium bromide as a labeling reagent was developed and used to measure energy barriers to the initial pre-amyloid structural change of β2m under different amyloid-forming conditions. The results represent the first ever measure of the activation barrier for a structural change initiating amyloid formation. The results also give new mechanistic insight into β2m's amyloidogenic structural change, particularly the role of Pro32 isomerization. The catalytic nature of Cu(II) as an initiator of the β2m pre-amyloid structural change was confirmed as

it significantly lowered the energy barrier to this structural change. It also appears that, when initiated by acid, the Pro32 isomerization may no longer be the rate limiting step in this process.

The same technique was further used to investigate the β2m structural change caused by its interaction with an amyloidogenic variant of β2m called ΔN6-β2m, which is missing its first six N-terminal residues. Both primary and secondary nucleation events involved in the β2m/ΔN6-β2m interaction were investigated. The measured barrier for the primary nucleation event seems to indicate that, like the acid induced structural change of β2m, the isomerization of Pro32 may not be the rate determining step. However, the measured barrier for the secondary nucleation event, similar to that of the Cu(II) induced structural change, indicates that the isomerization of Pro32 is the rate determining step. The use of point mutants gives further detail on the crucial residues and regions of the proteins required for a productive interaction to yield amyloids. The new kinetic and thermodynamic information gained in this work yields new insight into the mechanistic details of the biomedically important process of β2m amyloidosis.

TABLE OF CONTENTS

Page

LIST OF TABLES

LIST OF FIGURES

CHAPTER 1

INTRODUCTION

1.1 Amyloidosis

Protein folding diseases involve the misfolding or altered folding of proteins in the body and can lead to negative, sometimes fatal consequences. A subset of protein folding diseases are amyloid related diseases. Amyloids are insoluble protein aggregates characterized by their fibrillar morphology composed of β-sheet rich structures. Amyloid fibrils are implicated in well-known neurodegenerative diseases, such as Alzheimer's and Parkinson's diseases, but are also associated with over 20 other human diseases, each involving a different protein. Amyloid fibril formation is not only seen in the brain (as in Alzheimer's and Parkinson's diseases), but can be found in other soft tissues, such as the pancreas (in the case of islet amyloid polypeptide or amylin) or in the joints of dialysis patients (in the case of β-2-microglobulin).[1,2] Amyloid fibril formation typically begins with partial protein unfolding (or partial folding by an unstructured protein) into an intermediate followed by formation of soluble oligomeric species. The partially structured intermediate or oligomeric intermediates then self-assemble into a nucleus enriched in β-sheet structure. Growth of the nucleus by β-sheet extension leads to larger protofibrillar aggregates that eventually form mature insoluble fibrils.[1–6]

While general aspects of amyloid formation are well understood for many different amyloid-forming proteins, molecular-level information about the early stages of the amyloid reaction is only beginning to be revealed for most amyloid systems. The early steps of the reaction are important to understand because interrupting the reaction at these

stages can be one of the most effective means of preventing eventual fibril formation. Furthermore, evidence indicates that pre-amyloid oligomeric intermediates are pathogenic in some cases.[7–10] For some proteins, the global structural properties of amyloidogenic intermediates have been studied, but insights into amino acid-level structural changes are only starting to emerge for some amyloid protein systems.

1.2 β-2-microglobulin

One amyloid disease, dialysis-related amyloidosis (DRA), occurs when kidney function is impaired and patients undergo long term hemodialysis. In DRA, β-2-microglobulin (β2m) accumulates and aggregates, primarily in bone and joint tissue.[11] β2m is a small (~12 kDa) 99 residue protein comprised of 7 β-strands (A-G) organized in an anti-parallel β-sandwich held together by a disulfide bond (Figure 1.1).[12–14] It is a part of

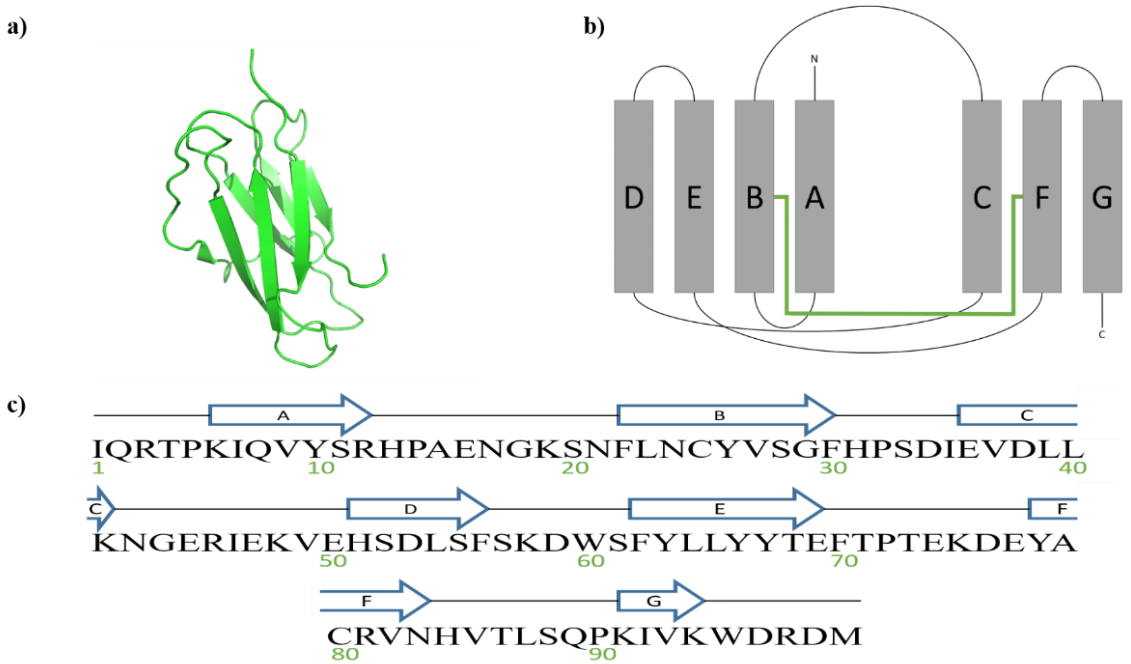

Figure 1.1: A breakdown of the structure of β2m. a) A cartoon representation of β2m (PDB: 2XKS). b) A representation of the nomenclature and connectivity of the β-strands in β2m. The green line represents the disulfide bond between the B strand and the F strand. c) The amino acid sequence of β2m. Arrows above the sequence show which residues make up each β-strand. The lines between the arrows represents the loops and unstructured regions between β-strands.

the major histocompatibility complex (MHC) class I molecule and is present in all nucleated cells in humans.

In patients with renal failure undergoing long term hemodialysis, the kidneys cannot keep up with the body's natural turnover of MHC I and β2m is not effectively removed, causing its concentration to increase up to 60-fold. Eventually, β2m forms amyloid fibrils in the joints of these patients.[11] The cause of β2m amyloidosis is still not well understood, but increased protein concentrations alone are insufficient. The resulting DRA can lead to arthralgia, carpal tunnel syndrome, and bone cysts and in extreme cases, death.[15] Several *in vitro* methods of inducing β2m amyloidogenesis have been established, including the addition of Cu(II), low pH, exposure to trifluoroethanol (TFE), and incubation with β2m truncation mutants, among others.[16–19]

The induction of amyloidosis is characterized by a hallmark structural change where native β2m monomers become destabilized and amyloid competent. In natively folded β2m, the His31-Pro32 bond, contained in the loop between strands B and C (the BC loop), adopts an unfavorable *cis* conformation stabilized by the N-terminal region of the protein. *Cis-trans* isomerization (CTI) of Pro32 in β2m has been identified as the rate determining step preceding β2m amyloid formation.[20–24] Displacement of this strand through truncation or interactions with metals or other molecules promotes CTI of Pro32 and subsequent conversion into the amyloidogenic precursor.[25] This structural change causes a repacking of the protein's hydrophobic core, particularly exposure of Phe30 (contained on the BC loop) and burial of Trp60 (contained on the DE loop), and other

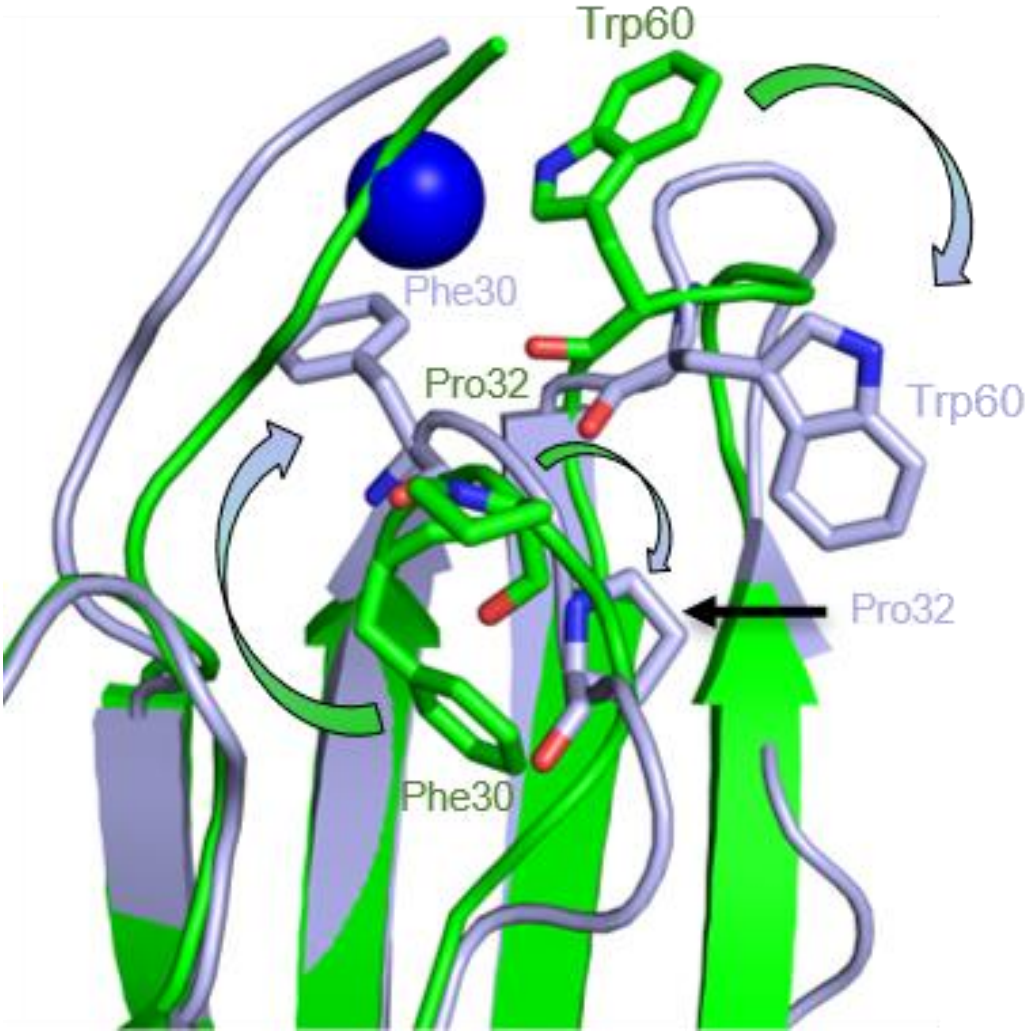

Figure 1.2: Pre-amyloid structural change of β2m from the native conformation (green) to the amyloid competent conformation (grey) characterized by the *cis-trans* isomerization of Pro32. Other key rearrangements include the exposure of Phe30 and the burial of Trp60.

structural changes that facilitate aggregation (Figure 1.2).[20–24,26–30] This conformational change results in subsequent oligomerization before eventual amyloid fibril formation.[20–24]

1.3 Mass Spectrometry and Covalent Labeling

The level of molecular detail available with X-ray crystallography and nuclear magnetic resonance (NMR) have made these popular tools for the analysis of amyloids, although most amyloid systems are not readily amenable to these techniques. The

application of these techniques has been somewhat limited in scope, however, because most pre-amyloid species are too short-lived, exist in mixtures, and cannot be readily crystallized. Low time resolution and need for high sample purity further limit their utility.

Mass spectrometry (MS) has emerged as a valuable tool for investigating amyloid-forming proteins because of its high sensitivity, specificity, and balance of analysis speed and moderate structural resolution. In contrast to NMR, it is not limited in terms of protein molecular size and can provide structural information in protein mixtures. Using MS to analyze protein structure typically requires encoding a protein's structural information into its mass and then detecting proteolytic fragments of that protein to localize the encoded structural information. One technique finding increased usage in the study of amyloid-forming proteins is covalent labeling. Covalent labeling (CL) has been coupled with MS to obtain insight into protein topologies, conformations, and interactions at residue level.[31–33] In CL-MS, a protein or protein complex is reacted with a reagent that covalently modifies the side chains of solvent exposed amino acids. A wide range of reagents have been developed and utilized in CL-MS experiments, both ones that react with specific amino acids[30] and those that react with a broad range of amino acids.[34] After the labeling reaction, which encodes the structural information, the protein is analyzed in a manner identical to most proteomics experiments: the protein is enzymatically digested, the resulting peptides are separated by liquid chromatography (LC), and these peptides are then sequenced by tandem mass spectrometry (MS/MS) to identify the modified residues. Most CL-MS experiments are conducted by comparing the modification percentages of a given protein under one condition to that of the same protein under another condition. Changes in the modification extent can reveal conformation changes, binding sites, and protein-

protein interfaces. CL-MS has unique attributes that enable this technique to reveal structural details about amyloid-forming proteins that is not accessible by other techniques. Two important features of CL-MS are its ability to analyze proteins in complex mixtures and to obtain structural information on protein systems that are undergoing structural changes on the timescales of minutes.

One specific type of CL, oxidative labeling, involves the covalent modification of solvent exposed amino acid side chains by reactive oxidants. This technique is useful for investigating protein-protein interaction sites by revealing differences in exposure of amino acid residues of protein monomers and complexes. In one example, Li *et al.* used fast photochemical oxidation of proteins (FPOP) to monitor the aggregation of $A\beta_{1-42}$.[35] The changes seen in percent modification of the peptide over time showed several distinct stages of aggregation. Using a nucleation-autocatalytic growth mechanism, the researchers were able to model $A\beta_{1-42}$ amyloidosis. They propose rapid dimer and small oligomer formation followed by nucleation of larger oligomers from these smaller species. This nucleation allows for catalysis of protofibril formation that eventually leads to formation of full amyloid fibrils. Further analysis via digestion and LC-MS/MS illustrates that association of $A\beta_{1-42}$ is driven by hydrophobic interactions of residues 16-27.

Oxidative labeling has also been used to investigate the conversion of the prion protein's cellular form, PrPc, into its β-oligomeric form, PrPb.[36] Isotopically labeled H_2O_2 ($H_2{}^{16}O_2$ and $H_2{}^{18}O_2$) were used to label Met and Trp residues in each conformer. After labeling, both forms of PrP were combined and analyzed by LC-MS/MS. The extent of modification on each form shows increased labeling on Met129, Met138, and Met213 of PrPc and increased labeling on Trp99, Met112, Met134, Met139, and Met206 of PrPb.

These labeling differences are due to the rotation of the β1-H1-β2 loop away from the core of the protein during the aggregation process.

FPOP has also been leveraged to look at structural differences between WT β2m and its naturally amyloidogenic variant ΔN6-β2m which is missing the first 6 residues. Cornwell *et al.* were able to determine 6 residues with significant differences in oxidation between the two proteins.[26] Unsurprisingly, most of these residues are near the N-terminal truncation. Through comparison with hydrogen deuterium exchange (HDX)/MS, it is revealed that all 6 of these residues fall in regions of ΔN6-β2m that are more dynamic than WT β2m. These results suggest that a reorganization of side chains in ΔN6-β2m as compared to WT β2m may lead to its high amyloidogenicity.

Metal catalyzed oxidation (MCO), another form of oxidative labeling, was used to identify the Cu(II) binding site of β2m. MCO reactions can quickly capture information on the Cu(II) binding site under conditions where the concentration of β2m is low enough (~2 μM) that there is no appreciable dimerization.[16,29,37] Our group was able to use this technique to identify the binding site of Cu(II) on monomeric β2m. This binding site involves the N-terminal amine, the backbone amide between Ile1 and Gln2, His31, and Asp59.[27] These data give insight into how metal binding induces the pre-amyloid structural change of β2m. In fully unfolded β2m, all four His residues can bind Cu(II), showing the specificity of the particular Cu(II) binding site that triggers the pre-amyloid structural change.[38] In addition, it was shown that Ni(II) binds to β2m in a slightly different way that does not lead to amyloid formation.[39] A 'detuned' variation of the MCO reaction that allows modification of residues within 10 Å shows a conformational change repositioning Arg3 and Asp59.[27] This subtle change allows for salt bridge formation in β2m dimers.[40]

Dimers and tetramers of β2m formed by initiation with Cu(II) were also investigated and slight binding site changes were found that are consistent with the loss of Cu(II) from β2m that occurs during the amyloid forming process.[29,37]

Residue-specific and pseudo-specific CL reagents can be used as a straightforward method for mapping binding sites because protein-ligand binding often involves interaction with specific side chains. Liu *et al.* were able to use CL to identify the binding sites of β2m inhibitors rifamycin SV and doxycycline and another small molecule, suramin, which binds to β2m but does not inhibit amyloid formation.[41] Several labeling reagents were used in parallel to increase confidence in binding site determination: diethylpyrocarbonate (DEPC), which labels several residues, including His, Lys, Thr, Ser, and Tyr; 2,3-butanedione (BD), which labels Arg residues; and the combination of 1-ethyl-3-(3-(dimethylamino) propyl) carbodiimide (EDC) and glycine ethyl ester (GEE), which labels Asp and Glu residues. The labeling reagents were each reacted with β2m in the presence or absence of small molecule ligand. Analysis by LC-MS/MS revealed the binding sites of rifamycin SV and doxycycline are regions of β2m known to mediate amyloid-competent tetramer formation. Suramin was found to interact with residues not known to facilitate formation of any oligomers. Further studies endeavored to use CL to determine the binding site of another amyloid inhibitor epigallocatechin-3-gallate (EGCG).[42]

β2m forms discrete, even-order oligomers including dimers, tetramers, and hexamers.[37] Selective CL with MS can be used to characterize these oligomeric species. Mendoza *et al.* studied the interfaces between monomer units in β2m dimers and tetramers using DEPC, BD, and sulfo-N-hydroxysuccinimide acetate (NHSA) as complementary labeling reagents.[43,44] The extent of labeling of β2m monomers and the oligomers were

compared to gain insight into the oligomeric interfaces. The dimer interface was found to be formed by an antiparallel arrangement of the ABED β-sheets of two monomers. The labeling pattern of the tetramer indicates an interface between the D β-strands of one dimer and the G β-strands of another dimer.

One residue specific covalent labeling reagent, Koshland's reagent (2-(Bromomethyl)-4-nitrophenol) is a tryptophan specific covalent label that has been used to investigate solvent accessibility of tryptophan residues. However, use of Koshland's reagent is limited due to its lack of solubility in aqueous solution. The reactivity of Koshland's reagent also varies greatly with pH of the solution and the molecule can hydrolyze rapidly at low pH. In addition, at various pHs, Koshland's reagent can also react with and label cysteine and tyrosine residues.[45,46] To avoid the issues surrounding the use of Koshland's reagent, a variant was created which is soluble in aqueous solutions, dimethyl(2-hydroxy-5-nitrobenzyl)sulfonium bromide (HNSB) (Figure 1.3). This reagent is still selective for tryptophan residues, but has also been known to label free cysteine residues to some extent, especially at low pH. HNSB is more stable than Koshland's reagent especially under acidic conditions, allowing for structural changes in protein to be monitored under a wider variety of incubation conditions.[47]

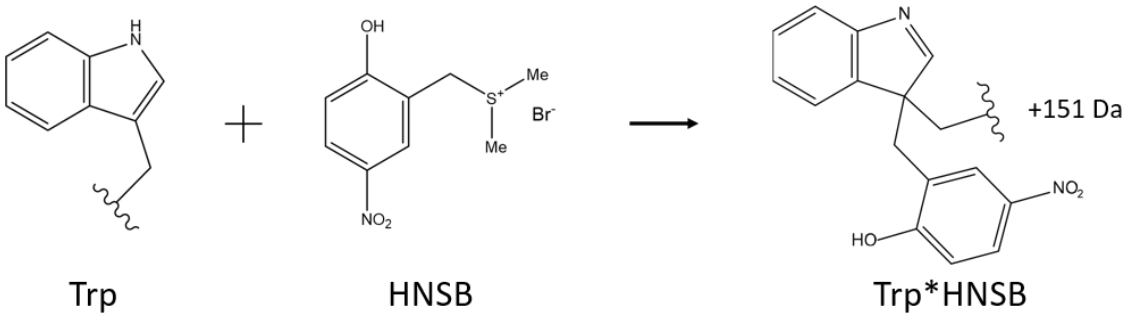

Figure 1.3: Reaction of HNSB with a Trp residue, yielding a mass addition of 151 Da.

Proteins or peptides that are labeled by HNSB can be analyzed by liquid chromatography mass spectrometry (LC-MS) to determine the extent and site(s) of labeling. From the MS data, a weighted average of the extent of tryptophan modification by HNSB can be calculated. The large change in solvent accessibility of Trp60 in β2m provides an excellent way to monitor the initial structural change that causes the conversion of the protein into the amyloidogenic precursor. Since there are only two Trp residues in β2m and only the Trp60 moves during the pre-amyloid structural change under most conditions, whole protein analysis CL-MS experiments can be carried out without proteolytic digestion or MS/MS, further simplifying experimentation.

1.4 Dissertation Overview

In this dissertation, a CL-MS method has been developed to monitor the burial of Trp60 in β2m as a proxy for the pre-amyloid structural change characterized by the CTI of Pro32. This technique was leveraged to gather energetic and mechanistic information about reactions leading to the amyloid competent state of β2m. This work represents the first-ever measurements of, not only the energy barrier to the pre-amyloid structural change of β2m, but of any structural change leading to amyloid formation. In addition to the knowledge gained about the β2m amyloid forming process, this work yields new insights that are applicable to all amyloid systems.

In chapter 2 (published data), the CL-MS method using HNSB labeling was developed to monitor the burial of Trp60 in β2m as a function of time as a means of determining the rate of β2m's amyloidogenic switch. These rate measurements were then used to determine the energy barriers associated with this structural switch under different amyloid forming conditions. The results confirmed the catalytic nature of Cu(II) by

demonstrating the significant drop in activation energy when Cu(II) is used as the amyloid inducer of β2m. TFE also acts by reducing the energy required for the CTI of Pro32, but not by nearly as much as Cu(II). Finally, it was revealed that when induced by low pH, the CTI of Pro32 may no longer be the rate determining step of β2m amyloidogenesis.

In chapter 3, the same CL-MS method is used to probe the primary and secondary nucleation dependent mechanisms of β2m amyloidosis as induced by interaction with the amyloidogenic variant ΔN6. Activation energy barriers for both the primary and secondary nucleation dependent mechanisms were determined. Additional work has begun to probe some of the molecular factors governing these energy barriers for each mechanism. The results show another structural change during the lag phase under primary nucleation conditions and indicate that the CTI of Pro32 may no longer be the rate determining step. The removal of the lag phase is demonstrated under secondary nucleation conditions as well as evidence that the CTI of Pro32 is the rate determining step when initiated by amyloid seeds. This chapter also leaves room for particularly interesting future work towards possible molecular factors able to inhibit amyloid seeding.

Chapter 4 summarize the work completed towards this dissertation. It also illustrates a myriad of ways in which this HNSB Trp labeling technique can be applied to further investigation of amyloidosis. Specifically, determination of the method of action of amyloid inhibitors, cross-seeding of β2m with other amyloid systems, and investigations into another amyloidogenic variant of β2m with interesting structural features, among others.

1.5 References

1. Rochet, J. & Lansbury, P. T. J. Amyloid fibrillogenesis: themes and variations. *Curr. Opin. Struct. Biol.* **10**, 60–68 (2000).

2. Chiti, F. & Dobson, C. M. Protein Misfolding, Functional Amyloid, and Human Disease. *Annu. Rev. Biochem.* **75**, 333–366 (2006).

3. Cohen, S. I. A., Vendruscolo, M., Dobson, C. M. & Knowles, T. P. J. From macroscopic measurements to microscopic mechanisms of protein aggregation. *J. Mol. Biol.* **421**, 160–171 (2012).

4. Cohen, S. I. A. *et al.* Distinct thermodynamic signatures of oligomer generation in the aggregation of the amyloid-β peptide. *Nat. Chem.* **10**, 523–531 (2018).

5. Hellstrand, E., Boland, B., Walsh, D. M. & Linse, S. Amyloid β-protein aggregation produces highly reproducible kinetic data and occurs by a two-phase process. *ACS Chem. Neurosci.* **1**, 13–18 (2010).

6. Cohen, S. I. A. *et al.* Nucleated polymerization with secondary pathways. I. Time evolution of the principal moments. *J. Chem. Phys.* **135**, 1–44 (2011).

7. Fändrich, M. Oligomeric intermediates in amyloid formation: Structure determination and mechanisms of toxicity. *J. Mol. Biol.* **421**, 427–440 (2012).

8. Hardy, J., Selkoe, D. J., Hardy, J. & Selkoe, D. J. Therapeutics Linked references are available on JSTOR for this article : The Amyloid Hypothesis of Alzheim Progress and Problems on the Road to. *Science (80-.).* **297**, 353–356 (2002).

9. Lambert, M. P. *et al.* Diffusible, nonfibrillar ligands derived from Aβ1-42 are potent central nervous system neurotoxins. *Proc. Natl. Acad. Sci. U. S. A.* **95**, 6448–6453 (1998).

10. Winner, B. *et al.* In vivo demonstration that α-synuclein oligomers are toxic. *Proc. Natl. Acad. Sci. U. S. A.* **108**, 4194–4199 (2011).

11. Gejyo, F. *et al.* β2-microglobulin: a new form of amyloid protein associated with chronic hemodialysis. *Kidney Int* **30**, 385–390 (1986).

12. Becker, J. W. & Reeke, G. N. Three-dimensional structure of beta 2-microglobulin. *Proc. Natl. Acad. Sci. U. S. A.* **82**, 4225–9 (1985).

13. Smith, D. P. & Radford, S. E. Role of the single disulphide bond of beta(2)-microglobulin in amyloidosis in vitro. *Protein Sci.* **10**, 1775–84 (2001).

14. Katou, H. *et al.* The role of disulfide bond in the amyloidogenic state of beta(2)-microglobulin studied by heteronuclear NMR. *Protein Sci.* **11**, 2218–29 (2002).

15. Gillmore, J. D., Hawkins, P. N. & Pepys, M. B. Amyloidosis: a review of recent diagnostic and therapeutic developments. *Br. J. Haematol.* **99**, 245–56 (1997).

16. Morgan, C. J., Gelfand, M., Atreya, C. & Miranker, A. D. Kidney dialysis-associated amyloidosis: a molecular role for copper in fiber formation. *J. Mol. Biol.* **309**, 339–45 (2001).

17. McParland, V. J. *et al.* Partially Unfolded States of β2-Microglobulin and Amyloid Formation in Vitro. *Biochemistry* **39**, 8735–8746 (2000).

18. Eichner, T., Kalverda, A. P., Thompson, G. S., Homans, S. W. & Radford, S. E. Conformational Conversion during Amyloid Formation at Atomic Resolution. *Mol. Cell* **41**, 161–172 (2011).

19. Stoppini, M. & Bellotti, V. Systemic amyloidosis: Lessons from β2-microglobulin. *J. Biol. Chem.* **290**, 9951–9958 (2015).

20. Jahn, T. R., Parker, M. J., Homans, S. W. & Radford, S. E. Amyloid formation under physiological conditions proceeds via a native-like folding intermediate. *Nat. Struct. Mol. Biol.* **13**, 195–201 (2006).

21. Eakin, C. M., Berman, A. J. & Miranker, A. D. A native to amyloidogenic transition regulated by a backbone trigger. *Nat. Struct. Mol. Biol.* **13**, 202–208 (2006).

22. Eichner, T. & Radford, S. E. A Generic Mechanism of β2-Microglobulin Amyloid Assembly at Neutral pH Involving a Specific Proline Switch. *J. Mol. Biol.* **386**, 1312–1326 (2009).

23. Torbeev, V. Y. & Hilvert, D. Both the cis-trans equilibrium and isomerization dynamics of a single proline amide modulate β2-microglobulin amyloid assembly. *Proc. Natl. Acad. Sci.* **110**, 20051–20056 (2013).

24. Esposito, G. *et al.* The Controlling Roles of Trp60 and Trp95 in β2-Microglobulin Function, Folding and Amyloid Aggregation Properties. *J. Mol. Biol.* **378**, 887–897 (2008).

25. Esposito, G. *et al.* Removal of the N-terminal hexapeptide from human β2-microglobulin facilitates protein aggregation and fibril formation. *Protein Sci.* **9**, 831–845 (2000).

26. Cornwell, O., Radford, S. E., Ashcroft, A. E. & Ault, J. R. Comparing Hydrogen Deuterium Exchange and Fast Photochemical Oxidation of Proteins: a Structural Characterisation of Wild-Type and ΔN6 β2-Microglobulin. *J. Am. Soc. Mass Spectrom.* **29**, 2413–2426 (2018).

27. Srikanth, R., Mendoza, V. L., Bridgewater, J. D., Zhang, G. & Vachet, R. W. Copper Binding to β-2-Microglobulin and its Pre-Amyloid Oligomers. *Biochemistry* **48**, 9871–9881 (2009).

28. Calabrese, M. F. & Miranker, A. D. Metal binding sheds light on mechanisms of amyloid assembly. *Prion* **3**, 1–4 (2009).

29. Antwi, K. *et al.* Cu (II) organizes β-2-microglobulin oligomers but is released upon amyloid formation. *Protein Sci.* **17**, 748–759 (2008).

30. Mendoza, V. L. & Vachet, R. W. Probing Protein Structure by Amino Acid-Specific Covalent Labeling and Mass Spectrometry. *Mass Spectrom. Rev.* **28**, 785–815 (2009).

31. Kaur, U. *et al.* Evolution of Structural Biology through the Lens of Mass Spectrometry. *Anal. Chem.* **91**, 142–155 (2019).

32. Limpikirati, P., Liu, T. & Vachet, R. W. Covalent labeling-mass spectrometry with non-specific reagents for studying protein structure and interactions. *Methods* **144**, 79–93 (2018).

33. Zhang, B., Cheng, M., Rempel, D. & Gross, M. L. Implementing fast photochemical oxidation of proteins (FPOP) as a footprinting approach to solve diverse problems in structural biology. *Methods* **144**, 94–103 (2018).

34. Xu, G. & Chance, M. R. Hydroxyl radical-mediated modification of proteins as probes for structural proteomics. *Chem. Rev.* **107**, 3514–3543 (2007).

35. Li, K. S., Rempel, D. L. & Gross, M. L. Conformational-Sensitive Fast Photochemical Oxidation of Proteins and Mass Spectrometry Characterize Amyloid Beta 1-42 Aggregation. *J. Am. Chem. Soc.* **138**, 12090–12098 (2016).

36. Serpa, J. J. *et al.* Using isotopically-coded hydrogen peroxide as a surface modification reagent for the structural characterization of prion protein aggregates. *J. Proteomics* **100**, 160–166 (2014).

37. Calabrese, M. F. & Miranker, A. D. Formation of a Stable Oligomer of β-2 Microglobulin Requires only Transient Encounter with Cu(II). *J. Mol. Biol.* **367**, 1–7 (2007).

38. Lim, J. & Vachet, R. W. Using mass spectrometry to study copper-protein binding under native and non-native conditions: β-2-microglobulin. *Anal. Chem.* **76**, 3498–3504 (2004).

39. Dong, J. *et al.* Unique Effect of Cu(II) in the Metal-Induced Amyloid Formation of β-2-Microglobulin. *Biochemistry* **53**, 1263–1274 (2014).

40. Calabrese, M. F., Eakin, C. M., Wang, J. M. & Miranker, A. D. A regulatable switch mediates self-association in an immunoglobulin fold. *Nat. Struct. Mol. Biol.* **15**, 965–71 (2008).

41. Liu, T., Marcinko, T. M., Kiefer, P. A. & Vachet, R. W. Using Covalent Labeling and Mass Spectrometry To Study Protein Binding Sites of Amyloid Inhibiting Molecules. *Anal. Chem.* **89**, 11583–11591 (2017).

42. Marcinko, T. M., Drews, T., Liu, T. & Vachet, R. W. Epigallocatechin-3-gallate Inhibits Cu(II)-Induced β-2-Microglobulin Amyloid Formation by Binding to the Edge of Its β-Sheets. *Biochemistry* **59**, 1093–1103 (2020).

43. Mendoza, V. L., Antwi, K., Barón-rodríguez, M. A., Blanco, C. & Vachet, R. W. Structure of the Pre-amyloid Dimer of β-2-microglobulin from Covalent Labeling and Mass Spectrometry. *Biochemistry* **49**, 1522–1532 (2010).

44. Mendoza, V. L., Barón-Rodríguez, M. A., Blanco, C. & Vachet, R. W. Structural insights into the pre-amyloid tetramer of β-2-microglobulin from covalent labeling and mass spectrometry. *Biochemistry* **50**, 6711–6722 (2011).

45. D. E. Koshland, Y. D. Karkhanis, H. G. L. An Environmentally-Sensitive Reagent with Selectivity for the Tryptophan Residue in Proteins. *J. Am. Chem. Soc.* **86**, 1448–1450 (1964).

46. Horton, H. R. & Koshland, D. E. A Highly Reactive Colored Reagent with Selectivity for the Tryptophan Residue in Proteins. 2-Hydroxy-5-nitrobenzyl Bromide. *J. Am. Chem. Soc.* **87**, 1126–1132 (1965).

47. Horton, H. R. & Tucker, W. P. Dimethyl(2-hydroxy-5-nitrobenzyl) sulfonium Salts. *J. Biol. Chem.* **245**, 3397–3401 (1970).

CHAPTER 2

MEASURING THE ENERGY BARRIER OF THE STRUCTURAL CHANGE THAT INITIATES AMYLOID FORMATION IN β-2-MICROGLOBULIN

2.1 Introduction

The formation of protein amyloid fibrils is associated with numerous devastating human diseases, including Alzheimer's, Parkinson's, and type II diabetes.[1,2] Amyloid fibril formation typically begins with partial protein unfolding (or partial folding by an unstructured protein) and formation of soluble oligomeric species before progressing to primary nucleation and elongation events that involve aggregate formation via the addition of monomers.[1–6] For several amyloid protein systems, a combination of new experimental and theoretical tools have recently led to a greater understanding of the kinetics and thermodynamics the amyloid pathway,[3–6] but almost no kinetic or thermodynamic information is available for the initial structural change for any amyloid system. Even so, it is generally recognized that measurements of kinetics and thermodynamics for amyloid systems more fully reveal the complex mechanisms involved in the process and can help better predict amyloid behavior under *in vivo* conditions that are more difficult to study directly.

We have sought to obtain the first-ever kinetic and energetic information about the initial structural change in amyloid formation using the protein β-2-microglobulin (β2m) as a model system. In patients with renal failure undergoing long term hemodialysis, β2m is not effectively removed, causing its concentration to increase up to 60-fold. Eventually, β2m forms amyloid fibrils in the joints of these patients.[7] The cause of β2m amyloidosis is not well understood, but increased protein concentrations alone are insufficient. Several *in*

vitro methods of inducing β2m amyloidogenesis have been established, including the addition of Cu(II), low pH, exposure to trifluoroethanol (TFE), and incubation with β2m truncation mutants, among others.[8–11]

Cis-trans isomerization (CTI) of Pro32 in β2m has been identified as an important structural change preceding β2m amyloid formation.[12–16] In natively folded β2m, the His31-Pro32 peptide bond adopts a *cis* conformation stabilized by the N-terminal strand. Displacement of this strand through truncation or interactions with metals or other molecules promotes CTI of Pro32 and subsequent conversion into the amyloidogenic precursor.[17] This structural change causes a repacking of the protein's hydrophobic core, particularly exposure of Phe30 and burial of Trp60, and other structural changes that facilitate aggregation.[12–16,18–22] Subsequent oligomerization to higher-order oligomers occurs before eventual amyloid fibril formation.[12–16]

The large change in solvent accessibility of Trp60 provides an excellent way to monitor the initial structural change that causes the conversion of the protein into the amyloidogenic precursor. Here, we use a covalent labeling (CL) mass spectrometry (MS) method[22,23] to monitor the burial of Trp60 as a function of time as a means of determining the rate of β2m's amyloidogenic switch. These rate measurements are used to determine the energy barriers associated with this structural switch under different amyloid forming conditions. Cohen *et al*. have recently reported energy barriers to the nucleation and elongation phases of amyloid formation by amyloid-β peptide,[4] but to the best of our knowledge, our measurements represent the first energy barriers ever measured for the structural change that initiates amyloid formation. Such measurements will be useful for more deeply understanding the mechanistic details of this process.

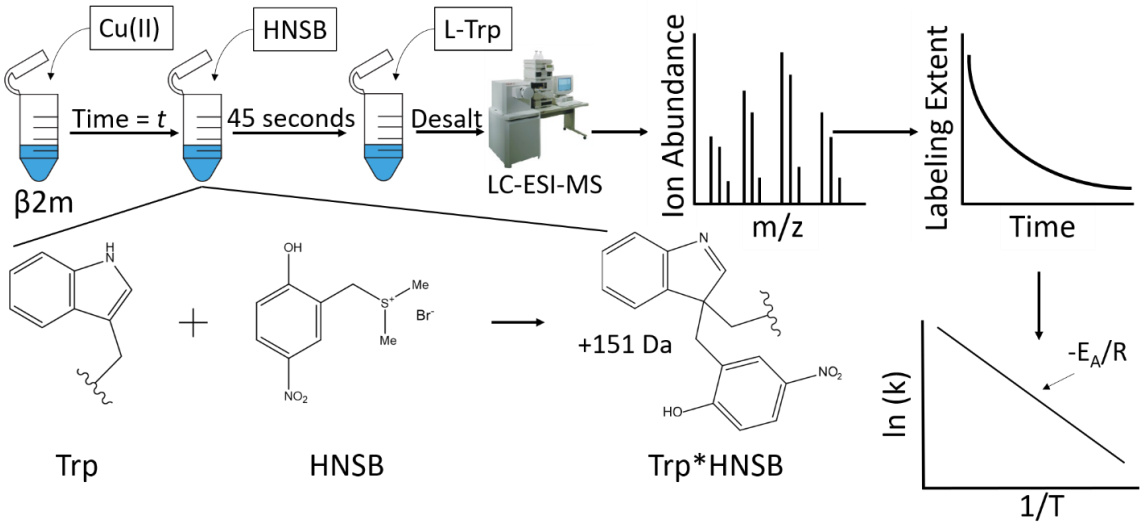

Figure 2.1: Experimental scheme for CL-MS of β2m using the reagent HNSB.

2.2 Experimental

Covalent labeling MS (CL-MS) along with fluorescence spectroscopy and dynamic light scattering (DLS) were used to monitor the structural and oligomeric changes of β2m under different amyloid forming conditions. CL-MS uses reagents to covalently modify solvent accessible amino acid residues,[23] with liquid chromatography MS (LC-MS) providing a readout of the extent of the modification (Figure 2.1 and Figure 2.2). The Trp-specific covalent labeling reagent dimethyl(2-hydroxy-5-nitrobenzyl) sulfonium bromide (HNSB) was used to monitor Trp60 burial over time by reacting it with β2m for 45 or 90 s at different time points after initiating amyloid formation with Cu(II), acid (at pH 3.5), or 20% TFE. The inherent reactivity of Trp with HNSB is lower at pH 3.5, and so a longer reaction time (i.e., 90 s) was used for those experiments. In all cases, the reaction is quenched by the addition of L-Trp and quickly desalted prior to MS analysis (Figure 2.1).

Covalent Labeling Sample Preparation. For all metal and TFE experiments, a 75 μM stock of β2m was made in 25 mM MOPS and 150 mM potassium acetate at pH 7.4. For all acid experiments, a 150 μM stock of β2m was made in HPLC water. For all

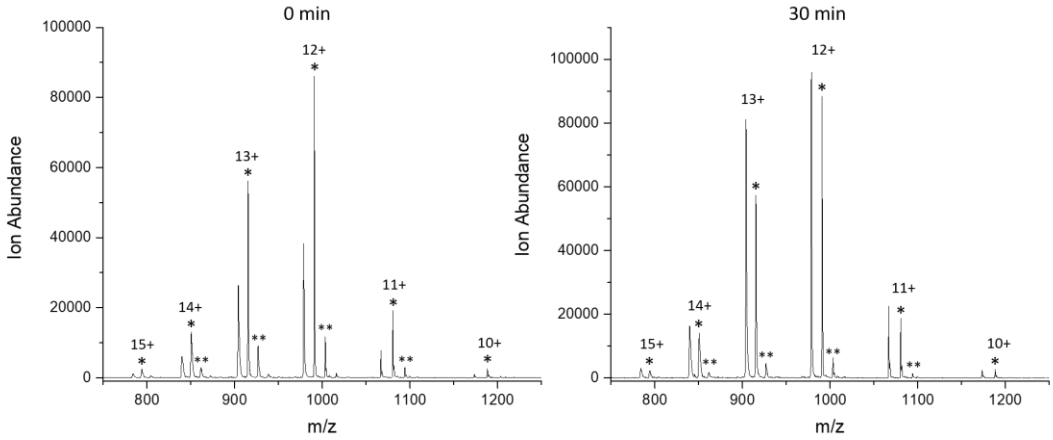

Figure 2.2: Example electrospray ionization mass spectra of β2m, showing a decreased extent of covalent labeling with HNSB 30 min after adding Cu(II). The asterisk (*) indicates the HNSB-labeled β2m peaks in the mass spectra.

experiments, molar ratios of metal to β2m were chosen such that 95% of proteins in solution were bound (based on previously reported measurements) and were as follows: Cu 2:1, Zn 4:1, and Ni 16:1.[24,25]

Thioflavin T Fluorescence. Fluorescence experiments were performed on a PTI QuantaMaster 4 SE spectrofluorometer. Measurements were taken at excitation and emission wavelengths of 437 nm and 483 nm, respectively. Cu(II) initiated samples contained 25 mM MOPS (at pH 7.4), 150 mM potassium acetate, 500 mM urea, 50 μM β2m, 80 μM ThT and were equilibrated at 37 °C for 15 minutes before adding Cu(II). After the addition of 100 μM Cu(II), the sample was immediately analyzed. Acid initiated samples contained 108 μM β2m and 160 μM ThT. Analysis was started immediately after introduction of β2m into the acidic buffer.

Dynamic Light Scattering. DLS was performed on a Malvern Zetasizer Nano ZSP set in size analysis mode. Data collection was performed at 22 °C. Samples contained 30 μM β2m in 150 mM citrate buffer at pH 3.5 and were analyzed immediately after introduction of β2m into the acidic condition.

Proteolytic Digestion and LC/MS/MS. HNSB labeled β2m samples were digested using chymotrypsin. First, labeled β2m samples were unfolded by 50 mM TEA with 10% ACN at 50°C for 45 min. Next, disulfide bonds were reduced by reaction with TCEP at 37°C for 15 min and cysteine's alkylated by reaction with iodoacetamide at room temperature for 30 min. Immobilized chymotrypsin was then added to yield an enzyme/protein ratio of 1:10 and incubated at 37°C for 3 hours. Digested samples were then centrifuged to separate the digestion enzyme and analyzed by LC/MS/MS. LC separation of the digests were performed on a C18 reverse phase column using water and ACN as mobile phases with a gradient from 1% ACN to 99% ACN over 80 min.

Data Fitting. HNSB labeling curves were fit with the exponential equation: $Y = Y_0 + Ae^{k_0 x}$. Where Y_0 is the asymptotic limit, k is the rate, A is a pre-exponential factor, and x is time.

Activation Energy Calculations. The Arrhenius equation of the form $\ln k_r = \ln A - \frac{E_a}{RT}$ was used to determine the activation energy (E_a) from the rates of Trp60 burial at different temperatures. k_r is the Trp60 burial rate, A is the Arrhenius preexponential factor, R is the gas constant, and T is the temperature. The Eyring equation of the form $k_r = \kappa e^2 B e^{\frac{\Delta S}{R}} e^{-\frac{E_a}{RT}}$ was used to relate activation energy (E_a) to activation entropy (ΔS) where $B = \frac{kT}{h}\frac{RT}{p^\circ}$. κ and p° are each taken to be 1, as is the most common form, and h is Planck's constant.

2.3 Results and Discussion

Upon adding Cu(II),[19,21] the extent of β2m labeling by HNSB decreases over time before leveling off at around 30 min (Figure 2.3). The labeling decrease and leveling off is consistent with Trp60 being partially, but not fully, buried as Cu(II) causes the CTI of Pro32.[13] β2m has two Trp residues, Trp60 and Trp95, but because Trp95 is more buried, >90% of the HNSB labeling occurs at Trp60, as determined by proteolysis and LC-MS/MS (Figure 2.4). Due to the low amount of labeling and lack of labeling change on Trp95, changes in total Trp labeling in the protein can be used to measure the burial of Trp60.

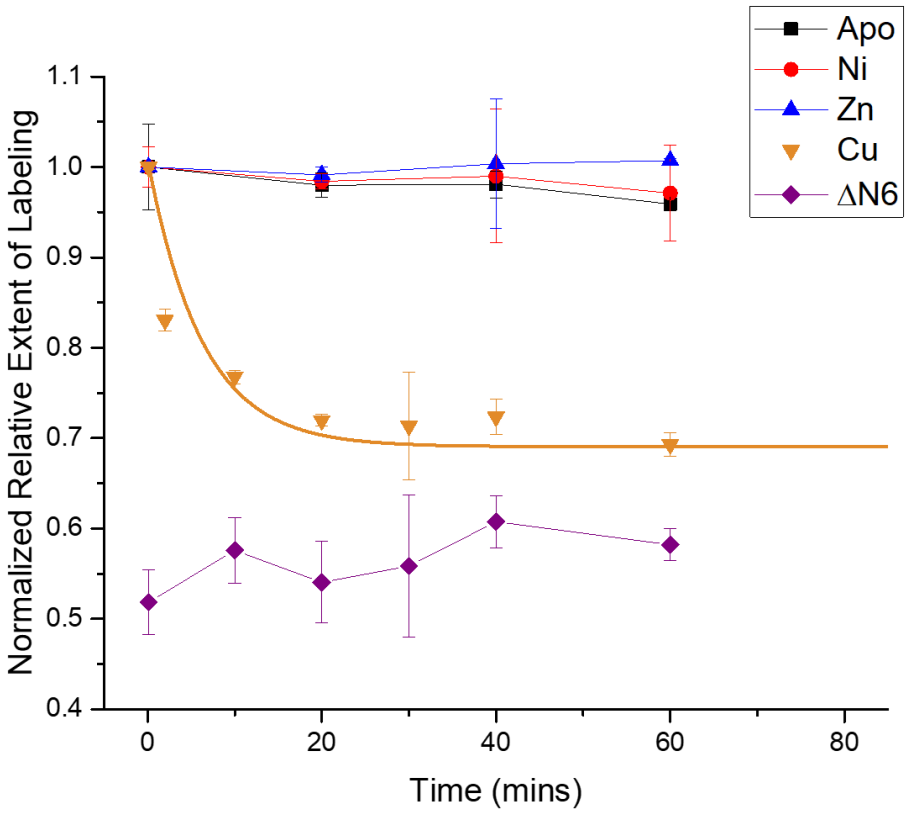

Figure 2.3: The rate of Trp burial under different conditions as determined by HNSB Trp labeling. Cu(II) induces the structural change leading to Trp60 burial while Ni and Zn do not. ΔN6-β2m reacts with HNSB to a lesser extent than wild-type β2m because Trp60 is more buried in that construct. Experiments were performed at 22 °C with 75 μM β2m in 25 mM MOPS and 150 mM potassium acetate at pH 7.

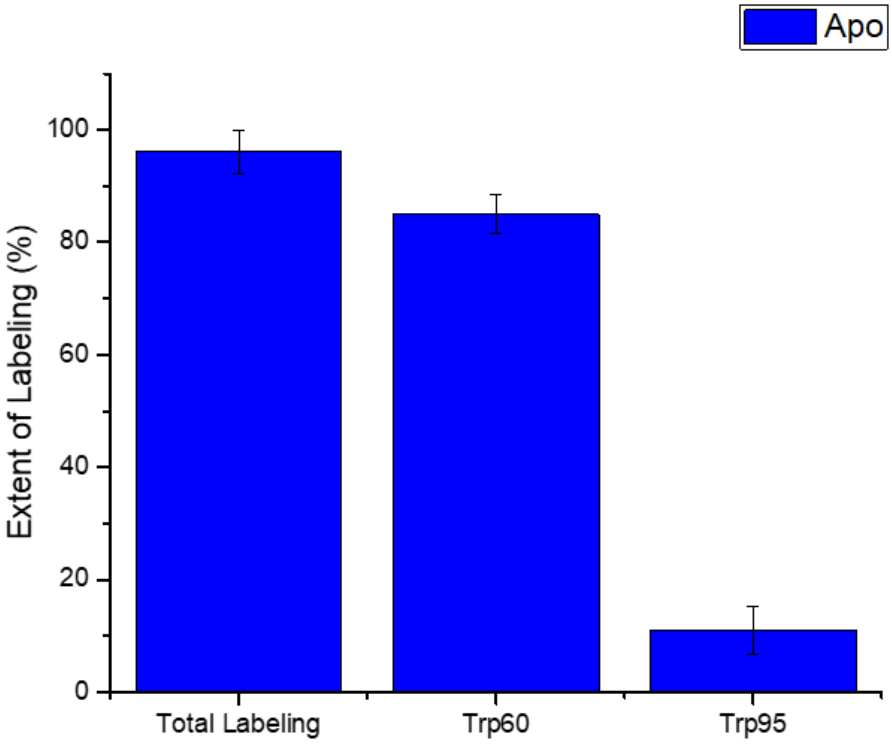

Figure 2.4: Extent of HNSB labeling from proteolytic digestion followed by LC-MS/MS of β2m, indicating total labeling and labeling at Trp60 from measured peptide Asp59-Tyr63 and labeling at Trp95 from measured peptides Trp95-97 and Trp95-Met99.

Without Cu(II), β2m demonstrates no change in Trp60 exposure over more than 6 h. As a control, the truncated β2m species, ΔN6- β2m, which is missing the first six N-terminal residues and has a *trans* Pro32 and thus a more buried Trp60,[17,18] was also reacted with HNSB. As expected, its reactivity is lower than wild type β2m and does not change significantly over time (Figure 2.3). To ensure that metal binding itself does not affect the HNSB labeling reaction, β2m was incubated with Ni(II) and Zn(II), which do not promote amyloidogenesis.[25] Trp labeling extents are similar to the metal-free protein, consistent with no Trp burial over time. Together, these data show that HNSB can be used to monitor Trp60 burial that coincides with Pro32 CTI.

From a fit of the Cu(II) data in Figure 2.3 using $Y = Y_0 + Ae^{k_0 x}$, a Trp60 burial rate of 0.16 ± 0.06 min^{-1} is determined. This burial rate is about the same when 500 mM

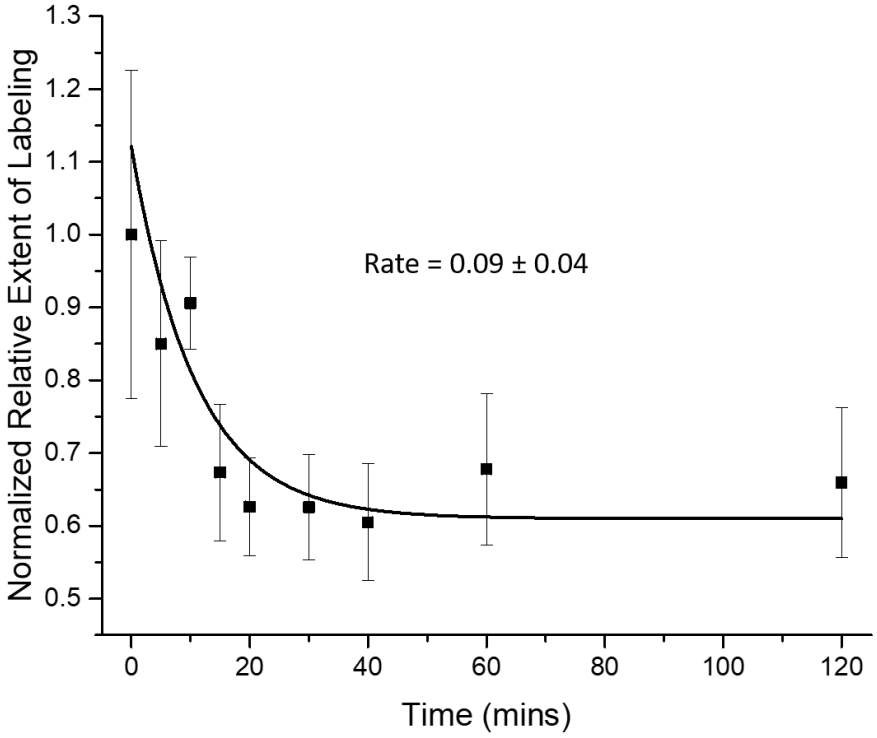

Figure 2.5: Extent of HNSB labeling on β2m when incubated with Cu(II) and 500 mM urea over a 120 min period.

urea is added with Cu(II) (Figure 2.5). This is important as 500 mM urea is often added during β2m amyloid formation reactions to mimic uremia in dialysis patients and is known to accelerate β2m amyloid formation *in vitro*,[8–11,21,24,26] so its small effect on the Trp60 burial rate likely indicates an effect later in the amyloidogenesis pathway. Because Trp60 burial is an essential part of the structural change, we propose that the rate of Trp60 burial is a good proxy of the rate of this amyloidogenic switch.[12–16] Consistent with the idea that Trp60 burial is an indicator of the amyloidogenic structural change is the fact that thioflavin T (ThT) data indicate amyloid oligomer formation is on a time scale that is slightly longer than the decrease in Trp60 labeling upon Cu(II) addition (Figure 2.6). A change in ThT fluorescence is a well-known indicator of protein amyloid formation in solution,[27] yet several studies have shown that ThT's fluorescence changes as β2m

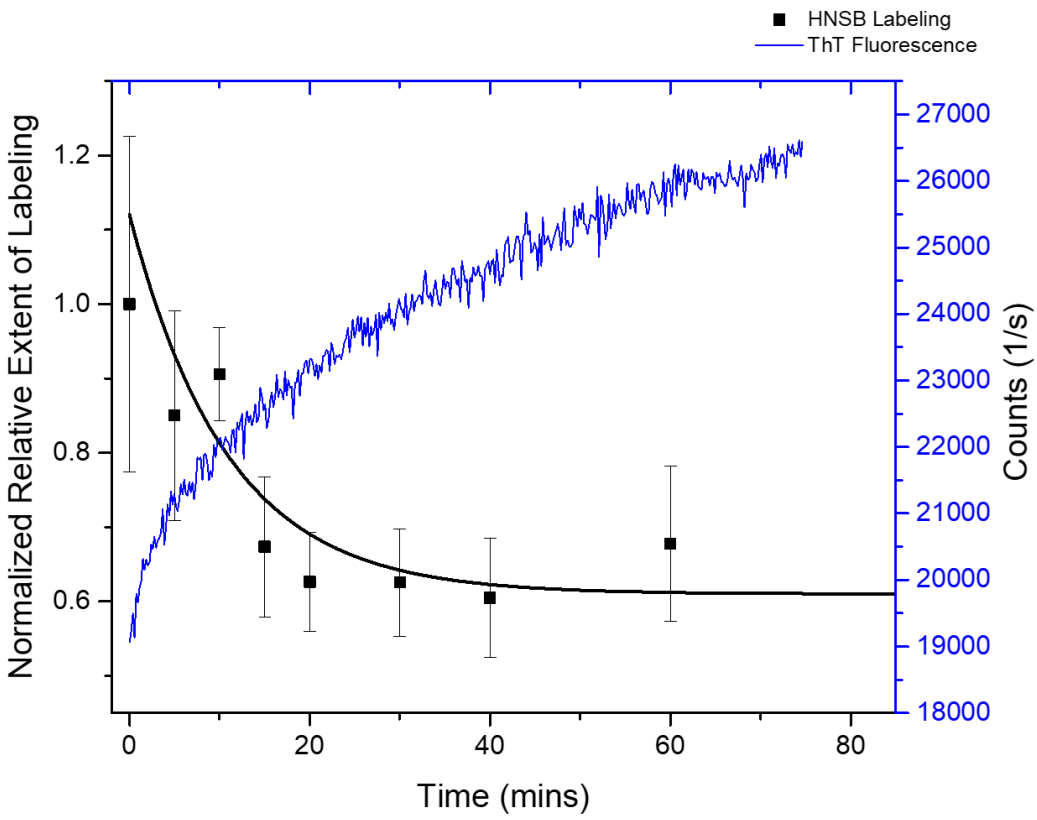

Figure 2.6: Comparison of HNSB Trp labeling data with ThT fluorescence data at 22 °C when incubated with Cu(II) and 500 mM urea.

oligomers form.[20,28,29] β2m oligomers should form after the amyloidogenic structural change has occurred,[10,12–16] and the rate of oligomer formation as revealed by ThT fluorescence (Figure 2.6) is 0.03 min^{-1} at 22°C, which, as expected, is slower than the rate of the amyloidogenic structural change in the presence of Cu(II) at 22°C.

HNSB labeling was also utilized to monitor the structural change initiated by 20% TFE (Figure 2.7) and acid at pH 3.5 (Figure 2.8).[8–11,30] There are stark differences in Trp labeling profiles as compared to initiation with Cu(II). With TFE, there is a 40-min lag period before Trp labeling decreases, resulting in a Trp60 burial rate of 0.013 ± 0.003 min^{-1}. The reason(s) for the lag period is unclear, but it is likely due to some conformational

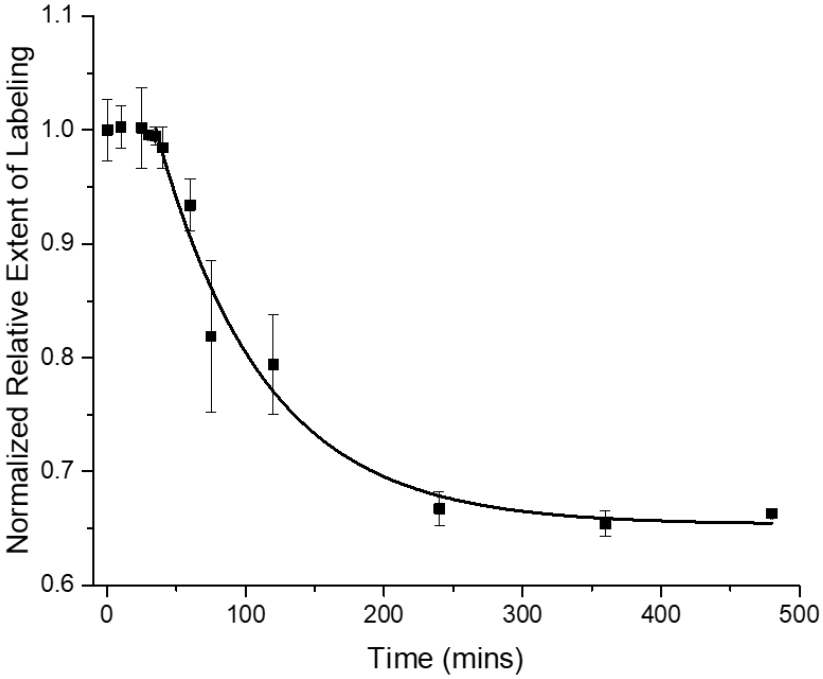

Figure 2.7: Trp burial in β2m using HNSB in the presence of 20% TFE at 22 °C. Data were fit after the 40-min lag period, giving a rate of 0.013 ± 0.003 min^{-1}. Experiments were conducted with 75 μM β2m in 25 mM MOPS and 150 mM potassium acetate at pH 7.4.

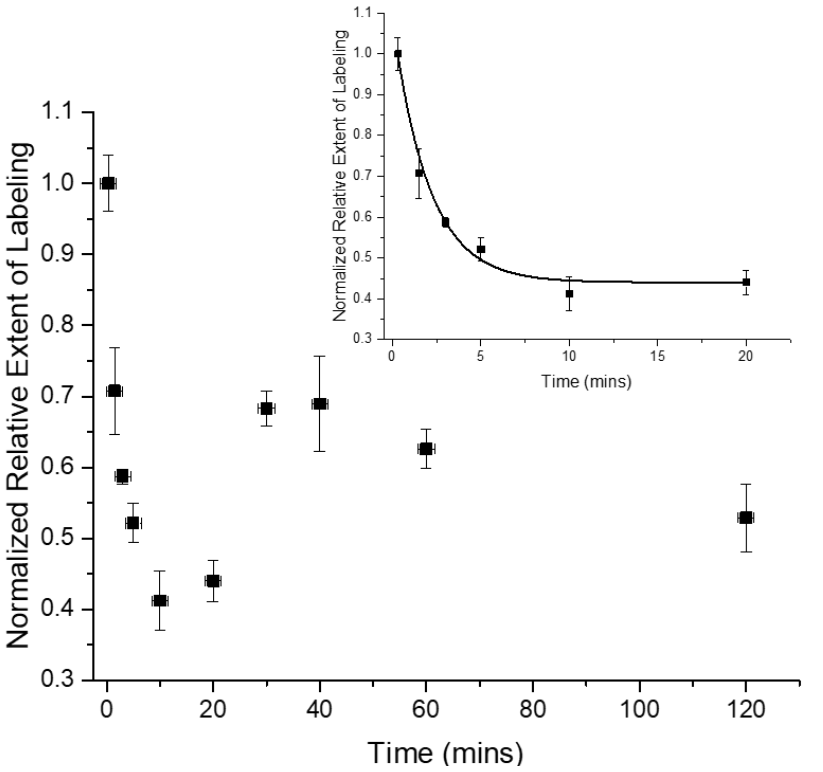

Figure 2.8: HNSB labeling of β2m at pH 3.5 (citrate buffer) at 22 °C. The initial decrease is due to Trp60 burial, but the sudden increase at 30 min is due to a structural change that causes the exposure and labeling of Trp95 (see Figure 2.9). Data were fit from 0-20 min (inset), giving a rate of 0.49 ± 0.05 min^{-1}.

change that needs to occur before the CTI of Pro32 can proceed, as the time scale of the lag is too long to be due to TFE-related solvent effects.[31–33] DLS measurements and ThT fluorescence show no oligomerization for up to 24 h after TFE addition, indicating that the structural change occurs long before aggregation. These data are the first evidence of TFE causing the β2m amyloidogenic structural change that is known to occur with Cu(II) and acid.

Trp labeling has a distinct profile when amyloid formation is initiated at pH 3.5 with a sharp decrease over about 20 min before undergoing a slight increase until around

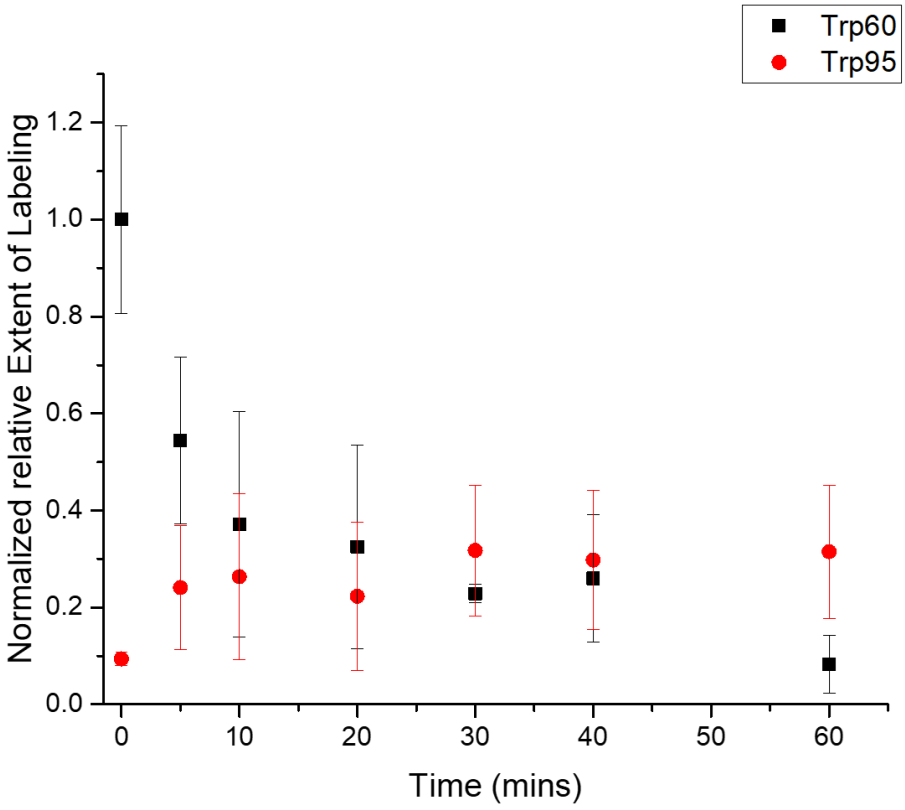

Figure 2.9: Extent of HNSB labeling on Trp60 and Trp95 over time after initiation with acid at pH 3.5. These data were obtained from proteolytic digestion followed by LC-MS/MS analysis of β2m. Trp labeling at Trp60 is an average of the values from the following measured peptides Ser55-Trp60, Ser57-Trp60, Ser57-Phe62, and Ser57-Tyr63, and labeling at Trp95 is an average of the values from the following measured peptides Ser88-Trp95, Val93-Met99, and Lys94-Met99. The error bars represent one standard deviation.

40 min when it levels off and then decreases again (Figure 2.8). This labeling profile is due to both structural and oligomeric changes in β2m. Proteolytic digestion followed by LC-MS/MS analyses indicate that this is a special case in which Trp60 labeling decreases steadily after the addition of acid, due to the amyloidogenic conformational change, while Trp95 labeling increases (Figure 2.9). Trp95 is relatively unreactive with HNSB, but over time at pH 3.5, the protein evidently unfolds to expose Trp95, leading to increased reactivity. The decrease in Trp60 labeling is on a comparable time scale with β2m oligomerization, as indicated by DLS and ThT measurements (Figure 2.10), again showing that Trp60 labeling probes the formation of the amyloid competent state that precedes oligomer formation. To determine the rate of the structural change, the labeling results were

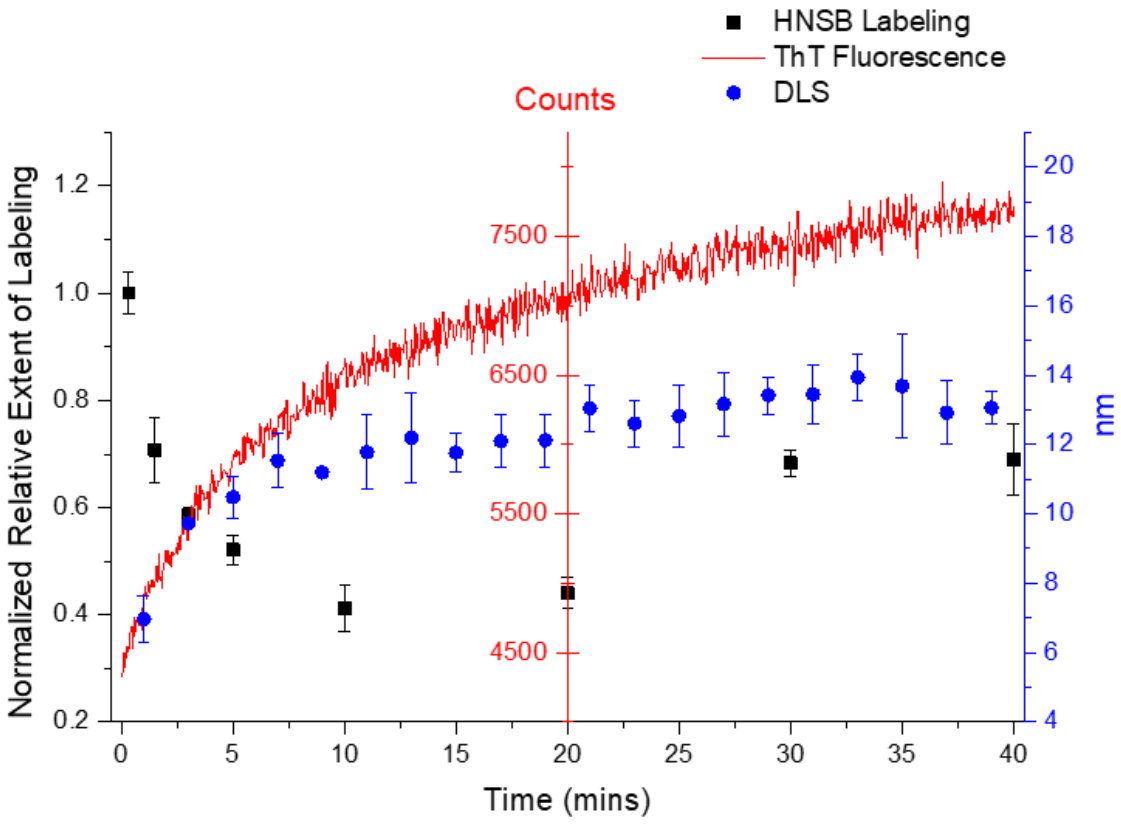

Figure 2.10: Comparison of CL-MS data with ThT fluorescence and DLS data during the pre-amyloid structural change. All experiments were conducted with 75 μM β2m at pH 3.5.

fit for the first 20 min, giving a rate of 0.49 ± 0.05 min^{-1} at 22 °C. For comparison, the oligomerization rates as indicated by ThT fluorescence and DLS changes (Figure 2.10) are 0.085 ± 0.001 min^{-1} and 0.08 ± 0.01 min^{-1}, respectively. These measurements are consistent with oligomerization occurring after the pre-amyloid structural change.

Activation barriers for the amyloidogenic structural change were determined by measuring the Trp60 burial rates at different temperatures. As an example, Figure 2.11 shows a comparison of Trp labeling in the presence of Cu(II) at 22°C and 37°C. At 37°C, the structural change occurs somewhat faster (0.21 ± 0.06 min^{-1} vs. 0.16 ± 0.06 min^{-1}). The Arrhenius Equation (Equation 2.1) was used to determine the activation energy barrier and

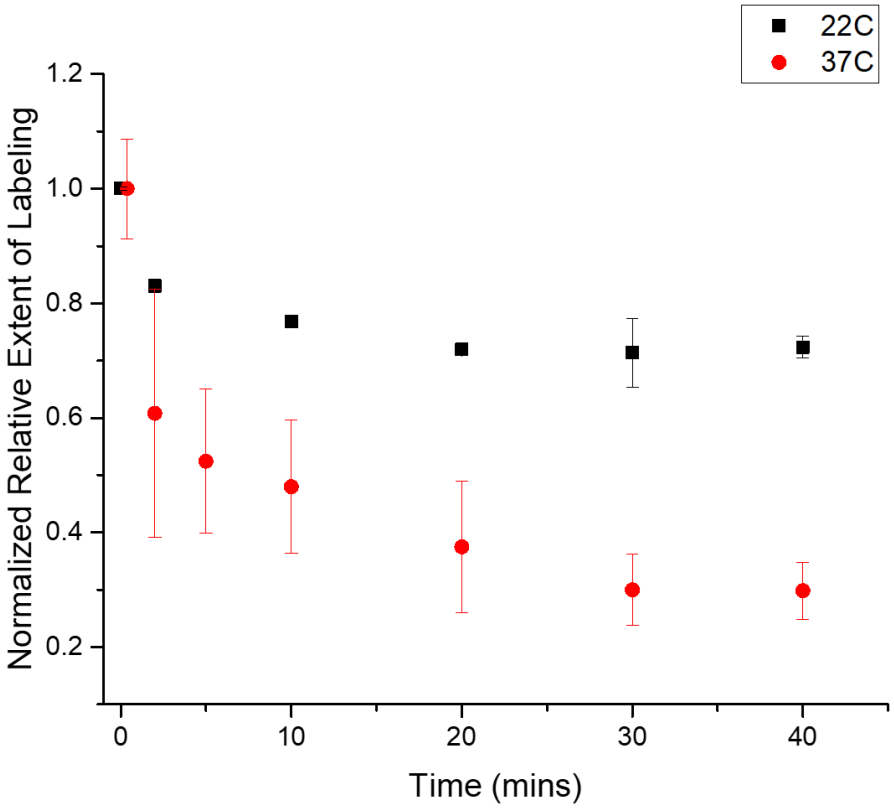

Figure 2.11: Comparison of the rate of Trp burial at 22 °C and 37 °C for Cu(II) initiated amyloid reaction. The normalized relative extent of labeling reaches a lower value at 37 °C primarily because the labeling reaction with HNSB is more extensive at this higher temperature.

the preexponential factor and the Eyring Equation (Equation 2.2) were used to relate the activation energy to the activation entropy of this reaction (Table 2.1).

Equation 2.1 $$\ln k_r = \ln A - \frac{E_a}{RT}$$

Equation 2.2 $$k_r = \kappa e^2 B e^{\frac{\Delta S}{R}} e^{-\frac{E_a}{RT}}$$

Of the conditions tested, the structural change in the presence of Cu(II) has the lowest activation energy and preexponential factor. The addition of urea with Cu(II) has little effect on the activation energy. In the presence of 20% TFE, the activation energy is higher and the frequency factor is several orders of magnitude higher. Despite acid causing the highest rate of Trp60 burial at 37 °C, the determined energy barrier is the highest of the

Condition	Temp (°C)	Rate (min^{-1})	E_a (kJ/mol)	Log(A) (min^{-1})	ΔS (J/K·mol)‡
Cu(II)	37	0.21 ± 0.06	15 ± 2	1.78 ± 0.02	-185.0 ± 0.4
	22	0.16 ± 0.06			
	12	0.12 ± 0.08			
Cu(II) w/Urea	37	0.11 ± 0.04	10.7 ± 0.7	0.846 ± 0.006	-202.9 ± 0.3
	22	0.09 ± 0.04			
	12	0.08 ± 0.06			
TFE	37	0.04 ± 0.01	57 ± 3	8.18 ± 0.02	-62.8 ± 0.4
	30*	0.03 ± 0.01			
	22**	0.013 ± 0.003			
Acid	37	5 ± 2	120 ± 10	21.3 ± 0.1	188 ± 2
	30	2 ± 1			
	22	0.49 ± 0.05			

Table 2.1: Rates of Trp60 burial, activation energy barriers (E_a), pre-exponential factors (A), and activation entropies (ΔS) for each amyloid formation condition.

*A lag of ~10 mins is seen prior to Trp60 burial. ** A lag of ~40 mins is seen prior to Trp60 burial.
‡The Eyring equation was used to relate E_a and ΔS.

three conditions. The high frequency factor associated with the structural change at pH 3.5 explains the apparent disconnect. Clearly, the acid-induced amyloidogenic structural change is very sensitive to temperature. Indeed, at 37 °C in acid, visual evidence for the formation of amyloid fibrils occurs within a week, but at 4 °C in acid, no fibrils are observed for over a year.

CTIs of Pro residues have energy barriers typically ranging between 60 and 100 kJ/mol in peptides and refolding proteins, depending on sequence and other effects.[34–37] His residues on the N-terminal side of Pro residues, as is the case in β2m, usually reduce Pro CTI barriers,[38] which likely means the barrier of wild-type β2m is lower than average. Our measurements indicate that Cu(II) binding leads to an energy barrier for the β2m pre-amyloid structural change that is much lower than typical CTI values for Pro, suggesting that Cu(II) binding reduces the Pro32 CTI barrier substantially. Metal cations are known to catalyze Pro CTI.[39,40] Cu(II) binding at His31 in β2m[19,41,42] presumably accelerates CTI at His31-Pro32 because the measured barrier for the conformational change is quite low. Given the low measured barrier, His31-Pro32 CTI is likely the rate-determining step for the pre-amyloid structural change in the presence of Cu(II). The measured energy barrier with TFE is slightly below typical Pro CTI barriers, suggesting that TFE may be influencing the Pro32 CTI barrier to a small extent. Hydrogen bonds donated by solvents are known to stabilize both the *cis* and *trans* isomers of Pro, increasing the barrier to isomerization.[43] The disrupted hydrogen bonding caused by TFE may have the opposite effect, destabilizing both isomers and lowering the barrier to Pro32 CTI.

Interestingly, the measured barrier at pH 3.5 is much higher than the typical Pro CTI activation barriers, even though acid is known to decrease Pro CTI barriers,

particularly in cases where His precedes the prolyl bond.[38] This high barrier for the amyloidogenic structural change suggests that His31-Pro32 CTI is not the rate-determining step for the pre-amyloid structural change in the presence of acid. Very likely another conformational change must occur in addition to His31-Pro32 CTI for β2m to proceed to form amyloids at pH 3.5. Acidic conditions also give a significantly higher preexponential factor than the other conditions, which is likely due to the protein rapidly fluctuating between several partially structured and unfolded states,[44] leading to increased conformational heterogeneity and an increased statistical probability of adopting the higher energy transition state. In contrast, the preexponential factor with Cu(II) is much lower, which can be rationalized by the tight transition state that is almost certainly imposed by Cu(II) coordination to the N-terminal amine, the Ile1-Gln2 backbone amide, His31, and Asp59,[19,40] which span a significant portion of the protein sequence. It is remarkable that β2m is capable of forming amyloid fibrils under conditions that have such distinct effects on the structure of the monomer.

2.4 Conclusions

To our knowledge, the results described here represent the first-ever measurements of energetic barriers for the structural change that initiates protein amyloid formation. These measurements yield new biochemical insight, specifically for β2m. Such measurements have great potential for further elucidating the mechanistic details of β2m amyloid formation. In future work, we will measure the activation barriers for various mutants of β2m as a means of revealing the specific structural features that control the pre-amyloid structural change. One could also envision using the Trp labeling reaction to screen for molecules that prevent the pre-amyloid structural change. More generally

speaking, because protein amyloidosis is typically triggered by large structural changes, CL-MS should be useful for measuring unfolding barriers for other amyloid systems where the burial or exposure of specific residues can be monitored over time to yield kinetic and energetic information.

2.5 References

1. Rochet, J. & Lansbury, P. T. J. Amyloid fibrillogenesis: themes and variations. *Curr. Opin. Struct. Biol.* **10**, 60–68 (2000).
2. Chiti, F. & Dobson, C. M. Protein Misfolding, Functional Amyloid, and Human Disease. *Annu. Rev. Biochem.* **75**, 333–366 (2006).
3. Cohen, S. I. A., Vendruscolo, M., Dobson, C. M. & Knowles, T. P. J. From macroscopic measurements to microscopic mechanisms of protein aggregation. *J. Mol. Biol.* **421**, 160–171 (2012).
4. Cohen, S. I. A. *et al.* Distinct thermodynamic signatures of oligomer generation in the aggregation of the amyloid-β peptide. *Nat. Chem.* **10**, 523–531 (2018).
5. Hellstrand, E., Boland, B., Walsh, D. M. & Linse, S. Amyloid β-protein aggregation produces highly reproducible kinetic data and occurs by a two-phase process. *ACS Chem. Neurosci.* **1**, 13–18 (2010).
6. Cohen, S. I. A. *et al.* Nucleated polymerization with secondary pathways. I. Time evolution of the principal moments. *J. Chem. Phys.* **135**, 1–44 (2011).
7. Gejyo, F. *et al.* β2-microglobulin: a new form of amyloid protein associated with chronic hemodialysis. *Kidney Int* **30**, 385–390 (1986).
8. Morgan, C. J., Gelfand, M., Atreya, C. & Miranker, A. D. Kidney dialysis-associated amyloidosis: a molecular role for copper in fiber formation. *J. Mol. Biol.* **309**, 339–45 (2001).
9. McParland, V. J. *et al.* Partially Unfolded States of β2-Microglobulin and Amyloid Formation in Vitro. *Biochemistry* **39**, 8735–8746 (2000).
10. Eichner, T., Kalverda, A. P., Thompson, G. S., Homans, S. W. & Radford, S. E. Conformational Conversion during Amyloid Formation at Atomic Resolution. *Mol. Cell* **41**, 161–172 (2011).
11. Stoppini, M. & Bellotti, V. Systemic amyloidosis: Lessons from β2-microglobulin. *J. Biol. Chem.* **290**, 9951–9958 (2015).
12. Jahn, T. R., Parker, M. J., Homans, S. W. & Radford, S. E. Amyloid formation under physiological conditions proceeds via a native-like folding intermediate. *Nat. Struct. Mol. Biol.* **13**, 195–201 (2006).

13. Eakin, C. M., Berman, A. J. & Miranker, A. D. A native to amyloidogenic transition regulated by a backbone trigger. *Nat. Struct. Mol. Biol.* **13**, 202–208 (2006).

14. Eichner, T. & Radford, S. E. A Generic Mechanism of β2-Microglobulin Amyloid Assembly at Neutral pH Involving a Specific Proline Switch. *J. Mol. Biol.* **386**, 1312–1326 (2009).

15. Torbeev, V. Y. & Hilvert, D. Both the cis-trans equilibrium and isomerization dynamics of a single proline amide modulate β2-microglobulin amyloid assembly. *Proc. Natl. Acad. Sci.* **110**, 20051–20056 (2013).

16. Esposito, G. *et al.* The Controlling Roles of Trp60 and Trp95 in β2-Microglobulin Function, Folding and Amyloid Aggregation Properties. *J. Mol. Biol.* **378**, 887–897 (2008).

17. Esposito, G. *et al.* Removal of the N-terminal hexapeptide from human β2-microglobulin facilitates protein aggregation and fibril formation. *Protein Sci.* **9**, 831–845 (2000).

18. Cornwell, O., Radford, S. E., Ashcroft, A. E. & Ault, J. R. Comparing Hydrogen Deuterium Exchange and Fast Photochemical Oxidation of Proteins: a Structural Characterisation of Wild-Type and ΔN6 β2-Microglobulin. *J. Am. Soc. Mass Spectrom.* **29**, 2413–2426 (2018).

19. Srikanth, R., Mendoza, V. L., Bridgewater, J. D., Zhang, G. & Vachet, R. W. Copper Binding to β-2-Microglobulin and its Pre-Amyloid Oligomers. *Biochemistry* **48**, 9871–9881 (2009).

20. Calabrese, M. F. & Miranker, A. D. Metal binding sheds light on mechanisms of amyloid assembly. *Prion* **3**, 1–4 (2009).

21. Antwi, K. *et al.* Cu (II) organizes β-2-microglobulin oligomers but is released upon amyloid formation. *Protein Sci.* **17**, 748–759 (2008).

22. Mendoza, V. L. & Vachet, R. W. Probing Protein Structure by Amino Acid-Specific Covalent Labeling and Mass Spectrometry. *Mass Spectrom. Rev.* **28**, 785–815 (2009).

23. Limpikirati, P., Liu, T. & Vachet, R. W. Covalent labeling-mass spectrometry with non-specific reagents for studying protein structure and interactions. *Methods* **144**, 79–93 (2018).

24. Eakin, C. M., Knight, J. D., Morgan, C. J., Gelfand, M. A. & Miranker, A. D. Formation of a copper specific binding site in non-native states of β-2-microglobulin. *Biochemistry* **41**, 10646–10656 (2002).

25. Dong, J. *et al.* Unique Effect of Cu(II) in the Metal-Induced Amyloid Formation of β-2-Microglobulin. *Biochemistry* **53**, 1263–1274 (2014).

26. Mendoza, V. L., Antwi, K., Barón-rodríguez, M. A., Blanco, C. & Vachet, R. W. Structure of the Pre-amyloid Dimer of β-2-microglobulin from Covalent Labeling and Mass Spectrometry. *Biochemistry* **49**, 1522–1532 (2010).

27. Naiki, H., Higuchi, K., Hosokawa, M. & Takeda, T. Fluorometric determination of amyloid fibrils in vitro using the fluorescent dye, thioflavine T. *Anal. Biochem.* **177**, 244–249 (1989).

28. Wolfe, L. S. *et al.* Protein-induced photophysical changes to the amyloid indicator dye thioflavin T. *Proc. Natl. Acad. Sci.* **107**, 16863–16868 (2010).

29. Eakin, C. M., Attenello, F. J., Morgan, C. J. & Miranker, A. D. Oligomeric assembly of native-like precursors precedes amyloid formation by β-2 microglobulin. *Biochemistry* **43**, 7808–7815 (2004).

30. Heegaard, N. H. H., Sen, J. W., Kaarsholm, N. C. & Nissen, M. H. Conformational Intermediate of the Amyloidogenic Protein β2-Microglobulin at Neutral pH. *J. Biol. Chem.* **276**, 32657–32662 (2001).

31. Takamuku, T., Kumai, T., Yoshida, K., Otomo, T. & Yamaguchi, T. Structure and dynamics of halogenoethanol-water mixtures studied by large-angle X-ray scattering, small-angle neutron scattering, and NMR relaxation. *J. Phys. Chem. A* **109**, 7667–7676 (2005).

32. Othon, C. M., Kwon, O.-H., Lin, M. M. & Zewail, A. H. Solvation in protein (un)folding of melittin tetramer-monomer transition. *Proc. Natl. Acad. Sci.* **106**, 12593–12598 (2009).

33. Hong, D. P., Hoshino, M., Kuboi, R. & Goto, Y. Clustering of fluorine-substituted alcohols as a factor responsible for their marked effects on proteins and peptides. *J. Am. Chem. Soc.* **121**, 8427–8433 (1999).

34. *cis-trans Isomerization in Biochemistry*. (Wiley-VCH Verlag GmbH & Co. KGaA, 2006).

35. Yonezawa, Y., Nakata, K., Sakakura, K., Takada, T. & Nakamura, H. Intra- And intermolecular interaction inducing pyramidalization on both sides of a proline dipeptide during isomerization: An ab initio QM/MM molecular dynamics simulation study in explicit water. *J. Am. Chem. Soc.* **131**, 4535–4540 (2009).

36. Craveur, P., Joseph, A. P., Poulain, P., De Brevern, A. G. & Rebehmed, J. Cis-trans isomerization of omega dihedrals in proteins. *Amino Acids* **45**, 279–289 (2013).

37. Kang, Y. K. Ring Flip of Proline Residue via the Transition State with an Envelope Conformation. *J. Phys. Chem. B* **108**, 5463–5465 (2004).

38. Reimer, U., Mokdad, N. El, Schutkowski, M. & Fischer, G. Intramolecular assistance of cis/trans isomerization of the histidine- proline moiety. *Biochemistry* **36**, 13802–13808 (1997).

39. Cox, C., Ferraris, D., Murthy, N. N. & Lectka, T. Copper(II)-catalyzed amide isomerization: Evidence for N-coordination. *J. Am. Chem. Soc.* **118**, 5332–5333 (1996).

40. Gaggelli, E., D'Amelio, N., Gaggelli, N. & Valensin, G. Metal ion effects on the cis/trans isomerization equilibrium of proline in short-chain peptides: a solution NMR study. *Chembiochem* **2**, 524–529 (2001).

41. Calabrese, M. F., Eakin, C. M., Wang, J. M. & Miranker, A. D. A regulatable switch mediates self-association in an immunoglobulin fold. *Nat. Struct. Mol. Biol.* **15**, 965–71 (2008).

42. Lim, J. & Vachet, R. W. Using mass spectrometry to study copper-protein binding under native and non-native conditions: β-2-microglobulin. *Anal. Chem.* **76**, 3498–3504 (2004).

43. Eberhardt, E. S., Loh, S. N., Hinck, A. P. & Raines, R. T. Solvent Effects on the Energetics of Prolyl Peptide Bond Isomerization. *J. Am. Chem. Soc.* **114**, 5437–5439 (1992).

44. Yanagi, K. *et al.* The monomer-seed interaction mechanism in the formation of the β2-microglobulin amyloid fibril clarified by solution NMR techniques. *J. Mol. Biol.* **422**, 390–402 (2012).

CHAPTER 3

PRIMARY AND SECONDARY NUCLEATION MEDIATED PROTEIN-PROTEIN INTERACTIONS FOR INITIATION OF A PRE-AMYLOID STRUCTURAL CHANGE

3.1 Introduction

Amyloid forming protein systems involve complex assembly mechanisms that lead to aggregation and eventual amyloid formation. Due to this complexity, little is still known about the mechanisms and energetics of assembly. Most amyloidogenesis, including that of β-2-microglobulin (β2m), is a nucleation dependent process. Two types of nucleation have been identified in amyloid formation: primary nucleation and secondary nucleation. Primary nucleation occurs when monomeric species interact, causing a changing in structure that leads to aggregation and amyloid formation. A hallmark of primary nucleation is a lag phase after mixing that precedes oligomerization. Secondary nucleation occurs when pre-formed oligomeric species or fibrils are present, allowing free monomers to template from them, causing continued aggregation. Under secondary nucleation, an elimination of the lag phase is seen, allowing the growth phase to proceed immediately. Secondary nucleation is commonly taken advantage of to shorten fibril growth times through the use of oligomeric seeds.[1–11] Amyloid seeds are metastable oligomeric species that are created from pre-formed amyloid fibrils. There are several ways they can be formed from fibrils including sonication, chemically, freeze-thawing, and homogenates of amyloid containing tissue, as well as combinations of techniques. Sonication is the most commonly used method for *in vitro* seed generation.[5–7,11–28] The metastability of amyloid seeds requires their rapid use after formation before they begin to reaggregate into fibrils.

Both primary and secondary nucleation have been identified in several amyloid systems, including amyloid-β (Aβ),[29,30] insulin,[31] islet amyloid polypeptide (IAPP),[32] α-synuclein,[33,34] and carbonic anhydrase.[35] Primary nucleation occurs when monomers dominate in solution, but secondary nucleation occurs when enough aggregates have formed or seeds are added to interact with the monomers. In all such systems, secondary nucleation creates a catalytic feedback that results in amplification of amyloid aggregation. The rate of aggregation for primary nucleation mechanisms depends on monomer concentration, while the rate of aggregation for secondary nucleation mechanisms depends on aggregate or seed concentration.[1] One group has recently determined activation energy barriers to fibril elongation for both primary and secondary nucleated versions of the Aβ amyloid forming process.[4] This work has inspired us to investigate energy barriers to primary and secondary nucleation dependent amyloidosis in β2m.

Primary and secondary nucleation in β2m amyloidogenesis has been investigated previously by the Radford group. For example, under the primary nucleation mechanism, they determined that the addition of certain glycosaminoglycans (GAGs) resulted in spontaneous amyloid growth by stabilizing rare and transient aggregates.[36] Through NMR studies, the Radford group was also able to characterize interactions inhibiting or promoting amyloid formation under primary nucleation by demonstrating that interactions between ΔN6-β2m and human WT β2m creates a productive structural change in WT β2m, while interactions between ΔN6-β2m and murine WT β2m (mβ2m) leads to kinetically trapped dimers.[37] Using ion mobility-MS and electron microscopy, the Radford group showed, that at low pH and under primary nucleation conditions, rapid interconversion between oligomeric species leading to short, curved fibrils that can be stabilized at high

ionic strength.[38] The secondary nucleation mechanism was probed by another comparison between human WT β2m and mβ2m, in which they demonstrated the importance of solubility of the protein and ionic strength of the solution during seeded amyloidosis. Much of the work on this topic has been done using a comparison between primary and secondary nucleation to reveal new information about β2m amyloidosis. Through this comparison they have been able to determine important regions of interaction for fibril formation (e.g. residues 62-70),[7] suggest physiological factors in synovial fluid that stabilize seeds *in vivo*,[18] show that ionic strength and population of different intermediates leads to differing fibril morphology,[40] and how amyloid inhibitors work by binding monomers and diverting them off pathway.[41] The Radford group has also used comparisons of primary and secondary nucleation mechanisms using ΔN6-β2m to demonstrate that *trans* Pro32 is critical to amyloidosis and that ΔN6-β2m can convert WT β2m to an amyloid competent state through transient head-to-head dimers.[10,42] Once aggregation has begun, molecular shedding from fibrils and seeds yield toxic oligomers at pH 6.4, but non-toxic native monomers at pH 7.4.[43] However, even through all this work, many of the molecular interactions occurring during primary and secondary nucleation are not well understood.

In this work, we have focused on primary and secondary nucleation dependent amyloidogenesis between WT β2m and an amyloidogenic variant ΔN6-β2m. ΔN6-β2m is a naturally occurring truncation of β2m missing the first 6 N-terminal amino acids.[44] These 6 amino acids play a key role in preserving the *cis* conformation of the Pro32 in WT β2m. Disruption of the interactions between this N-terminal strand and the His31-Pro32 amide bond, or removal of this six-residue strand, allows for the Pro32 to adopt the *trans* conformation. ΔN6-β2m has a *trans*-locked Pro32 and is naturally amyloidogenic.

Interestingly, not only can ΔN6-β2m spontaneously form amyloids, it has also been shown to interact with WT β2m and induce the pre-amyloid structural change characterized by the *cis-trans* isomerization (CTI) of His31-Pro32, thereby causing amyloidogenesis in WT β2m in a prion-like manner.[45,46] Based on NMR experiments, Karamanos, *et al* have proposed a transient head-to-head interaction between the two proteins that induces the pre-amyloid structural change in the WT.[37] This interaction involves several loops at the 'head' of the proteins, the end of the protein closest to the N-terminus that includes the BC, DE, and FG loops (Figure 3.1). This part of the protein contains not only the important H31 and Pro32 residues, but Trp60 and the N-terminal strand of WT as well. The goal of

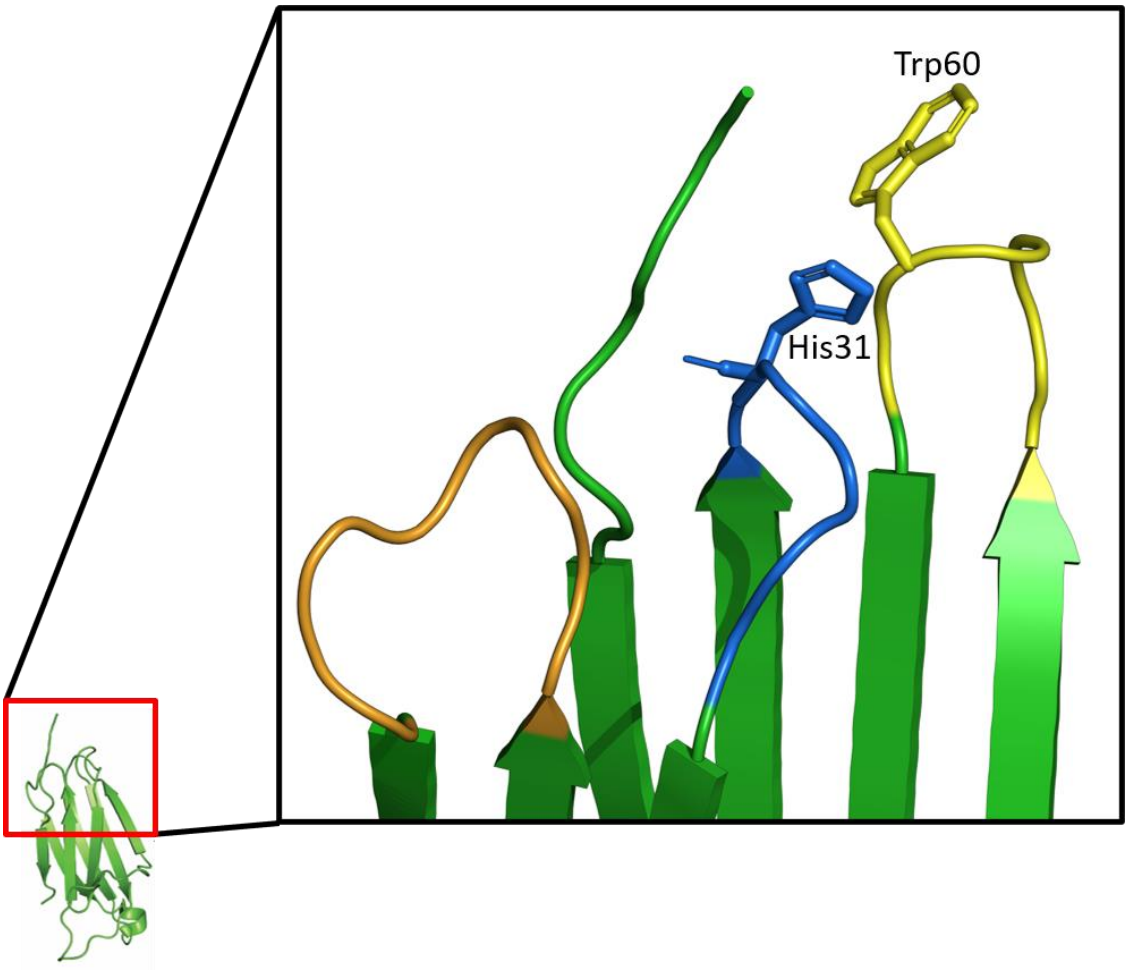

Figure 3.1: The head of the β2m protein comprised of the N-terminus (green strand), the BC loop (blue) including His31, the DE loop (yellow) including Trp60, and the FG loop (orange).

this work is to determine the energy barriers of the primary and secondary nucleation steps of WT β2m as induced by ΔN6-β2m. Further experiments endeavor to determine essential interactions between these two proteins in both the primary and secondary nucleation cases by studying what structural factors influence the CTI rates and energy barriers.

3.2 Experimental

Covalent labeling-mass spectrometry (CL-MS) was used in the same manner as in Chapter 2. The labeling reagent dimethyl(2-hydroxy-5-nitrobenzyl) sulfonium bromide (HNSB) was used to covalently label solvent accessible Trp residues in both WT and ΔN6-β2m. For these experiments, labeling, quenching, and injection were automated. An Agilent 1100 G1367A well plate autosampler was reprogrammed to perform all liquid handling portions of the experiment, from mixing of protein samples, to reacting with HNSB, to quenching with L-Trp, to injection on a desalting column (See Appendix). This setup includes tight temperature control of the samples within the well plate autosampler. Immediately after desalting, samples were analyzed on a Bruker SolariX FT-ICR mass spectrometer.

For primary nucleation experiments, ΔN6-β2m was incubated with WT β2m in a 3:1 (ΔN6:WT) ratio. At different time points, the proteins were reacted with HNSB for 45 seconds. The reaction was then quenched with the addition of L-Trp and the sample immediately desalted and analyzed. This process was repeated at different temperatures of incubation and the data analyzed in the same way as in Chapter 2. These primary nucleation experiments were also performed in the same manner by incubating the H31F mutant of β2m with ΔN6-β2m in the same ratio.

For secondary nucleation experiments, ΔN6-β2m was incubated at 37°C buffered to pH 6.2 until the formation of aggregates that could be seen by eye (usually 5-9 days). Seeds were then generated by sonication of the aggregate for 5 min. Any remaining solid was pelleted at the bottom of the tube by centrifugation and the supernatant removed and filtered with a 0.45 μm syringe filter. It is critical that the resulting amyloid seed solution be used immediately after filtration. The seed solution was then added to monomeric WT β2m at either pH 7.4 or 6.2 for differing incubation times using the same Agilent HPLC setup as the primary nucleation experiments and analyzed in the same way.

The primary nucleation reaction was also monitored by size exclusion chromatography (SEC), dynamic light scattering (DLS), and native MS to observe what, if any, oligomeric species might be present at different points during the reactions and the nature of these oligomeric species. SEC was performed by injection of the reaction mixture onto a size exclusion column at various time points after mixing ΔN6-β2m with WT. DLS was performed by constant measurements of the sample for up to 12 hours at different temperatures. Prior to performing native MS, each sample was rapidly desalted before analysis on a Waters Synapt G2Si.

3.3 Results and Discussion

When ΔN6-β2m and WT β2m are incubated at a 3:1 ratio, Trp labeling with HNSB shows an unexpected increase in labeling on WT before the extent of Trp labeling drops in a manner consistent with previously seen data reflecting CTI of Pro32 (see Chapter 2). The time of this increase in labeling is temperature dependent and likely reflects some other structural rearrangement that must occur during the lag phase prior to the pre-amyloid structural change. For example, the increase in labeling occurs over 1 h at 40°C, 2 h at

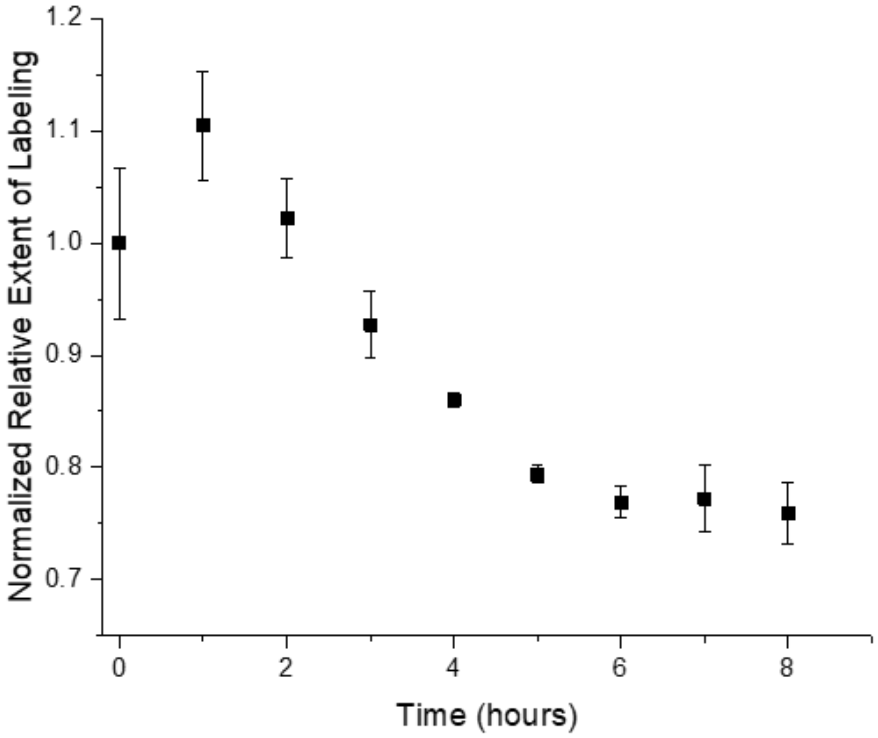

Figure 3.2: Extent of HNSB covalent labeling on wild-type (WT) β2m when incubated with ΔN6-β2m at a 3:1 ratio (ΔN6:WT)

37°C, and 3 h at 35°C. It is unclear what this other structural rearrangement might be, and further experimentation will be needed to ascertain its nature. Trp labeling data were fit from the end of the HNSB labeling rise (beginning of the labeling drop) using the same method as in Chapter 2. At 40°C, this corresponds to a fit from 1 h to 8 h, giving a rate of 0.32 ± 0.06 hr^{-1} or 0.005 ± 0.001 min^{-1} (Figure 3.2). The experiment was repeated at 37°C and 35°C and data fit (after the increase in labeling) in the same manner. The Arrhenius Equation (Equation 3.1) was used to determine the activation energy barrier and the preexponential factor and the Eyring Equation (Equation 3.2) was used to relate the activation energy to the activation entropy of this primary nucleation reaction.

Equation 3.1 $$\ln k_r = \ln A - \frac{E_a}{RT}$$

Equation 3.2

$$k_r = \kappa e^2 B e^{\frac{\Delta S}{R}} e^{-\frac{E_a}{RT}}$$

In comparison to most of the previously measured energy barriers for this *cis-trans* Pro32 isomerization, the ΔN6/WT monomeric coincubation shows a very high barrier of 136 ± 32 kJ/mol (Table 3.1).[47] This barrier is higher than the range that is typically expected from *cis-trans* Pro isomerizations (60-100 kJ/mol).[48–51] The only other condition previously measured that shows similar Arrhenius parameters is the amyloidogenesis of

Condition	Temp (°C)	Rate (min^{-1})	E_a (kJ/mol)	Log(A) (min^{-1})	ΔS (J/K·mol)‡
Cu(II)	37	0.21 ± 0.06	15 ± 2	1.78 ± 0.02	-185.0 ± 0.4
	22	0.16 ± 0.06			
	12	0.12 ± 0.08			
Cu(II) w/Urea	37	0.11 ± 0.04	10.7 ± 0.7	0.846 ± 0.006	-202.9 ± 0.3
	22	0.09 ± 0.04			
	12	0.08 ± 0.06			
TFE	37	0.04 ± 0.01	57 ± 3	8.18 ± 0.02	-62.8 ± 0.4
	30*	0.03 ± 0.01			
	22**	0.013 ± 0.003			
Acid	37	5 ± 2	120 ± 10	21.3 ± 0.1	188 ± 2
	30	2 ± 1			
	22	0.49 ± 0.05			
ΔN6+WT	40	0.005 ± 0.001	136 ± 32	20.4 ± 0.1	171 ± 2
	37	0.004 ± 0.002			
	35	0.002 ± 0.001			
Seeding	40	0.080 ± 0.002	15	1.42	-192.3 ± 0.2
	30	0.066 ± 0.013			

Table 3.2: Rates of Trp60 burial, activation energy barriers (E_a), pre-exponential factors (A), and activation entropies (ΔS) for each amyloid formation condition.
*A lag of ~10 mins is seen prior to Trp60 burial. ** A lag of ~40 mins is seen prior to Trp60 burial. ǂThe Eyring equation was used to relate E_a and ΔS.

WT β2m as induced by acid. We have previously hypothesized that the unexpectedly high energy barrier seen in the acid induced case may indicate that the *cis-trans* Pro32 isomerization is not the rate determining step under those conditions. Due to the similarity in Arrhenius parameters, it is possible that the CTI is also not the rate determining step in the primary nucleation mechanism between ΔN6-β2m and WT β2m. This speculation is supported by the presence of the other structural change preceding the CTI, the nature of which has yet to be determined.

In an effort to determine what oligomeric species might be present during the β2m structural change that is measured, the β2m/ΔN6-β2m sample was also monitored by SEC, DLS, and native MS. The purpose of these experiments was to confirm if monomer-monomer interactions between ΔN6-β2m and WT are responsible for initiating the pre-amyloid structural change or some other stoichiometry of the protein complex. Insight here may also suggest possibilities of the nature of the structural change that occurs before the CTI that gives rise to an increase in Trp labeling. SEC, DLS and native MS reveal that when ΔN6-β2m and WT are incubated together (3:1 ratio) at 40°C, formation of complexes and aggregates is seen more rapidly than expected. By SEC, we see a sudden sharp drop in the area under the curve of all species present, indicating a loss of concentration of the

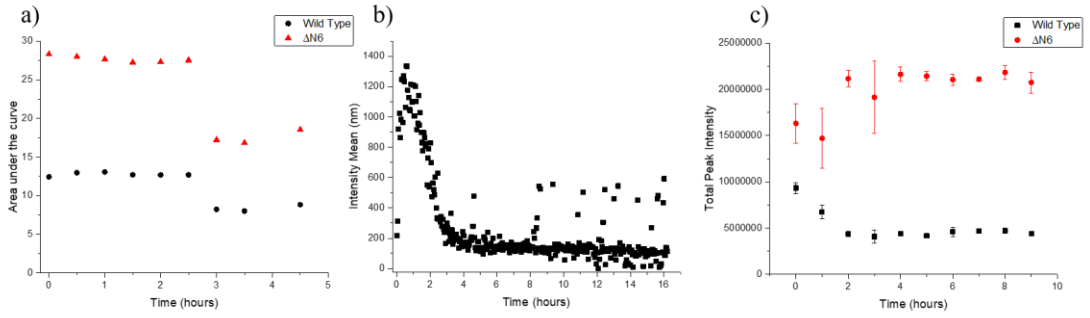

Figure 3.3: Coincubation of ΔN6-β2m and WT β2m at 40°C probed by a) Size exclusion chromatography (SEC) of the monomer peak, b) Dynamic light scattering (DLS), and c) Total ion intensity from ESI mass spectrometry measurements

proteins likely caused by aggregates dropping out of solution (Figure 3.3a). The precipitation of the aggregates coincides in time with the peak of the HNSB labeling data, where it begins to drop in a manner consistent with CTI of Pro32. DLS performed at 40°C shows the rapid evolution of very large aggregate species (up to ~1400 nm) followed by a sudden drop indicative of these large species precipitating out of solution (Figure 3.3b), further supporting what is seen by SEC. These appear to be amorphous aggregates as they are able to be solubilized by sodium dodecyl sulfate (SDS) indicating they may be off-pathway aggregates. Both SEC and DLS show these phenomena in a temperature dependent manner similar to HNSB labeling. The timing of the aggregation and precipitation shown by SEC and DLS shifts to match the timing of the peak and subsequent drop in HNSB labeling at each temperature measured. Additionally, ESI-MS measurements show a drop in total intensity of the WT peaks, at the same time period, further indicating aggregation (Figure 3.3c). The agreement between all these techniques leads us to believe that the formation of these aggregates prior to the amyloidogenic structural change are likely involved in changing the structure of WT β2m in some way, leading to the increase seen in HNSB labeling. Native MS experiments were also done to more closely observe the species that remain soluble in the system. After the drop seen

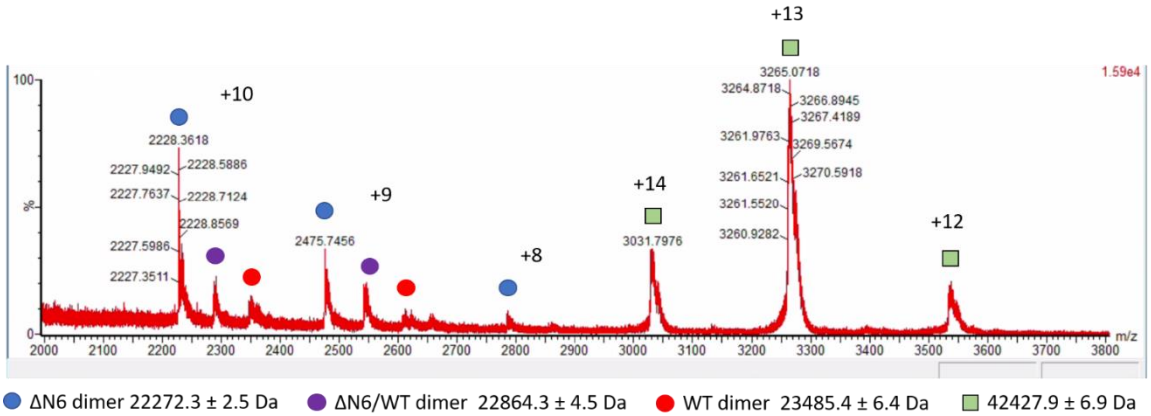

Figure 3.4: Native MS spectrum of a coincubation of ΔN6-β2m and WT β2m showing all three possible dimers, as well as larger, unidentified species.

with the other techniques, native MS shows peaks corresponding to monomeric ΔN6-β2m and monomeric WT β2m, as well as ΔN6-β2m homodimers, WT homodimers and ΔN6/WT heterodimers (Figure 3.4). Larger species were also observed that will require further experimentation to identify. These observations may indicate that the dimers observed or larger species that are observed, including precipitated aggregates, could be involved in the structural changes occurring to monomeric WT β2m. At this time, more experiments are needed to identify these potential interactions.

Other experiments were performed to elucidate some mechanistic information about the interaction between monomeric ΔN6-β2m and WT β2m leading to amyloidogenesis. First, the 40°C coincubation experiment was performed at pH 5, 6.2, and 8. These different solution pHs change the charge on His residues of both proteins (4 in

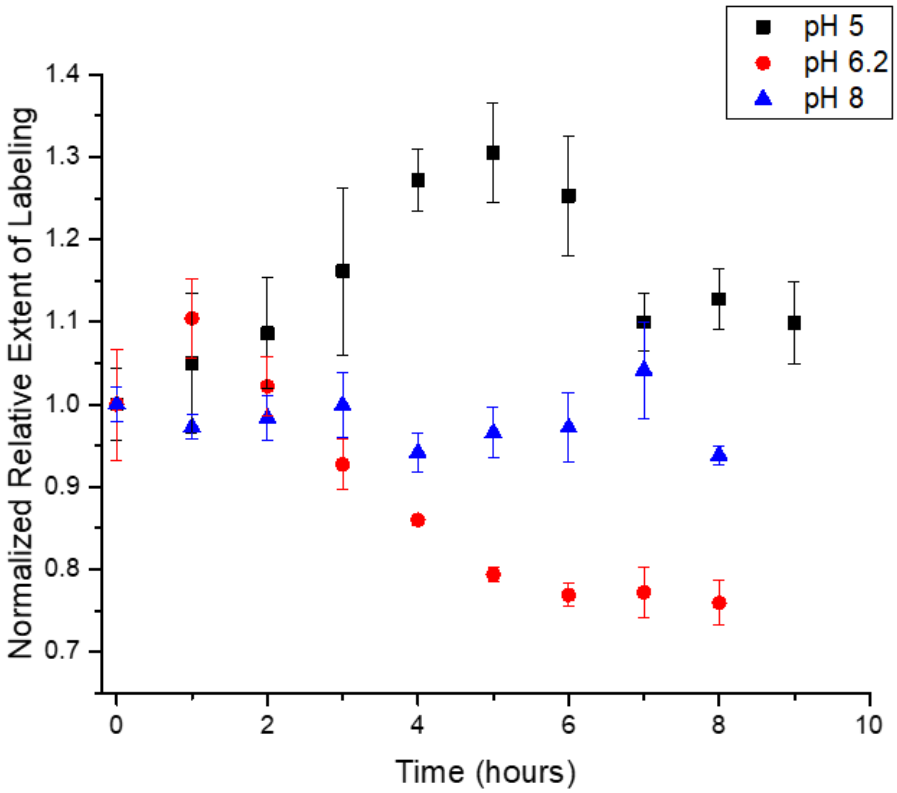

Figure 3.5: Extent of HNSB labeling on WT β2m when incubated at 40°C with ΔN6 at pH 5, 6.2, or 8.

each protein). His31 is an important residue because positively charged His residues on the N-terminal side of Pro residues is known to greatly speed up Pro CTI.[52] His31 is also on the BC loop which is part of the region of the proteins that are proposed to be part of the interaction site and could cause some repulsion when charged (Figure 3.1).[37] His51 is not involved in the pre-amyloid structural change, but may become an important part of the interface between monomer units as oligomers form.[53] As shown in Figure 3.5, at pH 8 there is no decrease in Trp labeling over 8 hours, while a significant decrease is seen at pH 6.2. This lack of labeling change is unsurprising as ΔN6-β2m is known to lose its amyloidogenic properties at pH ≥ 8.[42] Eichner *et al.* show that this is due to a complete suppression of the normally enhanced local dynamics of the BC and DE loops in ΔN6-β2m at pH ≥ 8.[42] At pH 5, when all the His residues will be positively charged, a long drawn-out increase in Trp labeling is seen for 5 hours (compared to 1 hour at pH 6.2). The Trp labeling then begins to drop again, but data needs to be acquired at longer time points to determine the rate of this decrease. The data at different pHs suggest that the potential structural change seen prior to CTI may involve interaction between the two proteins as a longer rise time may indicate some repulsion between key areas of the two proteins.

Targeted point mutations can be valuable to create directed changes to the charge, bulk, or hydrophobicity of certain regions in a protein. To this end, an H31F point mutant of β2m was incubated with ΔN6-β2m at pH 6.2 and 40°C in place of WT. Preliminary data indicate that while the increase in labeling during the lag period appears to be consistent with the WT, the rate of Trp labeling decrease is slightly, but not significantly, reduced when the H31F mutation is present (0.005 ± 0.001 min^{-1} with WT vs ~0.004 min^{-1} with H31F). This similarity in rates is further evidence that the CTI of Pro32 may not be the rate

determining step in the primary nucleation dependent reaction. While the measured rate at 40°C decreases with the H31F mutation, it is not significantly different. If it were the rate determining step, we would expect a significant change in the measured rate.

Amyloid seeding was used to examine the secondary nucleation dependent amyloidogenesis of β2m. Amyloid seeds were generated by sonication from ΔN6-β2m aggregates formed at pH 6.2. HNSB Trp labeling was also used here to monitor the Pro32 CTI of WT β2m when induced by seeds. When seeded at pH 6.2, no decrease in Trp labeling is seen. However, when seeding occurs at pH 7.4, Trp labeling decreases immediately, with the lag phase eliminated (Figure 3.6). From two different temperatures of incubation, we were able to calculate a preliminary energy barrier of ~15 kJ/mol (Table 3.1). More experiments at different temperatures should be performed to get a more

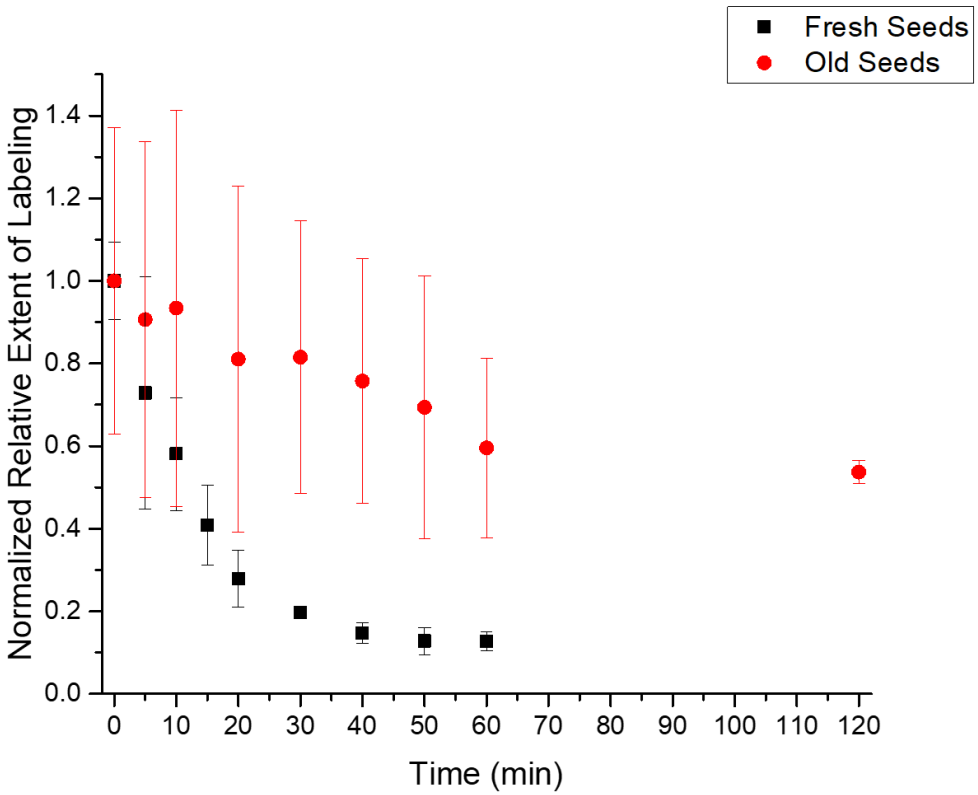

Figure 3.6: Extent of HNSB labeling on WT β2m when incubated with amyloid seeds generated from fresh ΔN6-β2m aggregates or old ΔN6-β2m aggregates.

accurate activation energy. It is important to note that no ΔN6-β2m peaks are observed in the mass spectra for these experiments, indicating that there is no monomer shedding occurring from the ΔN6-β2m seeds. In contrast to the acid induced and ΔN6-β2m induced primary nucleation cases, the Arrhenius parameters of the seed induced pre-amyloid conversion are much more consistent with Pro32 CTI being the rate determining step (as in the Cu(II) and TFE induced cases) (Table 3.1). In fact, the Arrhenius parameters match very closely to those of the Cu(II) induced case, indicating that, like Cu(II), the seeds are substantially lowering the Pro32 CTI barrier and are likely acting in a catalytic manner in the process. The specifics of how these seeds are interacting with β2m monomers has yet to be determined. Also, in contrast to the primary nucleation experiment, the soluble concentration of WT β2m remains constant over the period of the experiment. While pH of seeding seems critical to the amyloidogenic success of the reaction, the age of the aggregates from which the seeds are formed also plays a role. Seeds from 'fresh' aggregate (5-9 days of incubation) show different results from seeds formed from months-old aggregate (Figure 3.6). Seeds formed from older aggregates give a different rate of labeling change as well as a much higher error, perhaps indicating a more dynamic, heterogeneous system.

The seeding reactions were also done with two separate preparations of ΔN6-β2m, expressed and purified by two different people several years apart. One of the preparations contained as yet unidentified impurities. The preparation with the impurities did not yield seeding competent aggregates. This indicates that there may be some interference from these impurities inhibiting the secondary nucleation mechanism. Further investigation will be required to identify these impurities (Figure 3.7).

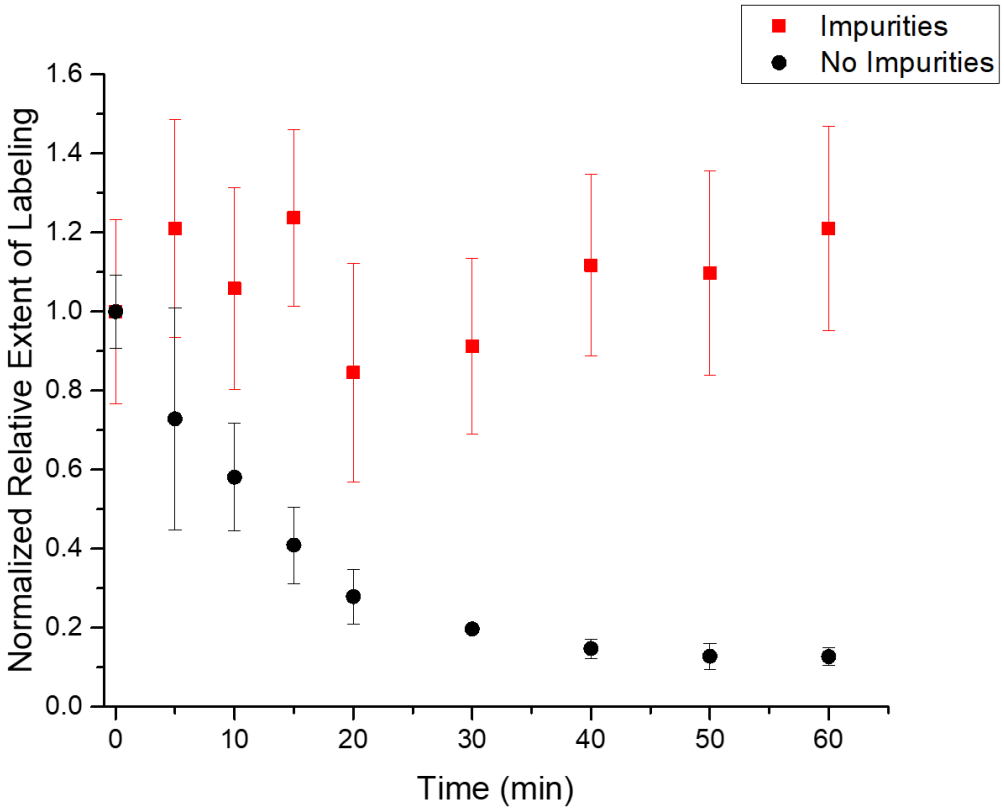

Figure 3.7: Extent of HNSB labeling on WT β2m when incubated with amyloid seeds generated from a ΔN6-β2m preparation with impurities or a ΔN6-β2m preparation without impurities.

As stated previously, the primary (soluble ΔN6-β2m) and secondary (ΔN6-β2m seeds) nucleated conversion of WT β2m show very different activation energy barriers. This difference is expected as seeding is commonly used in amyloid research to speed aggregation. The catalytic way in which seeds interact with monomeric WT β2m drastically lowers the energy barrier to CTI of Pro32. This also has the effect of removing the lag phase that is commonly seen when two monomeric amyloidogenic proteins interact. The results here are consistent with what has been seen for primary and secondary nucleation in the Aβ system. Our measurements differ, however, from what has been reported with the temperature dependence of the Aβ secondary nucleation reaction. Cohen *et al.* have shown that the rate increases with increase in temperature in the primary

nucleation mechanism but decreases with increasing temperature in the secondary nucleation mechanism.[4] Our work shows the rate increasing with increasing temperature for both primary and secondary nucleation. While these are both amyloid forming systems, it should be noted that there are several important differences between how the systems undergo amyloidogenesis. β2m undergoes a distinct conformational change gated by a CTI of Pro, whereas Aβ is not known to have such a conversion. This difference may explain the differences in thermodynamics of the secondary nucleation mechanism. However, as mentioned, β2m does maintain the lag phase in primary nucleation and has no lag phase in secondary nucleation, which is consistent among amyloid systems.

3.4 Conclusions and Future Work

Our work has shown that there are two distinct mechanisms for the induction of the pre-amyloid structural change as initiated by ΔN6-β2m. The primary nucleation mechanism is consistent with primary nucleation in other amyloid systems in terms of thermodynamics and the presence of the lag phase seen before amyloidogenesis. We determined the activation energy barrier of the primary nucleation reaction to be 136 ± 32 kJ/mol. This energy barrier is quite high and out of the range of typical Pro CTIs. This high barrier makes it likely that the CTI of Pro32 is no longer the rate determining step when ΔN6-β2m is used to induce amyloid formation. We have also identified the presence of another structural change that seems to occur causing the CTI of Pro32 to no longer be the rate determining step of the reaction. Future work should be focused on determining what this other structural change is and how it affects the amyloid forming process. Specifically, CL-MS with a more promiscuous reagent and/or hydrogen-deuterium

exchange (HDX)-MS may be needed to uncover what part of the protein's structure is changing.

A large sudden drop in the concentration of the soluble monomeric WT β2m was identified by MS. This concentration drop coincides in time with the rise in HNSB Trp labeling during the lag phase before the drop in labeling associated with the Pro32 CTI. SEC and DLS measurements reveal a rapid aggregation of large species that then precipitate out of solution. Native MS experiments show the quick evolution of all three possible dimer species: the ΔN6-β2m homodimer, the WT β2m homodimer, and the ΔN6/WT heterodimer. Also seen in native MS are larger species that have not yet been identified. Future experiments should focus on identification of the larger species seen and determining which species are involved in inducing the pre-amyloid structural change in the WT. Further native MS experiments, including ion mobility measurements would be useful for identifying these larger species. In addition, after the rapid aggregation, the precipitate and supernatant should be separated from each other and each mixed with fresh monomeric WT β2m to determine if it is truly monomeric ΔN6-β2m inducing the pre-amyloid structural change in the WT or if it is the evolution of the larger species that induces this change.

The charge on each protein was revealed to be critical by changing the pH of the reaction. At pH 8, all amyloidogenicity is lost, consistent with the suppression of enhanced dynamics of the BC and DE loops in ΔN6-β2m resulting in the loss of amyloidogenicity.[42] At pH 5, the lag phase is lengthened, further indicating that this lag phase may be associated with a structural change at the beginning of the ΔN6/WT interaction. At this pH, the His residues in the proteins would be charged, leading to some repulsion between the critical

head regions. Future work should include longer time points at pH 5 to see if, once the Trp labeling begins to drop, there is any change in the rate of Pro32 CTI. It may also be interesting to see what happens to the lag phase at pH 3.5, as WT β2m is known to be amyloidogenic at this pH.

We have also added evidence that the CTI of Pro32 may not be the rate determining step in the primary nucleation mechanism with ΔN6-β2m via studies of the point mutant H31F. Even though H31 has been shown to be important to the CTI of Pro32, its replacement does not drop the rate significantly as it should do for a rate determining CTI of Pro. Future work should repeat the ΔN6/H31F coincubations at different temperatures to elucidate an activation energy barrier for comparison with ΔN6/WT. Other point mutants should also be incubated with ΔN6-β2m to find their mechanistic effects. An H51F mutant would help determine if the species contributing to the induction of the pre-amyloid structural change are indeed monomeric or if they are some larger species because H51 is in a region of the protein involved in oligomerization.[53] If the rate is unaffected by the H51F mutation, that would be more evidence of a true monomer-monomer interaction between ΔN6-β2m and WT β2m. If the rate is greatly reduced by H51F, that may indicate a larger oligomeric species is involved in inducing the pre-amyloid structural change in WT. Another mutation of critical interest is R3A. The charged sidechain guanidinium group of Arg3 points at the H31-P32 bond and has significant electrostatic interactions that help stabilize the Pro32 in the *cis* conformation. Replacement of this Arg3 with an Ala should greatly reduce the energy needed to initiate the CTI. This change would also swap a large sidechain for a much smaller sidechain in the head region of the protein where WT β2m interacts with ΔN6-β2m. Additional mutants of interest are F30A, which would swap

a bulky sidechain for a small side chain in the head region of the protein while remaining hydrophobic and uncharged, and F62A for the same reason, but on a different loop in the head region of the protein. The F30A mutant is interesting because an important step in the cascade of events leading to aggregation of WT β2m when initiated by Cu(II) is the rotation and subsequent exposure of Phe30 out of the hydrophobic core.[54] However, the interaction between WT β2m and ΔN6-β2m stabilizes residues on the BC loop that contains Phe30.[42] Use of the F30A mutant could give insight as to the importance of the Phe30 in the WT β2m/ΔN6-β2m interaction. If this residue is as important to this process as it is to the Cu(II) induced aggregation, there would be a significant change in HNSB labeling. Phe62 is on the more dynamic DE loop which is implicated in the interaction between WT β2m and ΔN6-β2m.[42] If the reduction in bulk on this loop in the F62A mutant allows for increased interaction between WT β2m and ΔN6-β2m, it would result in a higher measured Pro32 CTI rate for this process. The use of these two point mutants would be helpful for investigating these necessary molecular interactions during the ΔN6-β2m initiated amyloidosis of WT β2m while controlling for charge and hydrophobicity.

The secondary nucleation mechanism is consistent with secondary nucleation in other amyloid systems in that the lag phase does not occur. The pre-amyloid structural change occurs directly and without any evidence of other structural changes happening first. The interaction between amyloid seeds and monomeric WT β2m appears catalytic in nature and greatly reduces the activation energy barrier. The activation barrier falls into a range that would indicate that, in contrast to the primary nucleation mechanism, the Pro32 CTI is the rate determining step. Charge is again critical here as seeding competency is removed when the pH is raised from 6.2 to 7.4. This pH effect may indicate that, while

charge on His residues is a hindrance in the primary nucleation reaction, charged His residues are required for the interaction between monomers and seeds. Future experiments should include a wider range of pHs to better understand this phenomenon. The 'freshness' of the seeds is also important as the rate changes when older seeds are used. Further work is needed to ascertain why this is the case. Finally, the seeding solutions are likely composed of a distribution of differently sized species. SEC, DLS, or ion mobility experiments are needed here to better characterize the species involved in inducing the pre-amyloid structural change.

Of two ΔN6-β2m preparations used, one contained impurities that appeared to hinder seeding. These impurities do not seem to inhibit the primary nucleation mechanism, but only the secondary nucleation mechanism. When these impurities are present, the ability for the seeds to induce the pre-amyloid structural change in monomeric WT β2m is completely removed. At this time, the identity of these impurities is unclear. Future work should be focused on identifying these impurities and how they inhibit the seeding process. These future studies would give interesting insight into the mechanisms of seeding and the molecular factors that interfere with that process. This insight could lead to the ability to design inhibitors for the secondary nucleation mediated amyloidosis process.

Other future work could include seeding experiments done with some of the mutants of β2m mentioned above. Using different mutants would be a good way to narrow down what regions of the protein may be interacting with the seed in the secondary nucleation dependent reaction. Seeding experiments should also be performed with seeds generated from WT aggregation in order to determine differences (if any) between the seeding propensity of WT and ΔN6-β2m. These seeding experiments can be accomplished

both through acid generated WT aggregates and Cu(II) generated WT aggregates using a Met0 version of WT. Using both methods of generation for WT seeds would reveal if the seeds created are morphologically different and if that difference affects the seeding ability. The M0WT would also allow us to see if any monomer shedding from the seeds occur during the experiment; though this is unlikely as we do not see any monomer shedding from the ΔN6-β2m seeds.

3.5 References

1. Törnquist, M. *et al.* Secondary nucleation in amyloid formation. *Chem. Commun.* **54**, 8667–8684 (2018).
2. Cohen, S. I. A., Vendruscolo, M., Dobson, C. M. & Knowles, T. P. J. From macroscopic measurements to microscopic mechanisms of protein aggregation. *J. Mol. Biol.* **421**, 160–171 (2012).
3. Chiti, F. *et al.* A Partially Structured Species of β 2 -Microglobulin Is Significantly Populated under Physiological Conditions and Involved in Fibrillogenesis. *J. Biol. Chem.* **276**, 46714–46721 (2001).
4. Cohen, S. I. A. *et al.* Distinct thermodynamic signatures of oligomer generation in the aggregation of the amyloid-β peptide. *Nat. Chem.* **10**, 523–531 (2018).
5. Blancas-Mejía, L. M. & Ramirez-Alvarado, M. Recruitment of Light Chains by Homologous and Heterologous Fibrils Shows Distinctive Kinetic and Conformational Specificity. *Biochemistry* **55**, 2967–2978 (2016).
6. Olsson, T. T., Klementieva, O. & Gouras, G. K. Prion-like seeding and nucleation of intracellular amyloid-β. *Neurobiol. Dis.* **113**, 1–10 (2018).
7. Platt, G. W., Routledge, K. E., Homans, S. W. & Radford, S. E. Fibril Growth Kinetics Reveal a Region of β2-microglobulin Important for Nucleation and Elongation of Aggregation. *J. Mol. Biol.* **378**, 251–263 (2008).
8. Cohen, S. I. A. *et al.* Nucleated polymerization with secondary pathways. I. Time evolution of the principal moments. *J. Chem. Phys.* **135**, 1–44 (2011).
9. Xue, W. F., Homans, S. W. & Radford, S. E. Systematic analysis of nucleation-dependent polymerization reveals new insights into the mechanism of amyloid self-assembly. *Proc. Natl. Acad. Sci. U. S. A.* **105**, 8926–8931 (2008).
10. Karamanos, T. K. *et al.* Structural mapping of oligomeric intermediates in an amyloid assembly pathway. *Elife* **8**, 1–32 (2019).

11. Natalello, A. *et al.* Co-fibrillogenesis of wild-type and D76N β2-microglobulin: The crucial role of fibrillar seeds. *J. Biol. Chem.* **291**, 9678–9689 (2016).

12. Xu, F. *et al.* Cerebral vascular amyloid seeds drive amyloid β-protein fibril assembly with a distinct anti-parallel structure. *Nat. Commun.* **7**, 1–10 (2016).

13. Sade, D., Shaham-Niv, S., Arnon, Z. A., Tavassoly, O. & Gazit, E. Seeding of proteins into amyloid structures by metabolite assemblies may clarify certain unexplained epidemiological associations. *Open Biol.* **8**, (2018).

14. O'Nuallain, B., Williams, A. D., Westermark, P. & Wetzel, R. Seeding Specificity in Amyloid Growth Induced by Heterologous Fibrils. *J. Biol. Chem.* **279**, 17490–17499 (2004).

15. Yang, X., Williams, J. K., Yan, R., Mouradian, M. M. & Baum, J. Increased Dynamics of α-Synuclein Fibrils by β-Synuclein Leads to Reduced Seeding and Cytotoxicity. *Sci. Rep.* **9**, 1–13 (2019).

16. Mirbaha, H. *et al.* Inert and seed-competent tau monomers suggest structural origins of aggregation. *Elife* **7**, 1–29 (2018).

17. Ohhashi, Y., Kihara, M., Naiki, H. & Goto, Y. Ultrasonication-induced amyloid fibril formation of beta2-microglobulin. *J. Biol. Chem.* **280**, 32843–32848 (2005).

18. Myers, S. L. *et al.* A systematic study of the effect of physiological factors on β2-microglobulin amyloid formation at neutral pH. *Biochemistry* **45**, 2311–2321 (2006).

19. Dzwolak, W., Smirnovas, V., Jansen, R. & Winter, R. Insulin forms amyloid in a strain-dependent manner: An FT-IR spectroscopic study. *Protein Sci.* **13**, 1927–1932 (2004).

20. Borysik, A. J. H. *et al.* Separation of β2-microglobulin conformers by high-field asymmetric waveform ion mobility spectrometry (FAIMS) coupled to electrospray ionisation mass spectrometry. *Rapid Commun. Mass Spectrom.* **18**, 2229–2234 (2004).

21. Müller, H. *et al.* Progress towards structural understanding of infectious sheep PrP-amyloid. *Prion* **8**, 344–358 (2014).

22. Yamamoto, S. Glycosaminoglycans Enhance the Trifluoroethanol-Induced Extension of 2-Microglobulin-Related Amyloid Fibrils at a Neutral pH. *J. Am. Soc. Nephrol.* **15**, 126–133 (2004).

23. JT, J. & Jr, L. P. T. Seeding 'one-dimensional crystallization' of amyloid: A pathogenic mechanism in Alzheimer's disease and scrapie? *Cell* **73**, 1055–8 (1993).

24. Yanagi, K. *et al.* The monomer-seed interaction mechanism in the formation of the β2-microglobulin amyloid fibril clarified by solution NMR techniques. *J. Mol. Biol.* **422**, 390–402 (2012).

25. Ma, T. *et al.* Structural Mechanism of Barriers to Interspecies Seeding Transmissibility of Full-Length Prion Protein Amyloid. *ChemBioChem* **20**, 2757–2766 (2019).

26. Saelices, L. *et al.* Amyloid seeding of transthyretin by ex vivo cardiac fibrils and its inhibition. *Proc. Natl. Acad. Sci. U. S. A.* **115**, E6741–E6750 (2018).

27. Saelices, L. *et al.* A pair of peptides inhibits seeding of the hormone transporter transthyretin into amyloid fibrils. *J. Biol. Chem.* **294**, 6130–6141 (2019).

28. Paravastu, A. K., Qahwash, I., Leapman, R. D., Meredith, S. C. & Tycko, R. Seeded growth of β-amyloid fibrils from Alzheimer's brain-derived fibrils produces a distinct fibril structure. *Proc. Natl. Acad. Sci. U. S. A.* **106**, 7443–7448 (2009).

29. Cohen, S. I. A. *et al.* Proliferation of amyloid-β42 aggregates occurs through a secondary nucleation mechanism. *Proc. Natl. Acad. Sci. U. S. A.* **110**, 9758–9763 (2013).

30. Meisl, G. *et al.* Differences in nucleation behavior underlie the contrasting aggregation kinetics of the Aβ40 and Aβ42 peptides. *Proc. Natl. Acad. Sci. U. S. A.* **111**, 9384–9389 (2014).

31. Foderà, V., Librizzi, F., Groenning, M., Van De Weert, M. & Leone, M. Secondary nucleation and accessible surface in insulin amyloid fibril formation. *J. Phys. Chem. B* **112**, 3853–3858 (2008).

32. Ruschak, A. M. & Miranker, A. D. Fiber-dependent amyloid formation as catalysis of an existing reaction pathway. *Proc. Natl. Acad. Sci. U. S. A.* **104**, 12341–12346 (2007).

33. Buell, A. K. *et al.* Solution conditions determine the relative importance of nucleation and growth processes in α-synuclein aggregation. *Proc. Natl. Acad. Sci. U. S. A.* **111**, 7671–7676 (2014).

34. Gaspar, R. *et al.* Secondary nucleation of monomers on fibril surface dominates α-synuclein aggregation and provides autocatalytic amyloid amplification. *Q. Rev. Biophys.* **50**, (2017).

35. Garg, D. K. & Kundu, B. Clues for divergent, polymorphic amyloidogenesis through dissection of amyloid forming steps of bovine carbonic anhydrase and its critical amyloid forming stretch. *Biochim. Biophys. Acta - Proteins Proteomics* **1864**, 794–804 (2016).

36. Borysik, a J., Morten, I. J., Radford, S. E. & Hewitt, E. W. Specific glycosaminoglycans promote unseeded amyloid formation from beta2-microglobulin under physiological conditions. *Kidney Int.* **72**, 174–81 (2007).

37. Karamanos, T. K., Kalverda, A. P., Thompson, G. S. & Radford, S. E. Visualization of Transient Protein-Protein Interactions that Promote or Inhibit Amyloid Assembly. *Mol. Cell* **55**, 214–226 (2014).

38. Smith, D. P., Woods, L. a, Radford, S. E. & Ashcroft, A. E. Structure and Dynamics of Oligomeric Intermediates in β(2)-Microglobulin Self-Assembly. *Biophys. J.* **101**, 1238–1247 (2011).

39. Pashley, C. L., Hewitt, E. W. & Radford, S. E. Comparison of the aggregation of homologous β2-microglobulin variants reveals protein solubility as a key determinant of amyloid formation. *J. Mol. Biol.* **428**, 631–643 (2016).

40. Smith, D. P., Jones, S., Serpell, L. C., Sunde, M. & Radford, S. E. A systematic investigation into the effect of protein destabilisation on beta 2-microglobulin amyloid formation. *J. Mol. Biol.* **330**, 943–954 (2003).

41. Woods, L. A. *et al.* Ligand binding to distinct states diverts aggregation of an amyloid-forming protein. **7**, 730–739 (2012).

42. Eichner, T., Kalverda, A. P., Thompson, G. S., Homans, S. W. & Radford, S. E. Conformational Conversion during Amyloid Formation at Atomic Resolution. *Mol. Cell* **41**, 161–172 (2011).

43. Tipping, K. W. *et al.* pH-induced molecular shedding drives the formation of amyloid fibril-derived oligomers. *Proc. Natl. Acad. Sci. U. S. A.* **112**, 5691–5696 (2015).

44. Linke, R. P. *et al.* Lysine-specific cleavage of β2-microglobulin in amyloid deposits associated with hemodialysis. *Kidney Int.* **36**, 675–681 (1989).

45. Cornwell, O., Radford, S. E., Ashcroft, A. E. & Ault, J. R. Comparing Hydrogen Deuterium Exchange and Fast Photochemical Oxidation of Proteins: a Structural Characterisation of Wild-Type and ΔN6 β2-Microglobulin. *J. Am. Soc. Mass Spectrom.* **29**, 2413–2426 (2018).

46. Esposito, G. *et al.* Removal of the N-terminal hexapeptide from human β2-microglobulin facilitates protein aggregation and fibril formation. *Protein Sci.* **9**, 831–845 (2000).

47. Arden, B. G. *et al.* Measuring the Energy Barrier of the Structural Change That Initiates Amyloid Formation. *Anal. Chem.* **92**, 4731–4735 (2020).

48. *cis-trans Isomerization in Biochemistry*. (Wiley-VCH Verlag GmbH & Co. KGaA, 2006).

49. Yonezawa, Y., Nakata, K., Sakakura, K., Takada, T. & Nakamura, H. Intra- And intermolecular interaction inducing pyramidalization on both sides of a proline dipeptide during isomerization: An ab initio QM/MM molecular dynamics simulation study in explicit water. *J. Am. Chem. Soc.* **131**, 4535–4540 (2009).

50. Craveur, P., Joseph, A. P., Poulain, P., De Brevern, A. G. & Rebehmed, J. Cis-trans isomerization of omega dihedrals in proteins. *Amino Acids* **45**, 279–289 (2013).

51. Kang, Y. K. Ring Flip of Proline Residue via the Transition State with an Envelope Conformation. *J. Phys. Chem. B* **108**, 5463–5465 (2004).

52. Reimer, U., Mokdad, N. El, Schutkowski, M. & Fischer, G. Intramolecular assistance of cis/trans isomerization of the histidine- proline moiety. *Biochemistry* **36**, 13802–13808 (1997).

53. Loureiro, R. J. S., Vila-Viçosa, D., Machuqueiro, M., Shakhnovich, E. I. & Faísca, P. F. N. The early phase of β2m aggregation: An integrative computational study framed on the d76n mutant and the dn6 variant. *Biomolecules* **9**, (2019).

54. Platt, G. W. & Radford, S. E. Glimpses of the molecular mechanisms of β2-microglobulin fibril formation in vitro: Aggregation on a complex energy landscape. *FEBS Lett.* **583**, 2623–2629 (2009).

CHAPTER 4

SUMMARY AND FUTURE OUTLOOK

4.1 Summary

A mass spectrometry (MS) and covalent labeling (CL) method has been developed to monitor the burial status of Trp60 in β-2-microglobulin (β2m) and, by proxy, the *cis-trans* isomerization (CTI) of Pro32 that initiates amyloid formation. This technique takes advantage of the Trp specificity of labeling reagent dimethyl(2-hydroxy-5-nitrobenzyl) sulfonium bromide (HNSB) and is straightforward enough to be applied broadly in many different amyloid-forming solution conditions. It has been demonstrated that this method can be automated through the repurposing of an autosampler and HPLC-MS system, allowing for higher throughput and more consistent experimentation.

Through method development it has become clear that each new solution condition investigated may require slight tweaking of the method. For example, under acidic conditions, the labeling efficiency of the HNSB reaction is reduced, requiring higher concentrations and/or longer labeling times. For each new experimental condition, it is important to confirm the HNSB labeling sites and even more critically, ensure that only Trp60 is changing over time. Whether the experiment is monitoring the movement of one or more Trp residues at a time becomes obvious from deviations from the standard labeling curve profile and can be confirmed by proteolytic digestion and LC-MS/MS. Dynamics of the system being investigated can make data analysis more complicated and may require more experimentation. For example, in the case of acid induced β2m amyloid formation, the high dynamic nature requires that many more time points, much closer together, are

run compared to the Cu(II) induced condition. The high dynamics also require more replicates to be performed to weed out any outliers and narrow in on the true rate of CTI. Overall, the developed HNSB CL method is a relatively simple and straightforward way to quickly gain structural insight into the pre-amyloid structural change of β2m. It can also be used as a quick and easy 'first pass' to identify systems warranting closer investigation. It would be easy to adapt the automation (using the autosampler) to other CL techniques that don't require proteolytic digestion for analysis.

In a published work, we have applied this technique to investigate the molecular factors governing the activation energy barrier to the CTI of Pro32 in the β2m amyloid forming process. Energy barriers were determined for the process as induced by Cu(II), trifluoroethanol (TFE), and acid. The catalytic nature of Cu(II) lowers the energy barrier substantially and does not appear to be affected by the use of urea, a common additive in amyloid fibril growth.[1–7] This is likely due to the Cu(II) binding close to Pro32 as metal ions are known to catalyze Pro CTIs.[8,9] It is likely, given the low energy barrier, that the CTI of Pro32 is the rate determining step in this process. While TFE lowers the energy barrier from a typical Pro CTI barrier, it does so significantly less than Cu(II). The donation of hydrogen bonds from TFE surrounding the protein likely stabilizes both the *cis* and *trans* conformation of Pro32, increasing the isomerization barrier.[10] The energy barrier is lowered enough that the CTI of Pro32 is still likely the rate determining step in this case. When initiated by acid, the measured rates are very high and yet, the massive temperature dependence of the pre-amyloid structural change under this condition yields a very high activation energy. This high activation barrier may be an indication that the CTI of Pro32 is no longer the rate determining step in this process. Having a different rate-determining

step would be more consistent with the fact that charged His residues on the N-terminal side of Pro resides (as His31 would be in this case) are known to greatly reduce the energy barrier to isomerization.[11] The activation energy barrier measurements under these three solution conditions represent some of the first for amyloid systems and, to our knowledge, the first of a structural change leading to amyloid formation. The new biological insights discovered here are valuable for future determination of the mechanistic details of β2m amyloidogenesis. These results are also a demonstration of how CL-MS can be a useful tool for measuring energy barriers for other amyloid systems that are triggered by large structural changes.

The Trp labeling technique developed here was also used to investigate the primary and secondary nucleation mediated mechanisms of β2m amyloid formation as induced by the amyloidogenic variant ΔN6-β2m. The activation energy barrier was determined for the primary nucleation mediated mechanism. The height of this barrier seems to indicate that in this condition (like that of the previously mentioned acid induced condition) the Pro32 CTI may not be the rate determining step. The use of an H31F mutant in place of wild type (WT) β2m is further evidence of this conclusion, as the measured rate is not significantly changed by this mutation. If the CTI of Pro32 were the rate determining step in this reaction, we would expect a significant difference in rate due to the substitution of a bulky, uncharged residue for His on the N-terminal side of Pro32. In addition, we have discovered a rise in HNSB Trp labeling, seen before the drop in labeling characterizing the Pro32 CTI, that indicates the presence of another structural change during this lag phase. What this structural change could be is still unclear but appears to be temperature and pH dependent. It is unlikely to involve the Pro32 CTI as it is unaffected by the H31F mutation. This

increase in HNSB labeling also coincides in time with a drop in soluble WT and rapid accumulation of amorphous aggregates as seen by MS, size exclusion chromatography (SEC), and dynamic light scattering (DLS). The extent of involvement of these aggregates in the process has yet to be determined.

The secondary nucleation mediated mechanism was probed by amyloid seeding using seeds generated from ΔN6-β2m. These seeds exhibited a catalytic-like effect, yielding a large drop in the Pro32 CTI activation energy barrier. The Arrhenius parameters for this reaction, similar to those of the Cu(II) induced amyloidogenesis, indicate that the Pro32 CTI is likely the rate determining step. In addition, under seeding conditions, there is no longer a lag phase seen, consistent with the differences between primary and secondary nucleation seen in other amyloid systems.[12] β2m appears to differ from the amyloid-β (Aβ) amyloid system in that Aβ exhibits an inverse relationship between temperature and rate under secondary nucleation, whereas β2m shows a correlation between rising temperature and rising rate. It also seems that pH changes can impede seeding competency as successful seeding is seen at pH 7.4, but not at pH 6.2. Interestingly, as-of-yet unidentified impurities in one of two ΔN6-β2m preparations used, possess the ability to inhibit the seeding of WT β2m. These impurities do not affect the energy barrier of the primary nucleation mechanism, but may length the lag period in this process.

These projects together have given new insight into the energetics of β2m amyloidosis. We have specifically gained new understanding of the mechanism of the Pro32 CTI leading to amyloid formation and the molecular factors governing it. Different conditions leading to amyloidosis can be investigated in the future to continue to further this understanding. A deeper understanding of these factors can aid in finding new methods

to manipulate and eventually inhibit amyloidosis of not only β2m, but amyloid systems generally. To this end, β2m can be seen as a model system for the determination of activation energy barriers leading to amyloid formation. The techniques developed in this dissertation also demonstrate the capability of CL-MS to measure these barriers, especially in cases where a large structural change triggers amyloidosis.

4.2 Future Directions

The relative ease and simplicity of the developed CL-MS technique could be applied to several additional analyses. Good candidates for investigation using this technique include: amyloid inhibitors and their effect on the CTI of Pro32, the interaction between amyloidogenic mutant D76N-β2m and WT β2m, seeding amyloidosis with peptide fragments of β2m, and cross-seeding β2m amyloidosis with other amyloid systems. These would also all be compatible with automation using the autosampler setup. This would help gain even further insight into the mechanism of β2m amyloidosis, particularly the biochemical factors governing the CTI of Pro32.

Several small molecule amyloid inhibitors have been developed for specific amyloid systems and broadly applicable inhibitors that can act on many amyloid systems.[13–18] Doxycycline, rifamycin and, epigallocatechin-3-gallate (EGCG) have been demonstrated as small molecule inhibitors of β2m amyloid formation that are able to bind to the WT β2m monomer.[14,19,20] However, the exact mechanism of inhibition is still not completely clear. Our method is uniquely suited to determine whether the inhibiting molecules act by preventing the CTI of Pro32. In fact, preliminary data indicates that these molecules seem to inhibit the CTI process at least up to 120 mins after incubation with Cu(II), while small molecule binding control suramin slows the onset of, but does not

inhibit this structural change (Figure 4.1). Further investigation is required to determine the extent of this inhibition. EGCG in particular seems to induce some structural change in the monomer as evidenced by the increase in Trp labeling over 120 mins. As we already have evidence that some molecular factors can inhibit the secondary nucleation mechanism of β2m amyloidosis but not the primary nucleation mechanism, it would be interesting to evaluate whether these small molecules can inhibit both mechanisms or just one. These experiments would be relatively simple to investigate with the ΔN6-β2m induced system. Furthermore, our automation of the technique can be leveraged to screen for likely inhibition candidates that act by preventing the CTI of Pro32. The automated labeling (see Appendix) can include the addition of inhibitor molecules. In this way, several inhibitor

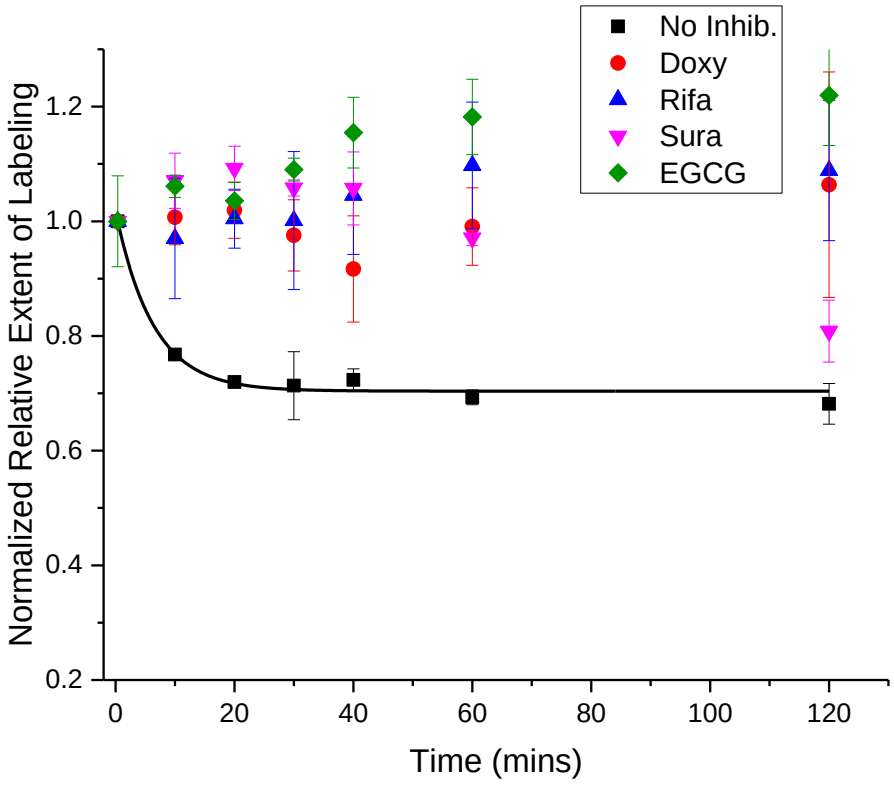

Figure 4.1: HNSB Trp labeling of WT β2m bound to small molecule inhibitors doxycycline, rifamycin, or EGCG or small molecule binding control suramin. Cu(II) was used as the amyloid initiator in these cases.

candidates can be placed in vials within the autosampler. β2m can be mixed with each candidate at a 0 time point and a time point several hours later. If there is a significant decrease in HNSB labeling indicating Pro32 CTI after several hours, that compound would be a good candidate for further testing as to its inhibitory effects.

Several cases have been identified of amyloid forming proteins and peptides cross-seeding other amyloid forming systems.[21–25] An interesting application of our technique would be the seeding of WT β2m amyloidosis with another amyloid. Specifically, Aβ and the prion protein would be good candidates. Aβ is a peptide and would likely be able to interact with β2m easily. The prion protein is known to be infective and have the ability to cross-seed other systems and would compare well with ΔN6-β2m.[25]

Peptide fragments of the β2m sequence have been identified which have shown the ability to form amyloid-like fibrils on their own as well as induce aggregation in the full WT protein (Figure 4.2).[26] These observations give an opportunity to investigate their potential to seed WT β2m under both primary and secondary nucleation conditions. Because each of the peptide fragments are from regions of the full β2m protein, studies of these peptides could give important insight into which sections of the protein are involved in primary and secondary nucleation dependent amyloid formation. If the use of one

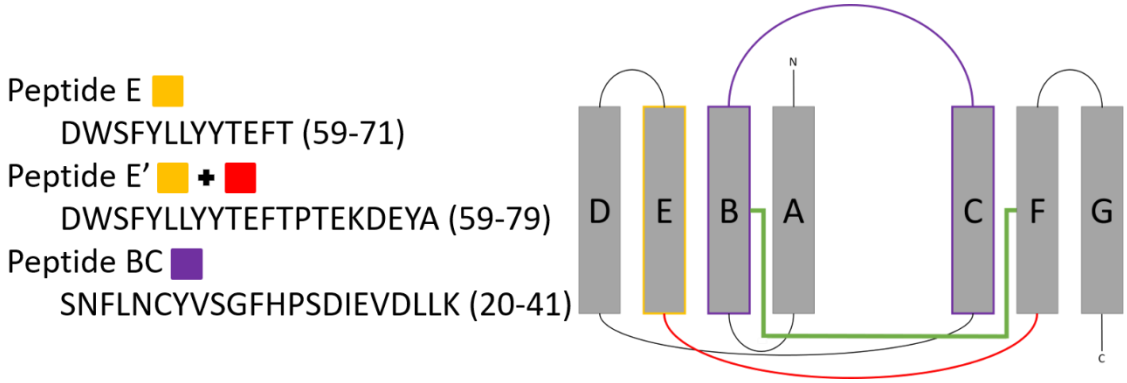

Figure 4.2: Select peptide fragments of the β2m sequence that are known to aggregate as well as induce aggregation in the full-length protein

peptide yields a larger reduction in the activation energy barrier than the others, that would be an indication of the importance of that stretch of the sequence to the amyloid forming process under either primary or secondary nucleation conditions.

In addition to the use of mutants R3A, H51F, F30A, and F62A as mentioned in Chapter 3, other point mutants would be useful in future experiments to reveal regions of β2m that are most critical to the activation energy of the pre-amyloid structural change whether induced by Cu(II) or the interaction between WT β2m and ΔN6-β2m. The amyloidogenesis of several point mutants of β2m have been compared to WT β2m. Most interestingly D53P[27] aggregates to amyloids slower that WT β2m and D59P[28] yield amyloids faster than WT β2m. Our technique would be useful for determining whether these mutants effect the energy barrier to the Pro32 CTI as induced by Cu(II) or if they are more critical downstream of the CTI, but before full amyloid formation. D53P is not likely to greatly affect the CTI as it is far from the region of the protein involved but may slow aggregation by disrupting oligomerization as it replaces a negatively charged residue with a neutral residue that introduces a kink into the amino acid chain.

It was demonstrated by Karamanos *et al*. that the BC, DE, and FG loops (Figure 4.3) are important in the transient head-to-head interactions between WT β2m and ΔN6-β2m that lead to amyloidosis.[29] However, it is still unclear if any of these three loops are more critical than the others for this process or the importance of specific residues. The AB loop has also been shown to be an important driver of monomer association at a range of pHs.[30] Additional point mutants could help shed some light on the importance of these various loops. H13F and N17D mutants would be valuable for probing the AB loop where higher mobility of the loop leads to improved adhesion between monomers.[30] H13F and

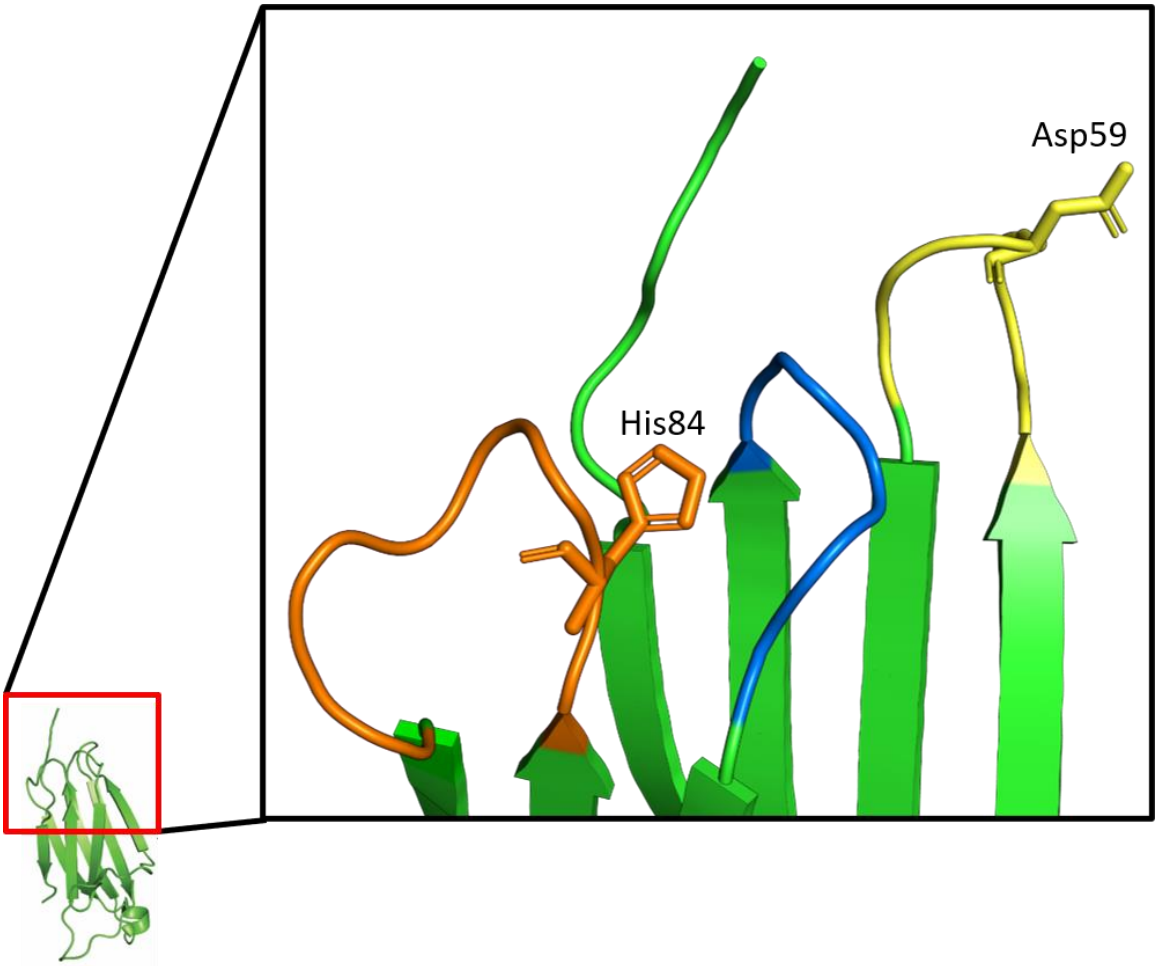

Figure 4.3: The head of the β2m protein comprised of the N-terminus (green strand), the BC loop (blue), the DE loop (yellow) including Asp59, and the FG loop (orange) including His84.

N17D would both likely slow the ΔN6-β2m initiated amyloidosis of WT β2m as they would promote non-productive interactions between the two proteins. The DE loop (Figure 4.3) can be probed with the D59P mutant which introduces a significant change in size and charge as well as another proline to a critical region. D59P would likely reduce productive head-to-head interactions with ΔN6-β2m due to a reduction in the possibility of salt bridge formation. A dimer-stabilizing intermolecular salt bridge is seen between D59 and K19 of two WT β2m molecules in the amyloid competent state, of which ΔN6-β2m is a structural mimic.[3,31] The resulting reduction in interaction between ΔN6-β2m and WT β2m would

then decrease the CTI rate of Pro32. The FG loop (Figure 4.3) can be probed by H84A as H84 is positively charged and would be replaced by a much smaller, uncharged, and hydrophobic residue. This mutation would likely result in a decrease in Pro32 CTI rate.

The amyloidogenic mutant D76N-β2m has similar properties to ΔN6-β2m. It is naturally occurring, self-amyloidogenic, and can also induce amyloidogenicity in the WT protein.[30,32–39] Interestingly, however, D76N-β2m shows only subtle structural differences from the WT.[40] This mutant would be a great candidate for comparing the primary and secondary nucleation mechanisms in a manner similar to ΔN6-β2m. Such studies would also contribute to the currently sparse knowledge of the D76N-β2m aggregation mechanism. Our Trp labeling technique could be applied in almost exactly the same way as we have investigated ΔN6-β2m. In all, these future works would add to the mechanistic information of β2m amyloidogenesis we have gained here as well as amyloid systems generally.

4.3 References

1. Morgan, C. J., Gelfand, M., Atreya, C. & Miranker, A. D. Kidney dialysis-associated amyloidosis: a molecular role for copper in fiber formation. *J. Mol. Biol.* **309**, 339–45 (2001).
2. McParland, V. J. *et al.* Partially Unfolded States of β2-Microglobulin and Amyloid Formation in Vitro. *Biochemistry* **39**, 8735–8746 (2000).
3. Eichner, T., Kalverda, A. P., Thompson, G. S., Homans, S. W. & Radford, S. E. Conformational Conversion during Amyloid Formation at Atomic Resolution. *Mol. Cell* **41**, 161–172 (2011).
4. Stoppini, M. & Bellotti, V. Systemic amyloidosis: Lessons from β2-microglobulin. *J. Biol. Chem.* **290**, 9951–9958 (2015).
5. Antwi, K. *et al.* Cu (II) organizes β-2-microglobulin oligomers but is released upon amyloid formation. *Protein Sci.* **17**, 748–759 (2008).

6. Mendoza, V. L., Antwi, K., Barón-rodríguez, M. A., Blanco, C. & Vachet, R. W. Structure of the Pre-amyloid Dimer of β-2-microglobulin from Covalent Labeling and Mass Spectrometry. *Biochemistry* **49**, 1522–1532 (2010).

7. Eakin, C. M., Knight, J. D., Morgan, C. J., Gelfand, M. A. & Miranker, A. D. Formation of a copper specific binding site in non-native states of β-2-microglobulin. *Biochemistry* **41**, 10646–10656 (2002).

8. Cox, C., Ferraris, D., Murthy, N. N. & Lectka, T. Copper(II)-catalyzed amide isomerization: Evidence for N-coordination. *J. Am. Chem. Soc.* **118**, 5332–5333 (1996).

9. Gaggelli, E., D'Amelio, N., Gaggelli, N. & Valensin, G. Metal ion effects on the cis/trans isomerization equilibrium of proline in short-chain peptides: a solution NMR study. *Chembiochem* **2**, 524–529 (2001).

10. Eberhardt, E. S., Loh, S. N., Hinck, A. P. & Raines, R. T. Solvent Effects on the Energetics of Prolyl Peptide Bond Isomerization. *J. Am. Chem. Soc.* **114**, 5437–5439 (1992).

11. Reimer, U., Mokdad, N. El, Schutkowski, M. & Fischer, G. Intramolecular assistance of cis/trans isomerization of the histidine- proline moiety. *Biochemistry* **36**, 13802–13808 (1997).

12. Cohen, S. I. A. *et al.* Distinct thermodynamic signatures of oligomer generation in the aggregation of the amyloid-β peptide. *Nat. Chem.* **10**, 523–531 (2018).

13. Liu, T., Marcinko, T. M., Kiefer, P. A. & Vachet, R. W. Using Covalent Labeling and Mass Spectrometry To Study Protein Binding Sites of Amyloid Inhibiting Molecules. *Anal. Chem.* **89**, 11583–11591 (2017).

14. Marcinko, T. M., Drews, T., Liu, T. & Vachet, R. W. Epigallocatechin-3-gallate Inhibits Cu(II)-Induced β-2-Microglobulin Amyloid Formation by Binding to the Edge of Its β-Sheets. *Biochemistry* **59**, 1093–1103 (2020).

15. Saelices, L. *et al.* Amyloid seeding of transthyretin by ex vivo cardiac fibrils and its inhibition. *Proc. Natl. Acad. Sci. U. S. A.* **115**, E6741–E6750 (2018).

16. Cao, Q. *et al.* Inhibiting amyloid-ß cytotoxicity through its interaction with the cell surface receptor LilrB2 by structure-based design. *Nat. Chem.* 1 (2018).

17. Marcinko, T. M., Dong, J., LeBlanc, R., Daborowski, K. V. & Vachet, R. W. Small Molecule-mediated Inhibition of β-2-Microglobulin Amyloid Fibril Formation. *J. Biol. Chem.* jbc.M116.774083 (2017).

18. Thomas, A., Kaur, G., Ali, R. & Verma, S. Small Molecule Inhibitors for Amyloid Aggregation. in *Biological Soft Matter: Fundamentals, Properties, and Applications* (eds. Nardin, C. & Schlaad, H.) 153–194 (WILEY-VCH, 2021).

19. Woods, L. A. *et al.* Ligand binding to distinct states diverts aggregation of an amyloid-forming protein. **7**, 730–739 (2012).

20. Giorgetti, S. *et al.* Effect of tetracyclines on the dynamics of formation and destructuration of β2-microglobulin amyloid fibrils. *J. Biol. Chem.* **286**, 2121–2131 (2011).

21. Ma, T. *et al.* Structural Mechanism of Barriers to Interspecies Seeding Transmissibility of Full-Length Prion Protein Amyloid. *ChemBioChem* **20**, 2757–2766 (2019).

22. Yang, X., Williams, J. K., Yan, R., Mouradian, M. M. & Baum, J. Increased Dynamics of α-Synuclein Fibrils by β-Synuclein Leads to Reduced Seeding and Cytotoxicity. *Sci. Rep.* **9**, 1–13 (2019).

23. Dzwolak, W., Smirnovas, V., Jansen, R. & Winter, R. Insulin forms amyloid in a strain-dependent manner: An FT-IR spectroscopic study. *Protein Sci.* **13**, 1927–1932 (2004).

24. Wasmer, C. *et al.* Structural similarity between the prion domain of HET-s and a homologue can explain amyloid cross-seeding in spite of limited sequence identity. *J. Mol. Biol.* **402**, 311–325 (2010).

25. Chaudhuri, P., Prajapati, K. P., Anand, B. G., Dubey, K. & Kar, K. Amyloid cross-seeding raises new dimensions to understanding of amyloidogenesis mechanism. *Ageing Res. Rev.* **56**, 100937 (2019).

26. Jones, S., Manning, J., Kad, N. M. & Radford, S. E. Amyloid-forming peptides from β2-microglobulin - Insights into the mechanism of fibril formation in vitro. *J. Mol. Biol.* **325**, 249–257 (2003).

27. Azinas, S. *et al.* D-strand perturbation and amyloid propensity in beta-2 microglobulin. *FEBS J.* **278**, 2349–2358 (2011).

28. Ricagno, S. *et al.* DE loop mutations affect β2-microglobulin stability and amyloid aggregation. *Biochem. Biophys. Res. Commun.* **377**, 146–150 (2008).

29. Karamanos, T. K., Kalverda, A. P., Thompson, G. S. & Radford, S. E. Visualization of Transient Protein-Protein Interactions that Promote or Inhibit Amyloid Assembly. *Mol. Cell* **55**, 214–226 (2014).

30. Loureiro, R. J. S., Vila-Viçosa, D., Machuqueiro, M., Shakhnovich, E. I. & Faísca, P. F. N. The early phase of β2m aggregation: An integrative computational study framed on the d76n mutant and the dn6 variant. *Biomolecules* **9**, (2019).

31. Srikanth, R., Mendoza, V. L., Bridgewater, J. D., Zhang, G. & Vachet, R. W. Copper Binding to β-2-Microglobulin and its Pre-Amyloid Oligomers. *Biochemistry* **48**, 9871–9881 (2009).

32. Natalello, A. *et al.* Co-fibrillogenesis of wild-type and D76N β2-microglobulin: The crucial role of fibrillar seeds. *J. Biol. Chem.* **291**, 9678–9689 (2016).

33. Mangione, P. P. *et al.* Structure, folding dynamics, and amyloidogenesis of D76N β2-microglobulin roles of shear flow, hydrophobic surfaces, and α-crystallin. *J. Biol. Chem.* **288**, 30917–30930 (2013).

34. Smith, H. I. *et al.* The role of the IT-state in D76N β2-microglobulin amyloid assembly: A crucial intermediate or an innocuous bystander? *J. Biol. Chem.* **295**, 12474–12484 (2020).

35. Lucato, C. M., Lupton, C. C., Halls, M. L. & Ellisdon, A. M. Amyloidogenicity at a distance: How distal protein regions modulate aggregation in disease. *J. Mol. Biol.* **429**, 1289–1304 (2017).

36. Hall, Z., Schmidt, C. & Politis, A. Uncovering the early assembly mechanism for amyloidogenic β2-microglobulin using cross-linking and native mass spectrometry. *J. Biol. Chem.* **291**, 4626–4637 (2016).

37. Mizuno, H. *et al.* Dialysis-related amyloidosis associated with a novel β2-microglobulin variant. *Amyloid* **0**, 1–8 (2020).

38. Chong, S.-H. *et al.* Structural and Thermodynamic Characteristics of Amyloidogenic Intermediates of β-2-Microglobulin. *Sci. Rep.* **5**, 13631 (2015).

39. Le Marchand, T. *et al.* Conformational dynamics in crystals reveal the molecular bases for D76N beta-2 microglobulin aggregation propensity. *Nat. Commun.* **9**, 1–11 (2018).

40. Cornwell, O., Ault, J. R., Bond, N. J., Radford, S. E. & Ashcroft, A. E. Investigation of D76N β2-Microglobulin Using Protein Footprinting and Structural Mass Spectrometry. *J. Am. Soc. Mass Spectrom.* (2021).

APPENDIX

AUTOMATION AND USE OF AGILENT 1100 LC SYSTEM FOR COVALENT LABELING

Set up of 1100 system modules

For all automated covalent labeling (CL) experiments in this dissertation, the following Agilent 1100 modules were used: G1367A well plate autosampler with temperature control, G1379A degasser, and G1312A binary pump. Other Agilent 1100 modules can easily be integrated into this setup for a variety of measurements (e.g., G1315B diode array detector).

Ensure that each module being used is connected via CAN cable to another module being used. The chain of CAN cables should end at the module with the networking card. Good practice dictates that the networking card be in the module that collects data (i.e., diode array detector or similar). For our experiments, all data was collected by the mass spectrometer, therefore any module can have the network card.

Connect the network card to the computer with a crossover shielded LAN patch cable. When setting up the ethernet adapter on the computer for communication with the Agilent modules, ensure you match the IP address to that of the Agilent system. This IP address can be found and/or changed in the settings on the Agilent handheld control module.

Vial placement in the well plate autosampler

The vials in the well plate of the autosampler will contain all reagents needed for the CL reaction. This may include: the protein sample, labeling reagent, quencher, and any other reagents needed depending on the CL reaction being performed. Vials should be placed as close to the injection inlet of the autosampler as possible to minimize the injector needle's travel time around the compartment. Figure A.1 shows an example well plate set up for an HNSB labeling reaction on Cu(II) induced β2m. This can be expanded for more sample vials/more time points, but it is recommended to continue keeping all sample vials as close to the inlet as possible. This method can be customized to add any and all reagents needed for a CL procedure.

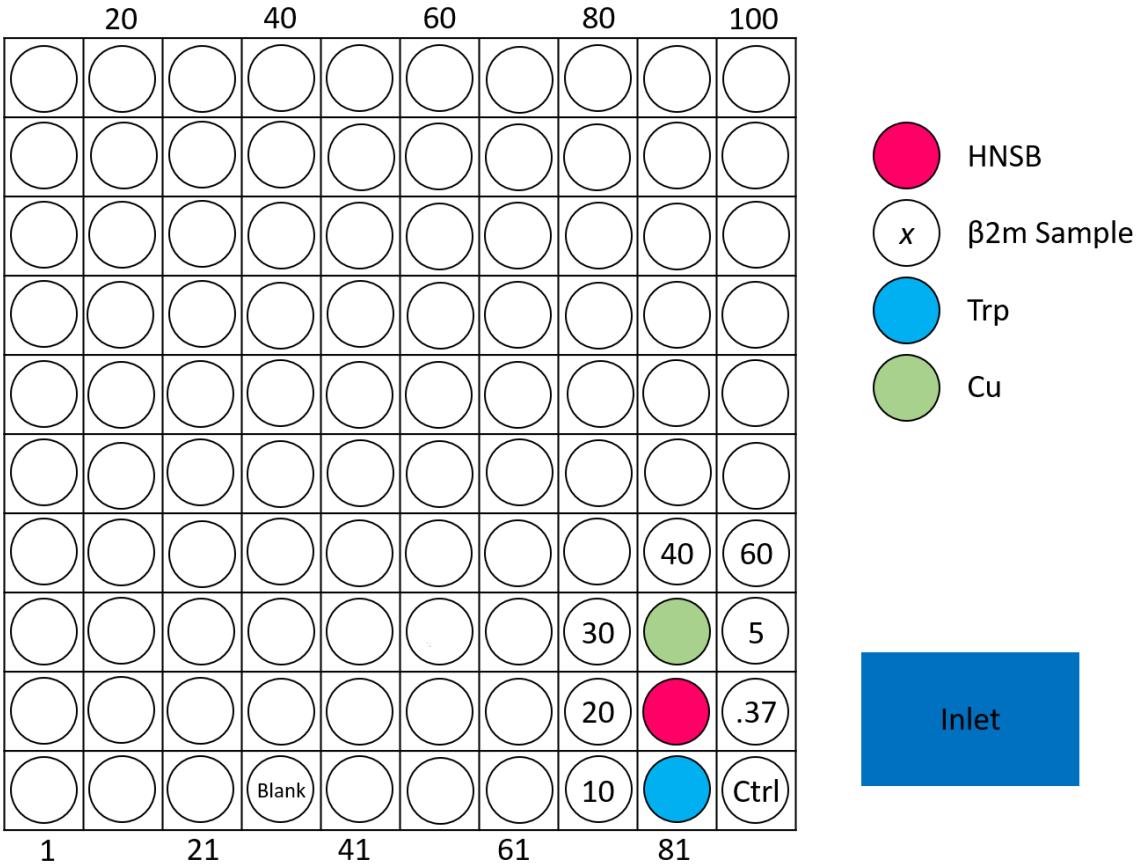

Figure A.1: Well plate setup for an HNSB labeling reaction on Cu(II) induced β2m. Included are the HNSB reagent (pink), Cu(II) (green), L-Trp quenching agent (blue), and β2m protein samples (white) to be incubated with Cu(II) for *x* minutes.

Software set up

For all automated CL experiments in this dissertation, Bruker Hystar software was used to jointly control the LC set up and the mass spectrometers used. However, any software that supports the integration of Agilent LC systems will work (ChemStation, etc.) It is critical that the firmware versions on all modules matches. Additionally, the firmware of all modules may need to be updated or downgraded for compatibility with the software you choose (see Agilent website for more information).

The gradient and flow rate can be set in the bin pump section of the method. These will depend on the particular CL reaction and column being used. For our experiments we used a protein desalting column with a max flow rate of 0.2 mL/min and a short (2 min)

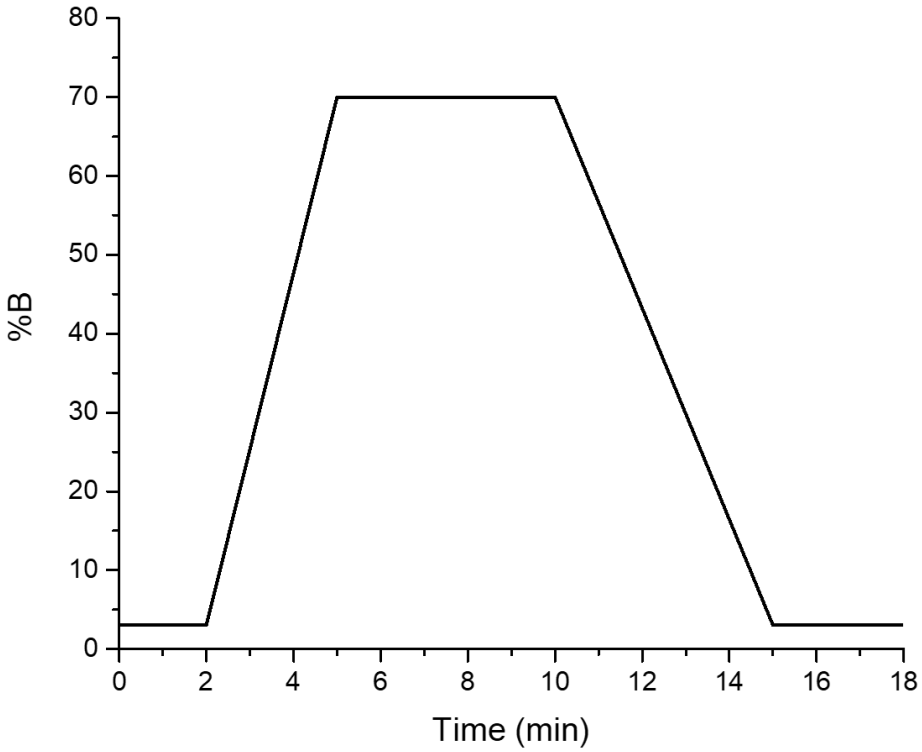

Figure A.2: Example LC gradient for desalting of an HNSB reaction with β2m. It begins at 3%B until 2 min when it starts to rapidly rise to 70% B. The gradient sits at 70% B until min 10 to ensure all protein has eluted off the column followed by a slow return to 3% B at min 15.

desalting time at 3%B followed by a quick jump to 70% B to release the protein sample from the column (Figure A.2).

Within the settings for the autosampler part of the method, an ‘injector program’ can be written. This uses command lines such as ‘DRAW’ to pull solution from a vial or ‘EJECT’ to place solution into a different vial. This allows for granular control of the autosampler allowing it to be used as a pseudo liquid handing robot. In this way, the autosampler can completely take over all steps of a CL reaction. The following is an example injector program for an HNSB labeling reaction on Cu(II) induced β2m that goes with the well plate setup in Figure A.1. In all capital letters are the base commands found in the programming window and what follows each base command are the variables.

- VALVE: bypass
- DRAW: from vial *83, 1 uL,* 500 *u*L/min
- EJECT: into *sample*, 500 uL/min
- NEEDLE: wash in flush port, 1 sec
- DRAW: from vial *82*, 5 *uL,* 500 uL/min
- WAIT: *x* min-22 sec
- EJECT: into *sample*, 500 uL/min
- NEEDLE: wash in flush port, 10 sec
- DRAW: from vial *81*, 4 *u*L, DEF.
- WAIT: 14 sec
- EJECT into *sample,* DEF.
- DRAW from *sample,* 10 *u*L, DEF.
- INJECT 10 *u*L, DEF.
- VALVE mainpass+start
- NEEDLE wash in flush port, 10 sec

Note that the autosampler completes all steps, including initiation with Cu(II), reaction with HNSB, and quenching with Trp before injecting the sample onto the column. These commands can be customized for nearly any CL reaction. Note that due to slight movement differences in each individual autosampler, it is recommended to determine travel times of the injector needle to various vial locations as this may affect how long the WAIT steps should be.

Notes

- Ensure proper cleaning of the system after every experiment. Neglecting this can lead to clogs in the system.
- Firmware versions can be update or downgraded using Agilent's Lab Advisor software (see Agilent website).

BIBLIOGRAPHY

Antwi, K. *et al.* Cu (II) organizes β-2-microglobulin oligomers but is released upon amyloid formation. *Protein Sci.* **17**, 748–759 (2008).

Arden, B. G. *et al.* Measuring the Energy Barrier of the Structural Change That Initiates Amyloid Formation. *Anal. Chem.* **92**, 4731–4735 (2020).

Azinas, S. *et al.* D-strand perturbation and amyloid propensity in beta-2 microglobulin. *FEBS J.* **278**, 2349–2358 (2011).

Becker, J. W. & Reeke, G. N. Three-dimensional structure of beta 2-microglobulin. *Proc. Natl. Acad. Sci. U. S. A.* **82**, 4225–9 (1985).

Blancas-Mejía, L. M. & Ramirez-Alvarado, M. Recruitment of Light Chains by Homologous and Heterologous Fibrils Shows Distinctive Kinetic and Conformational Specificity. *Biochemistry* **55**, 2967–2978 (2016).

Borysik, a J., Morten, I. J., Radford, S. E. & Hewitt, E. W. Specific glycosaminoglycans promote unseeded amyloid formation from beta2-microglobulin under physiological conditions. *Kidney Int.* **72**, 174–81 (2007).

Borysik, A. J. H. *et al.* Separation of β2-microglobulin conformers by high-field asymmetric waveform ion mobility spectrometry (FAIMS) coupled to electrospray ionisation mass spectrometry. *Rapid Commun. Mass Spectrom.* **18**, 2229–2234 (2004).

Buell, A. K. *et al.* Solution conditions determine the relative importance of nucleation and growth processes in α-synuclein aggregation. *Proc. Natl. Acad. Sci. U. S. A.* **111**, 7671–7676 (2014).

Calabrese, M. F. & Miranker, A. D. Formation of a Stable Oligomer of β-2 Microglobulin Requires only Transient Encounter with Cu(II). *J. Mol. Biol.* **367**, 1–7 (2007).

Calabrese, M. F. & Miranker, A. D. Metal binding sheds light on mechanisms of amyloid assembly. *Prion* **3**, 1–4 (2009).

Calabrese, M. F., Eakin, C. M., Wang, J. M. & Miranker, A. D. A regulatable switch mediates self-association in an immunoglobulin fold. *Nat. Struct. Mol. Biol.* **15**, 965–71 (2008).

Cao, Q. *et al.* Inhibiting amyloid-ß cytotoxicity through its interaction with the cell surface receptor LilrB2 by structure-based design. *Nat. Chem.* **1** (2018).

Chaudhuri, P., Prajapati, K. P., Anand, B. G., Dubey, K. & Kar, K. Amyloid cross-seeding raises new dimensions to understanding of amyloidogenesis mechanism. *Ageing Res. Rev.* **56**, 100937 (2019).

Chiti, F. & Dobson, C. M. Protein Misfolding, Functional Amyloid, and Human Disease. *Annu. Rev. Biochem.* **75**, 333–366 (2006).

Chiti, F. *et al.* A Partially Structured Species of β 2 -Microglobulin Is Significantly Populated under Physiological Conditions and Involved in Fibrillogenesis. *J. Biol. Chem.* **276**, 46714–46721 (2001).

Chong, S.-H. *et al.* Structural and Thermodynamic Characteristics of Amyloidogenic Intermediates of β-2-Microglobulin. *Sci. Rep.* **5**, 13631 (2015).

cis-trans Isomerization in Biochemistry. (Wiley-VCH Verlag GmbH & Co. KGaA, 2006).

Cohen, S. I. A. *et al.* Distinct thermodynamic signatures of oligomer generation in the aggregation of the amyloid-β peptide. *Nat. Chem.* **10**, 523–531 (2018).

Cohen, S. I. A. *et al.* Nucleated polymerization with secondary pathways. I. Time evolution of the principal moments. *J. Chem. Phys.* **135**, 1–44 (2011).

Cohen, S. I. A. *et al.* Proliferation of amyloid-β42 aggregates occurs through a secondary nucleation mechanism. *Proc. Natl. Acad. Sci. U. S. A.* **110**, 9758–9763 (2013).

Cohen, S. I. A., Vendruscolo, M., Dobson, C. M. & Knowles, T. P. J. From macroscopic measurements to microscopic mechanisms of protein aggregation. *J. Mol. Biol.* **421**, 160–171 (2012).

Cornwell, O., Ault, J. R., Bond, N. J., Radford, S. E. & Ashcroft, A. E. Investigation of D76N β2-Microglobulin Using Protein Footprinting and Structural Mass Spectrometry. *J. Am. Soc. Mass Spectrom.* **32**, 1583-1592 (2021).

Cornwell, O., Radford, S. E., Ashcroft, A. E. & Ault, J. R. Comparing Hydrogen Deuterium Exchange and Fast Photochemical Oxidation of Proteins: a Structural Characterisation of Wild-Type and ΔN6 β2-Microglobulin. *J. Am. Soc. Mass Spectrom.* **29**, 2413–2426 (2018).

Cox, C., Ferraris, D., Murthy, N. N. & Lectka, T. Copper(II)-catalyzed amide isomerization: Evidence for N-coordination. *J. Am. Chem. Soc.* **118**, 5332–5333 (1996).

Craveur, P., Joseph, A. P., Poulain, P., De Brevern, A. G. & Rebehmed, J. Cis-trans isomerization of omega dihedrals in proteins. *Amino Acids* **45**, 279–289 (2013).

Dong, J. *et al.* Unique Effect of Cu(II) in the Metal-Induced Amyloid Formation of β-2-Microglobulin. *Biochemistry* **53**, 1263–1274 (2014).

Dzwolak, W., Smirnovas, V., Jansen, R. & Winter, R. Insulin forms amyloid in a strain-dependent manner: An FT-IR spectroscopic study. *Protein Sci.* **13**, 1927–1932 (2004).

Eakin, C. M., Attenello, F. J., Morgan, C. J. & Miranker, A. D. Oligomeric assembly of native-like precursors precedes amyloid formation by β-2 microglobulin. *Biochemistry* **43**, 7808–7815 (2004).

Eakin, C. M., Berman, A. J. & Miranker, A. D. A native to amyloidogenic transition regulated by a backbone trigger. *Nat. Struct. Mol. Biol.* **13**, 202–208 (2006).

Eakin, C. M., Knight, J. D., Morgan, C. J., Gelfand, M. A. & Miranker, A. D. Formation of a copper specific binding site in non-native states of β-2-microglobulin. *Biochemistry* **41**, 10646–10656 (2002).

Eberhardt, E. S., Loh, S. N., Hinck, A. P. & Raines, R. T. Solvent Effects on the Energetics of Prolyl Peptide Bond Isomerization. *J. Am. Chem. Soc.* **114**, 5437–5439 (1992).

Eichner, T. & Radford, S. E. A Generic Mechanism of β2-Microglobulin Amyloid Assembly at Neutral pH Involving a Specific Proline Switch. *J. Mol. Biol.* **386**, 1312–1326 (2009).

Eichner, T., Kalverda, A. P., Thompson, G. S., Homans, S. W. & Radford, S. E. Conformational Conversion during Amyloid Formation at Atomic Resolution. *Mol. Cell* **41**, 161–172 (2011).

Esposito, G. *et al.* Removal of the N-terminal hexapeptide from human β2-microglobulin facilitates protein aggregation and fibril formation. *Protein Sci.* **9**, 831–845 (2000).

Esposito, G. *et al.* The Controlling Roles of Trp60 and Trp95 in β2-Microglobulin Function, Folding and Amyloid Aggregation Properties. *J. Mol. Biol.* **378**, 887–897 (2008).

Fändrich, M. Oligomeric intermediates in amyloid formation: Structure determination and mechanisms of toxicity. *J. Mol. Biol.* **421**, 427–440 (2012).

Foderà, V., Librizzi, F., Groenning, M., Van De Weert, M. & Leone, M. Secondary nucleation and accessible surface in insulin amyloid fibril formation. *J. Phys. Chem. B* **112**, 3853–3858 (2008).

Gaggelli, E., D'Amelio, N., Gaggelli, N. & Valensin, G. Metal ion effects on the cis/trans isomerization equilibrium of proline in short-chain peptides: a solution NMR study. *Chembiochem* **2**, 524–529 (2001).

Garg, D. K. & Kundu, B. Clues for divergent, polymorphic amyloidogenesis through dissection of amyloid forming steps of bovine carbonic anhydrase and its critical amyloid forming stretch. *Biochim. Biophys. Acta - Proteins Proteomics* **1864**, 794–804 (2016).

Gaspar, R. *et al.* Secondary nucleation of monomers on fibril surface dominates α-synuclein aggregation and provides autocatalytic amyloid amplification. *Q. Rev. Biophys.* **50**, (2017).

Gejyo, F. *et al.* β2-microglobulin: a new form of amyloid protein associated with chronic hemodialysis. *Kidney Int* **30**, 385–390 (1986).

Gillmore, J. D., Hawkins, P. N. & Pepys, M. B. Amyloidosis: a review of recent diagnostic and therapeutic developments. *Br. J. Haematol.* **99**, 245–56 (1997).

Giorgetti, S. *et al.* Effect of tetracyclines on the dynamics of formation and destructuration of β2-microglobulin amyloid fibrils. *J. Biol. Chem.* **286**, 2121–2131 (2011).

Hall, Z., Schmidt, C. & Politis, A. Uncovering the early assembly mechanism for amyloidogenic β2-microglobulin using cross-linking and native mass spectrometry. *J. Biol. Chem.* **291**, 4626–4637 (2016).

Hardy, J., Selkoe, D. J., Hardy, J. & Selkoe, D. J. Therapeutics Linked references are available on JSTOR for this article : The Amyloid Hypothesis of Alzheim Progress and Problems on the Road to. *Science (80-.).* **297**, 353–356 (2002).

Heegaard, N. H. H., Sen, J. W., Kaarsholm, N. C. & Nissen, M. H. Conformational Intermediate of the Amyloidogenic Protein β2-Microglobulin at Neutral pH. *J. Biol. Chem.* **276**, 32657–32662 (2001).

Hellstrand, E., Boland, B., Walsh, D. M. & Linse, S. Amyloid β-protein aggregation produces highly reproducible kinetic data and occurs by a two-phase process. *ACS Chem. Neurosci.* **1**, 13–18 (2010).

Hong, D. P., Hoshino, M., Kuboi, R. & Goto, Y. Clustering of fluorine-substituted alcohols as a factor responsible for their marked effects on proteins and peptides. *J. Am. Chem. Soc.* **121**, 8427–8433 (1999).

Horton, H. R. & Koshland, D. E. A Highly Reactive Colored Reagent with Selectivity for the Tryptophan Residue in Proteins. 2-Hydroxy-5-nitrobenzyl Bromide. *J. Am. Chem. Soc.* **87**, 1126–1132 (1965).

Horton, H. R. & Tucker, W. P. Dimethyl(2-hydroxy-5-nitrobenzyl) sulfonium Salts. *J. Biol. Chem.* **245**, 3397–3401 (1970).

Jahn, T. R., Parker, M. J., Homans, S. W. & Radford, S. E. Amyloid formation under physiological conditions proceeds via a native-like folding intermediate. *Nat. Struct. Mol. Biol.* **13**, 195–201 (2006).

Jones, S., Manning, J., Kad, N. M. & Radford, S. E. Amyloid-forming peptides from β2-microglobulin - Insights into the mechanism of fibril formation in vitro. *J. Mol. Biol.* **325**, 249–257 (2003).

JT, J. & Jr, L. P. T. Seeding 'one-dimensional crystallization' of amyloid: A pathogenic mechanism in Alzheimer's disease and scrapie? *Cell* **73**, 1055–8 (1993).

Kang, Y. K. Ring Flip of Proline Residue via the Transition State with an Envelope Conformation. *J. Phys. Chem. B* **108**, 5463–5465 (2004).

Karamanos, T. K. *et al.* Structural mapping of oligomeric intermediates in an amyloid assembly pathway. *Elife* **8**, 1–32 (2019).

Karamanos, T. K., Kalverda, A. P., Thompson, G. S. & Radford, S. E. Visualization of Transient Protein-Protein Interactions that Promote or Inhibit Amyloid Assembly. *Mol. Cell* **55**, 214–226 (2014).

Katou, H. *et al.* The role of disulfide bond in the amyloidogenic state of beta(2)-microglobulin studied by heteronuclear NMR. *Protein Sci.* **11**, 2218–29 (2002).

Kaur, U. *et al.* Evolution of Structural Biology through the Lens of Mass Spectrometry. *Anal. Chem.* **91**, 142–155 (2019).

Koshland, D. E., Karkhanis, Y. D., H. G. L. An Environmentally-Sensitive Reagent with Selectivity for the Tryptophan Residue in Proteins. *J. Am. Chem. Soc.* **86**, 1448–1450 (1964).

Lambert, M. P. *et al.* Diffusible, nonfibrillar ligands derived from Aβ1-42 are potent central nervous system neurotoxins. *Proc. Natl. Acad. Sci. U. S. A.* **95**, 6448–6453 (1998).

Le Marchand, T. *et al.* Conformational dynamics in crystals reveal the molecular bases for D76N beta-2 microglobulin aggregation propensity. *Nat. Commun.* **9**, 1–11 (2018).

Li, K. S., Rempel, D. L. & Gross, M. L. Conformational-Sensitive Fast Photochemical Oxidation of Proteins and Mass Spectrometry Characterize Amyloid Beta 1-42 Aggregation. *J. Am. Chem. Soc.* **138**, 12090–12098 (2016).

Lim, J. & Vachet, R. W. Using mass spectrometry to study copper-protein binding under native and non-native conditions: β-2-microglobulin. *Anal. Chem.* **76**, 3498–3504 (2004).

Limpikirati, P., Liu, T. & Vachet, R. W. Covalent labeling-mass spectrometry with non-specific reagents for studying protein structure and interactions. *Methods* **144**, 79–93 (2018).

Linke, R. P. *et al.* Lysine-specific cleavage of β2-microglobulin in amyloid deposits associated with hemodialysis. *Kidney Int.* **36**, 675–681 (1989).

Liu, T., Marcinko, T. M., Kiefer, P. A. & Vachet, R. W. Using Covalent Labeling and Mass Spectrometry To Study Protein Binding Sites of Amyloid Inhibiting Molecules. *Anal. Chem.* **89**, 11583–11591 (2017).

Loureiro, R. J. S., Vila-Viçosa, D., Machuqueiro, M., Shakhnovich, E. I. & Faísca, P. F. N. The early phase of β2m aggregation: An integrative computational study framed on the d76n mutant and the dn6 variant. *Biomolecules* **9**, (2019).

Lucato, C. M., Lupton, C. C., Halls, M. L. & Ellisdon, A. M. Amyloidogenicity at a distance: How distal protein regions modulate aggregation in disease. *J. Mol. Biol.* **429**, 1289–1304 (2017).

Ma, T. *et al.* Structural Mechanism of Barriers to Interspecies Seeding Transmissibility of Full-Length Prion Protein Amyloid. *ChemBioChem* **20**, 2757–2766 (2019).

Mangione, P. P. *et al.* Structure, folding dynamics, and amyloidogenesis of D76N β2-microglobulin roles of shear flow, hydrophobic surfaces, and α-crystallin. *J. Biol. Chem.* **288**, 30917–30930 (2013).

Marcinko, T. M., Dong, J., LeBlanc, R., Daborowski, K. V. & Vachet, R. W. Small Molecule-mediated Inhibition of β-2-Microglobulin Amyloid Fibril Formation. *J. Biol. Chem.* **292**, 10630-10638 (2017).

Marcinko, T. M., Drews, T., Liu, T. & Vachet, R. W. Epigallocatechin-3-gallate Inhibits Cu(II)-Induced β-2-Microglobulin Amyloid Formation by Binding to the Edge of Its β-Sheets. *Biochemistry* **59**, 1093–1103 (2020).

McParland, V. J. *et al.* Partially Unfolded States of β2-Microglobulin and Amyloid Formation in Vitro. *Biochemistry* **39**, 8735–8746 (2000).

Meisl, G. *et al.* Differences in nucleation behavior underlie the contrasting aggregation kinetics of the Aβ40 and Aβ42 peptides. *Proc. Natl. Acad. Sci. U. S. A.* **111**, 9384–9389 (2014).

Mendoza, V. L. & Vachet, R. W. Probing Protein Structure by Amino Acid-Specific Covalent Labeling and Mass Spectrometry. *Mass Spectrom. Rev.* **28**, 785–815 (2009).

Mendoza, V. L., Antwi, K., Barón-rodríguez, M. A., Blanco, C. & Vachet, R. W. Structure of the Pre-amyloid Dimer of β-2-microglobulin from Covalent Labeling and Mass Spectrometry. *Biochemistry* **49**, 1522–1532 (2010).

Mendoza, V. L., Barón-Rodríguez, M. A., Blanco, C. & Vachet, R. W. Structural insights into the pre-amyloid tetramer of β-2-microglobulin from covalent labeling and mass spectrometry. *Biochemistry* **50**, 6711–6722 (2011).

Mirbaha, H. *et al.* Inert and seed-competent tau monomers suggest structural origins of aggregation. *Elife* **7**, 1–29 (2018).

Mizuno, H. *et al.* Dialysis-related amyloidosis associated with a novel β2-microglobulin variant. *Amyloid* **0**, 1–8 (2020).

Morgan, C. J., Gelfand, M., Atreya, C. & Miranker, A. D. Kidney dialysis-associated amyloidosis: a molecular role for copper in fiber formation. *J. Mol. Biol.* **309**, 339–45 (2001).

Müller, H. *et al.* Progress towards structural understanding of infectious sheep PrP-amyloid. *Prion* **8**, 344–358 (2014).

Myers, S. L. *et al.* A systematic study of the effect of physiological factors on β2-microglobulin amyloid formation at neutral pH. *Biochemistry* **45**, 2311–2321 (2006).

Naiki, H., Higuchi, K., Hosokawa, M. & Takeda, T. Fluorometric determination of amyloid fibrils in vitro using the fluorescent dye, thioflavine T. *Anal. Biochem.* **177**, 244–249 (1989).

Natalello, A. *et al.* Co-fibrillogenesis of wild-type and D76N β2-microglobulin: The crucial role of fibrillar seeds. *J. Biol. Chem.* **291**, 9678–9689 (2016).

O'Nuallain, B., Williams, A. D., Westermark, P. & Wetzel, R. Seeding Specificity in Amyloid Growth Induced by Heterologous Fibrils. *J. Biol. Chem.* **279**, 17490–17499 (2004).

Ohhashi, Y., Kihara, M., Naiki, H. & Goto, Y. Ultrasonication-induced amyloid fibril formation of beta2-microglobulin. *J. Biol. Chem.* **280**, 32843–32848 (2005).

Olsson, T. T., Klementieva, O. & Gouras, G. K. Prion-like seeding and nucleation of intracellular amyloid-β. *Neurobiol. Dis.* **113**, 1–10 (2018).

Othon, C. M., Kwon, O.-H., Lin, M. M. & Zewail, A. H. Solvation in protein (un)folding of melittin tetramer-monomer transition. *Proc. Natl. Acad. Sci.* **106**, 12593–12598 (2009).

Paravastu, A. K., Qahwash, I., Leapman, R. D., Meredith, S. C. & Tycko, R. Seeded growth of β-amyloid fibrils from Alzheimer's brain-derived fibrils produces a distinct fibril structure. *Proc. Natl. Acad. Sci. U. S. A.* **106**, 7443–7448 (2009).

Pashley, C. L., Hewitt, E. W. & Radford, S. E. Comparison of the aggregation of homologous β2-microglobulin variants reveals protein solubility as a key determinant of amyloid formation. *J. Mol. Biol.* **428**, 631–643 (2016).

Platt, G. W. & Radford, S. E. Glimpses of the molecular mechanisms of β2-microglobulin fibril formation in vitro: Aggregation on a complex energy landscape. *FEBS Lett.* **583**, 2623–2629 (2009).

Platt, G. W., Routledge, K. E., Homans, S. W. & Radford, S. E. Fibril Growth Kinetics Reveal a Region of β2-microglobulin Important for Nucleation and Elongation of Aggregation. *J. Mol. Biol.* **378**, 251–263 (2008).

Reimer, U., Mokdad, N. El, Schutkowski, M. & Fischer, G. Intramolecular assistance of cis/trans isomerization of the histidine- proline moiety. *Biochemistry* **36**, 13802–13808 (1997).

Ricagno, S. *et al.* DE loop mutations affect β2-microglobulin stability and amyloid aggregation. *Biochem. Biophys. Res. Commun.* **377**, 146–150 (2008).

Rochet, J. & Lansbury, P. T. J. Amyloid fibrillogenesis: themes and variations. *Curr. Opin. Struct. Biol.* **10**, 60–68 (2000).

Ruschak, A. M. & Miranker, A. D. Fiber-dependent amyloid formation as catalysis of an existing reaction pathway. *Proc. Natl. Acad. Sci. U. S. A.* **104**, 12341–12346 (2007).

Sade, D., Shaham-Niv, S., Arnon, Z. A., Tavassoly, O. & Gazit, E. Seeding of proteins into amyloid structures by metabolite assemblies may clarify certain unexplained epidemiological associations. *Open Biol.* **8**, (2018).

Saelices, L. *et al.* A pair of peptides inhibits seeding of the hormone transporter transthyretin into amyloid fibrils. *J. Biol. Chem.* **294**, 6130–6141 (2019).

Saelices, L. *et al.* Amyloid seeding of transthyretin by ex vivo cardiac fibrils and its inhibition. *Proc. Natl. Acad. Sci. U. S. A.* **115**, E6741–E6750 (2018).

Serpa, J. J. *et al.* Using isotopically-coded hydrogen peroxide as a surface modification reagent for the structural characterization of prion protein aggregates. *J. Proteomics* **100**, 160–166 (2014).

Smith, D. P. & Radford, S. E. Role of the single disulphide bond of beta(2)-microglobulin in amyloidosis in vitro. *Protein Sci.* **10**, 1775–84 (2001).

Smith, D. P., Jones, S., Serpell, L. C., Sunde, M. & Radford, S. E. A systematic investigation into the effect of protein destabilisation on beta 2-microglobulin amyloid formation. *J. Mol. Biol.* **330**, 943–954 (2003).

Smith, D. P., Woods, L. a, Radford, S. E. & Ashcroft, A. E. Structure and Dynamics of Oligomeric Intermediates in β(2)-Microglobulin Self-Assembly. *Biophys. J.* **101**, 1238–1247 (2011).

Smith, H. I. *et al.* The role of the IT-state in D76N β2-microglobulin amyloid assembly: A crucial intermediate or an innocuous bystander? *J. Biol. Chem.* **295**, 12474–12484 (2020).

Srikanth, R., Mendoza, V. L., Bridgewater, J. D., Zhang, G. & Vachet, R. W. Copper Binding to β-2-Microglobulin and its Pre-Amyloid Oligomers. *Biochemistry* **48**, 9871–9881 (2009).

Stoppini, M. & Bellotti, V. Systemic amyloidosis: Lessons from β2-microglobulin. *J. Biol. Chem.* **290**, 9951–9958 (2015).

Takamuku, T., Kumai, T., Yoshida, K., Otomo, T. & Yamaguchi, T. Structure and dynamics of halogenoethanol-water mixtures studied by large-angle X-ray scattering, small-angle neutron scattering, and NMR relaxation. *J. Phys. Chem. A* **109**, 7667–7676 (2005).

Thomas, A., Kaur, G., Ali, R. & Verma, S. Small Molecule Inhibitors for Amyloid Aggregation. in *Biological Soft Matter: Fundamentals, Properties, and Applications* (eds. Nardin, C. & Schlaad, H.) 153–194 (WILEY-VCH, 2021).

Tipping, K. W. *et al.* pH-induced molecular shedding drives the formation of amyloid fibril-derived oligomers. *Proc. Natl. Acad. Sci. U. S. A.* **112**, 5691–5696 (2015).

Torbeev, V. Y. & Hilvert, D. Both the cis-trans equilibrium and isomerization dynamics of a single proline amide modulate β2-microglobulin amyloid assembly. *Proc. Natl. Acad. Sci.* **110**, 20051–20056 (2013).

Törnquist, M. *et al.* Secondary nucleation in amyloid formation. *Chem. Commun.* **54**, 8667–8684 (2018).

Wasmer, C. *et al.* Structural similarity between the prion domain of HET-s and a homologue can explain amyloid cross-seeding in spite of limited sequence identity. *J. Mol. Biol.* **402**, 311–325 (2010).

Winner, B. *et al.* In vivo demonstration that α-synuclein oligomers are toxic. *Proc. Natl. Acad. Sci. U. S. A.* **108**, 4194–4199 (2011).

Wolfe, L. S. *et al.* Protein-induced photophysical changes to the amyloid indicator dye thioflavin T. *Proc. Natl. Acad. Sci.* **107**, 16863–16868 (2010).

Woods, L. A. *et al.* Ligand binding to distinct states diverts aggregation of an amyloid-forming protein. **7**, 730–739 (2012).

Xu, F. *et al.* Cerebral vascular amyloid seeds drive amyloid β-protein fibril assembly with a distinct anti-parallel structure. *Nat. Commun.* **7**, 1–10 (2016).

Xu, G. & Chance, M. R. Hydroxyl radical-mediated modification of proteins as probes for structural proteomics. *Chem. Rev.* **107**, 3514–3543 (2007).

Xue, W. F., Homans, S. W. & Radford, S. E. Systematic analysis of nucleation-dependent polymerization reveals new insights into the mechanism of amyloid self-assembly. *Proc. Natl. Acad. Sci. U. S. A.* **105**, 8926–8931 (2008).

Yamamoto, S. Glycosaminoglycans Enhance the Trifluoroethanol-Induced Extension of 2-Microglobulin-Related Amyloid Fibrils at a Neutral pH. *J. Am. Soc. Nephrol.* **15**, 126–133 (2004).

Yanagi, K. *et al.* The monomer-seed interaction mechanism in the formation of the β2-microglobulin amyloid fibril clarified by solution NMR techniques. *J. Mol. Biol.* **422**, 390–402 (2012).

Yang, X., Williams, J. K., Yan, R., Mouradian, M. M. & Baum, J. Increased Dynamics of α-Synuclein Fibrils by β-Synuclein Leads to Reduced Seeding and Cytotoxicity. *Sci. Rep.* **9**, 1–13 (2019).

Yonezawa, Y., Nakata, K., Sakakura, K., Takada, T. & Nakamura, H. Intra- And intermolecular interaction inducing pyramidalization on both sides of a proline dipeptide during isomerization: An ab initio QM/MM molecular dynamics simulation study in explicit water. *J. Am. Chem. Soc.* **131**, 4535–4540 (2009).

Zhang, B., Cheng, M., Rempel, D. & Gross, M. L. Implementing fast photochemical oxidation of proteins (FPOP) as a footprinting approach to solve diverse problems in structural biology. *Methods* **144**, 94–103 (2018).